MODEL ANALYSIS OF A TEN STOREY BUILDING

A Thesis

Presented to

the Faculty of Engineering

The University of Manitoba

In Partial Fulfillment

of the Requirements for the Degree

Master of Science in Civil Engineering

by

Robert Petri

May 1965

© Robert Petri 1965

THE UNIVERSITY OF MANITOBA ELIZABETH DAFOE LIBRARY

PREFACE

This thesis was carried out with the intent of determining the reliability of small scale reinforced concrete models of complex structures as a method of design. A 1/16 scale model of a typical ten story building having shear walls for lateral stability was chosen as the subject for investigation. Theoretical design methods of shear walls and the experimental results determined from testing were to be compared and the interaction of the shear wall with its component parts investigated.

The content of this thesis really has two phases. First the reliability and technical accuracy of the model was investigated and secondly the actual deflected shape of the model under lateral loading was compared to a theoretical derivation. Chapters I to V deal mainly with the accuracy of the model and a determination of the material properties of the model. Chapters VI to IX deal with the experimental results derived from loading the model and a comparison to theory.

ACKNOWLEDGEMENTS

The author wishes to express his sincere appreciation to the following for their help in the preparation of this thesis:

R. Lazar, Assistant Professor, Department of Civil Engineering, the University of Manitoba for his interest and advice in carrying out this thesis.

G. A. Morris, Assistant Professor, Department of Civil Engineering, for the use of his computer programme and his diligent and conscientious help in applying the programme to this thesis.

The Civil Engineering laboratory staff for their careful and constructive help in the structural laboratory.

Johnston Industrial Plastics, Bristol Aero-Industries Limited, and Acklands Limited for their technical advice.

TABLE OF CONTENTS

CHAPTER		PAGE
I	INTRODUCTION	1
	i. Purpose	2
	ii. Scope	2
	iii. Theory of Model Studies	2
II	DESCRIPTION AND DESIGN OF MODEL AND PROTOTYPE	4
	i. Description	4
	ii. Design of Prototype	4
	iii. Design of the Model	5
III	MATERIALS	13
	i. Mortar	13
	ii. Reinforcing Steel	23
IV	CONTROL OF MATERIAL PROPERTIES	26
	i. Mortar Test Cylinders	26
	ii. Beam Tests	33
	iii. Column Tests	43
	iv. Slab Tests	48
	v. Discussion on Adequacy of Model Similarity	51
V	METHODS OF CONSTRUCTION	59
	i. Placing and Fabrication of Column and Shear Wall Steel	59
	ii. Placing of Slab Steel	59
	iii. Fabrication of Forms	60
	iv. Construction Procedure	62
VI	INSTRUMENTATION AND LOADING PROCEDURE	79
	i. SR-4 Gages	79

TABLE OF CONTENTS (CONT'D)

CHAPTER		PAGE
	ii. Mechanical Dial Gages	79
	iii. Loading Apparatus	80
VII	TEST PROCEDURE AND EXPERIMENTAL RESULTS	83
	i. Lateral Deflections	83
	ii. Slab Deformations	97
	iii. Joint Deformations	97
VIII	DISCUSSION OF RESULTS	98
	i. Theoretical Results	98
	ii. Lateral Deflections	100
	iii. Slab Deformations	103
	iv. Joint Deformations	104
IX	CONCLUSIONS	107
	i. Adequacy of Model Similarity	107
	ii. Frame Rigidity	108
BIBLIOGRAPHY		110
APPENDIX I		
	Design of Prototype	
APPENDIX II		
	Tabulation of Experimental Results	
APPENDIX III		
	Computer Application of Kani Method	

LIST OF FIGURES

FIGURE		PAGE
1	Section Through a Shear Wall.	8
2	Section Through an Exterior Frame.	9
3	Floor Plan for First, Second and Third Floor.	10
4	Floor Plan for Fourth, Fifth, Sixth and Seventh Floors.	11
5	Floor Plan for Eighth, Ninth, and Tenth Floors.	12
6	Typical Crack Distribution on Failure of Prototype and Model Beams.	42
7.	Location of Top Steel Reinforcing Mats.	61
8.	Location of SR-4 Gages.	79
9.	Total Lateral Design Load for the Model.	82
10.	Interaction of Shear Wall, Slab and Columns.	107

LIST OF PLATES

PLATE		PAGE
1	Use of 30,000# Testing Machine for Cold-working of Reinforcing Steel.	55
2	Testing of Model Concrete Cylinders in 300,000# Testing Machine.	55
3	Testing of Model Beams in 30,000# Testing Machine.	56
4	Testing of Model Columns in 30,000# Testing Machine.	56
5	Model Column Test Specimen After Failure.	57
5a	Model Slabs.	57
5b	Model Beams.	58
5c	Crack Distribution of Prototype Beams.	58
6	Mortar Mixer (capacity 3/4 cubic ft.).	65
7	Placing of Column Steel Using a Grid System.	65
8	Method of Pouring Slabs.	66
9	Method of Forming Columns.	66
10	Removal of Column Forms.	67
11	Replacing Column Forms with Filler Plexiglass Pieces.	67
12	Fabrication of Shear Wall Reinforcing Steel.	68
13	Plexiglass Column Forms.	68
14	Base of Model.	69
15	Forming of First to Second Columns.	69
16	Forming of Second Floor.	70
17	Finished Second Floor.	70
18	Forming of Second to Third Columns.	71
19	Forming of Third Floor.	71
20	Finished Fourth Floor.	72
21	Forming of Fifth Floor.	72

LIST OF PLATES (CONT'D)

PLATE		PAGE
22	Forming of Fifth to Sixth Columns.	73
23	Finished Sixth Floor.	73
24	Finished Eighth Floor.	74
25	Poured Ninth Floor.	74
26	Forming of Tenth to Roof Columns.	75
27	Finished Model.	75
28	Detail Showing Supporting Frame.	76
29	Detail of Loading Apparatus.	76
30	Detail of Method of Applying Lateral Loads.	77

LIST OF GRAPHS

GRAPH		PAGE
IIIa	w/c ratio versus strength.	21
IVa	Mortar strength vs time.	28
IVb	Cumulative probability curve.	29
IVc	Mortar stress vs strain curve.	30
IVd	Stress vs strain curves for meam tests.	38
VIIa	Deflected shape of model due to point loads (Test Series 1).	87
VIIb	Theoretical derivation of deflected shape of the model due to lateral loading in direction of shear walls.	88
VIIc	Comparison of deflected shape of the model at design load between Test Series 1, Test Series 11, and the theoretical results of Graph VIIb.	89
VIId	Deflected shape of model due to different uniform lateral loads and comparison with theoretical results.	90
VIIe	Deflected shape of model due to 10# point loads. (Test Series IV).	91
VIIf	Deflected shape of model due to 20# point loads. (Test Series V).	92
VIIg	Deflected shape of model due to point loads from Test Series VI.	93
VIIh	Deflected shape of model due to point loads from Test Series VII.	94
VIIj	Deflected shape of model due to unfirm load application of 10#/floor and 20#/floor. (Test Series IV and V)	95
VIIk	Load Deflection Curve From Test Series 111.	96

LIST OF TABLES

TABLE		PAGE
IIa	Design of Prototype Columns.	7
IIIa	Sieve Analysis of Model Sand.	14
IIIb	Sieve Analysis of Model Sand.	15
IIIc	Sieve Analysis of Model Sand.	16
IIId	Preliminary Mortar Design.	19
IIIe	Typical Mortar Mixes (by weight) Used in Different Laboratories.	22
IIIf	Sizes of Black Annealed Wire.	23
IIIg	Yield Strength of Column and Shear Wall Steel.	24
IVa	Mortar Test Cylinders.	31
IVb	Structural Properties of Prototype and Model Beams.	34
IVc	Test Results of Model Beam Series 1.	35
IVd	Test Results of Model Beam Series 11.	36
IVe	Test Results of Prototype Beams.	37
IVf	Column Test Series 1.	46
IVg	Column Test Series 11.	47
IVh	Structural Properties of Test Slabs.	49
Va	Construction Timetable.	64
VIIa (Trial # 1)	Lateral Deflection Readings for Test Series 1.	Appendix II
VIIa (Trial # 2)	Lateral Deflection Readings for Test Series 1.	Appendix II
VIIa (Trial # 3)	Lateral Deflection Readings for Test Series 1.	Appendix II
VIIa (Average)	Lateral Deflection Readings for Test Series 1.	Appendix II

LIST OF TABLES (CONT'D)

TABLE		PAGE
VIIa	(Results by Superposition) Lateral Deflection Readings for Test Series I.	Appendix II
VIIb	(Trial #1 to #3) Lateral Deflection Readings for Test Series II.	Appendix II
VIIc	(Trial #1 and #2) Lateral Deflection Readings for Test Series III.	Appendix II
VIIc	(Trial #3 and #4) Lateral Deflection Readings for Test Series III.	Appendix II
VIId	Lateral Deflection Readings for Test Series IV.	Appendix II
VIIe	Lateral Deflection Readings for Test Series V.	Appendix II
VIIf	Lateral Deflection Readings for Test Series VI.	Appendix II
VIIg	Lateral Deflection Readings for Test Series VII.	Appendix II
VIIh	(Average of Three Trials) Slab Deformations in the Plane of the Shear Wall for Test Series I.	Appendix II
VIIh	(Results by Superpositions) Slab Deformations in the Plane of the Shear Wall Test Series I.	Appendix II
VIIj	(Trial #1 to #3) Slab Deformations in the Plane of the Shear Wall For Test Series II.	Appendix II
VIIk	(Trial #1 and #2) Slab Deformations in the Plane of the Shear Wall For Test Series III.	Appendix II
VIIk	(Trial #3 and #4) Slab Deformations in the Plane of the Shear Wall for Test Series III.	Appendix II
VIIl	(Average of Three Trials) Joint Deformations for Test Series I.	Appendix II
VIIl	(Results by Superposition) Joint Deformations for Test Series I.	Appendix II
VIIm	(Trial #1 to #3) Joint Deformations for Test Series II.	Appendix II

LIST OF TABLES (CONT'D)

TABLE		PAGE
VIIn	(Trial #1 and #2) Joint Deformations for Test Series 111.	Appendix II
VIIn	(Trial #3 and #4) Joint Deformations for Test Series 111.	Appendix II
VIIIa	Increase in Flexibility with Increase in Number of Cycles.	101
VIIIb	Location of Points of Inflection in the Slab.	103

LIST OF SYMBOLS

K = scale factor

f'c = compressive strength of concrete

fy = yield strength of reinforcing steel

Es = modulus of elasticity of steel

Ec = modulus of elasticity of concrete

n = modular ratio

lm = length of model

lp = length of prototype

fm = stress in model

fp = stress in prototype

Em = modulus of elasticity in model

Ep = modulus of elasticity in prototype

Wm = unit load on the model

Wp = unit load on the prototype

Δ m = deflection of the model

Δ p = deflection of the prototype

Mm = moment in the model

Mp = moment in the prototype

$A_s m$ = area of steel in the model

$A_s p$ = area of steel in the prototype

Pm = load on the model

Pp = load on the prototype

Im = moment of inertia of the model

Ip = moment of inertia of the prototype

% = percent

LIST OF SYMBOLS (CONT'D)

#30 - number thirty

30# - thirty pounds

w/c ratio - water-cement ratio

b - width of compression face of flexural member

d - distance from extreme compression fibre to centroid of tension reinforcement.

Pu - ultimate load capacity

p - ratio of area of tension reinforcement to effective area of concrete

Ag - gross area of tied columns

Pg - ratio of area of vertical reinforcement to the gross area, Ag

Pt - total load

Pc - load supported by concrete

Ps - load supported by reinforcing steel

Sc - stress developed in the concrete

Ss - stress developed in the reinforcing steel

Ac - area of concrete

As - area of reinforcing steel

ϵ - unit strain

$\emptyset$ - reduction factor for unavoidable eccentricity in columns

Chapter I

INTRODUCTION

Model analysis as a method of design or as a check on various theoretical designs has been used to some extent on this continent but to a larger degree in European countries, i.e., Portugal, Spain, Italy, and Britain. The importance of model analysis as a check on theoretical designs has been recognized more in this country and U.S.A. as evidenced by the numerous articles printed on this topic in the Portland Cement Association, American Concrete Institute, and American Society of Civil Engineering Journals. Until recently plexiglass has mainly been used for small scale models because of its ease of shaping, homogeniety, and low modulus of elasticity. However it was difficult to justify using this material to simulate reinforced concrete. Thus many Universities and other scientific bodies have been exploring the use of model concrete as a model material. Whereas with plexiglass it was not uncommon to use a scale factor as low as 1/40, a minimum scale factor for reinforced concrete would have to be established. A scale of 1/16 has been suggested as giving satisfactory results by the University of Illinois in their analysis of flat slabs. However European sources seemed to indicate that undesirable scale effects may be introduced in models of a smaller scale than 1/4. It appeared that as yet not enough research has occurred using concrete as a model material to justify any one scale factor as being a minimum.

i. Purpose

The purpose of this thesis project was to investigate the theoretical analysis presently in use for shear wall designs, and check these methods with the experimental results obtained from a model. The only scale factor involved in the model was that of dimension and therefore theoretically it was called an "exact model". An important corollary to this objective was to show that the 1/16 scale model of a ten story reinforced concrete building was in all practicality an exact model. A large portion of the work involved construction of the model to the proper degree of accuracy and in keeping sufficient checks on material properties.

ii Scope.

The experimental work has been limited to the analysis of the shear walls. This has resulted in a comparison of the experimental results with various theoretical methods of design.

iii Theory of Model Studies.

Two ways to look at the experimental and theoretical analysis of this model exist. One was that the model is in effect a model and there is a prototype. However, since the prototype exists on paper only there was no real way of comparing the experimental results with that of the prototype. There were slight differences between the material properties of the proposed prototype and that of the existing model. These differences were listed in Chapter IV, section v as the differences between the theoretical model and the actual model. But

these differences had no effect on the accuracy of the model properties themselves if these actual properties were used in predicting the behaviour of the model. The model itself was used in prototype form as a comparison with various theoretical designs.

The relationship between a model and its prototype can be summarized in one general statement; If the linear dimensions of a structure are scaled by a factor K, then the applied forces are scaled by a factor K^2, the applied moments will be scaled by a factor K^3, the deflections will be scaled by a factor K, and the strains and stresses will be unchanged. This statement applied only if the pertinent material properties of model and prototype, as in this thesis, were the same.

Chapter II

DESCRIPTION AND DESIGN OF MODEL AND PROTOTYPE

i. Description.

The prototype building was a hypothetical case and might represent a typical multistory office tower or apartment block built of reinforced concrete and containing a shear wall design. The building for ease of construction consisted of a minimum number of bays in either direction. Thus 3 bays 16' in length in one direction and 4 bays 16' in length in the other were used. The number of bays was chosen for ease of loading with a wiffle tree system. The building was 10 stories high with 2 shear walls running from the first floor to roof, the building being designed for lateral support in one direction only. To be consistent with common practise the column and shear wall design was changed only 3 times in the 10 stories.

ii. Design of Prototype.

The entire design was of reinforced concrete. The empirical design methods as set out in the ACI Building Code (ACI 318-56) were used for the flat plate design, design of columns and partially for the design of the shear walls. The complete design with calculations can be found in Appendix I. The shear walls were assumed to take all lateral loads and were designed as two vertical cantilever beams. The lateral wind loads were obtained from the NBC Supplement #1. The equivalent wind load was 17 psf with further appropriate modifications for height coefficients and height : breadth : length ratio. Each clear

floor height was 10' except for the first storey. With the intention of increasing stresses in this area and being consistent with practical architectural features the first clear storey height was chosen as 16'. Cross-sections showing the shear walls and exterior frame were shown in figures 1 and 2. Figures 3, 4, and 5 show the different floor plans for the three changes in column and shear wall design. Table IIa gave the final design for the columns and shear walls.

The entire design was chosen with the prime purpose of having a structure consistent with present practical design methods. The existing office tower at the Mall Centre Project in Winnipeg had a similar design in that it had 4 shear walls for the full height of its 10 stories designed as vertical cantilever beams. Similarly, the new Millbank Tower in London, a 34 storey office tower, consisted of a stiff central core which acted as a massive cantilever from the foundation. The exterior columns were not considered to offer any resistance to wind loading

The unit stresses used for design were as follows:

$f'c = 3{,}000$ psi

$fy = 40{,}000$ psi

$Es = 30 \times 10^6$ psi

$Ec = 3 \times 10^6$ psi

$n = 10$

iii. Design of the Model.

The model was built as an exact model on a scale of 1/16 of the prototype. Thus the model characteristics were as follows:

$$l_m = 1/16\ l_p$$

$$f_m = f_p$$

$$E_m = E_p$$

$$W_m = W_p$$

$$\Delta_m = 1/16\ \Delta_p$$

$$M_m = (1/16)^3\ M_p$$

$$A_{s_m} = (1/16)^2\ A_{s_p}$$

$$P_m = (1/16)^2\ P_p$$

$$I_m = (1/16)^4\ I_p$$

The model materials were chosen so as to have the same pertinent properties as the prototype materials. Chapters III and IV describe the materials used and the check recorded on the actual properties. A discussion on the adequacy of model similarity was given in Chapter IV section v. The design of the model itself consisted of applying the above model characteristics to the prototype design to arrive at the appropriate reinforcing steel and concrete dimensions.

The model was designed such that its foundation was perfectly rigid and there was no possibility of sliding. A base of standard 3,000 psi concrete was poured in a form 7½" x 5'9" x 5'6" giving a total weight of approximately 3,000 lbs. To prevent sliding this base was butted against a rigid steel testing frame. On top of this base a 1½" slab 4'3" x 3'3" was poured using the model concrete. This slab was securely anchored to the 7½" base with nails acting as steel dowels. The column and shear wall steel was set in the 1½" slab as it was poured. This insured no uplifting of the slab or rotation of

the foundation.

TABLE IIa

Design of Prototype Columns

	3B, 3C, (2)	A2, A3, A4, D2, D3, B1, C1, B5, C5. (10)	A1, D1, A5, D5. (4)	Shear Walls (2)
1st	18" x 18"	14" x 14"	14" x 14"	16^{10} x 10"
Verticals	10# 10	8# 10	6# 8	10# 10
Ties	#3 ties ¢ 18"	#3 ties @ 14"	#3 ties @ 14"	#3 ties @ 10"
Vert. Wall Steel				#6 @ 18"
Horiz. Wall Steel				#6 @ 11"
4th	16" x 16"	14" x 14"	12" x 12"	16^{10} x 8"
Verticals	6# 10	6# 8	4# 8	7# 8
Ties	#3 ties @ 16"	#3 ties @ 14"	#3 ties @ 12"	#3 ties @ 8"
Vert. Wall Steel				#6 @ 18"
Horiz. Wall Steel				#6 @ 13"
8th	12" x 12"	12" x 12"	12" x 12"	16^{10} x 8"
Verticals	4# 8	4# 8	4# 8	4# 8
Ties	#3 ties @ 12"	#3 ties @ 12"	#3 ties @ 12"	#3 ties @ 8"
Vert. Wall Steel				#6 @ 18"
Horiz. Wall Steel				#6 @ 13"

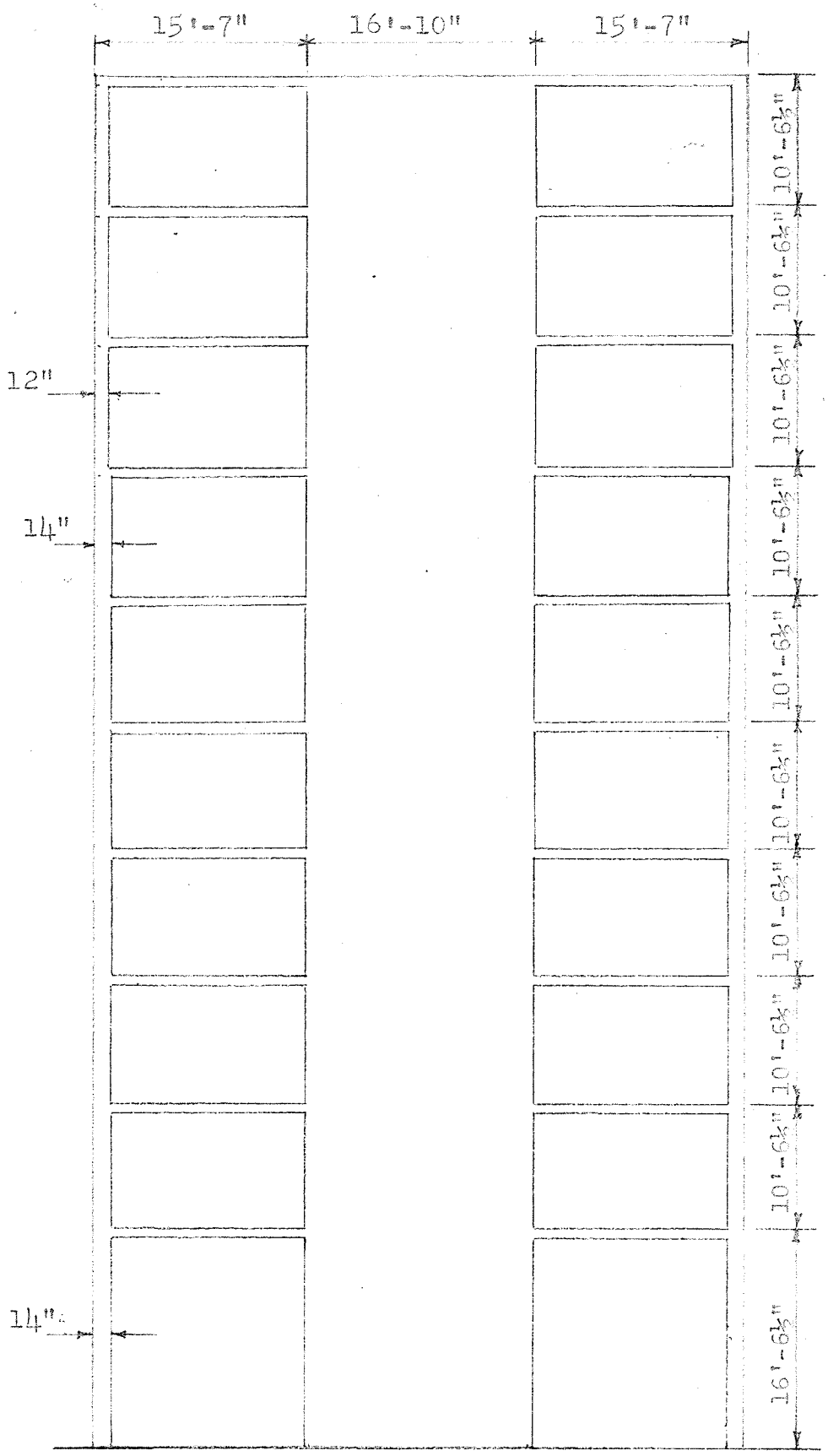

Section Through a Shear Wall

Figure 1.

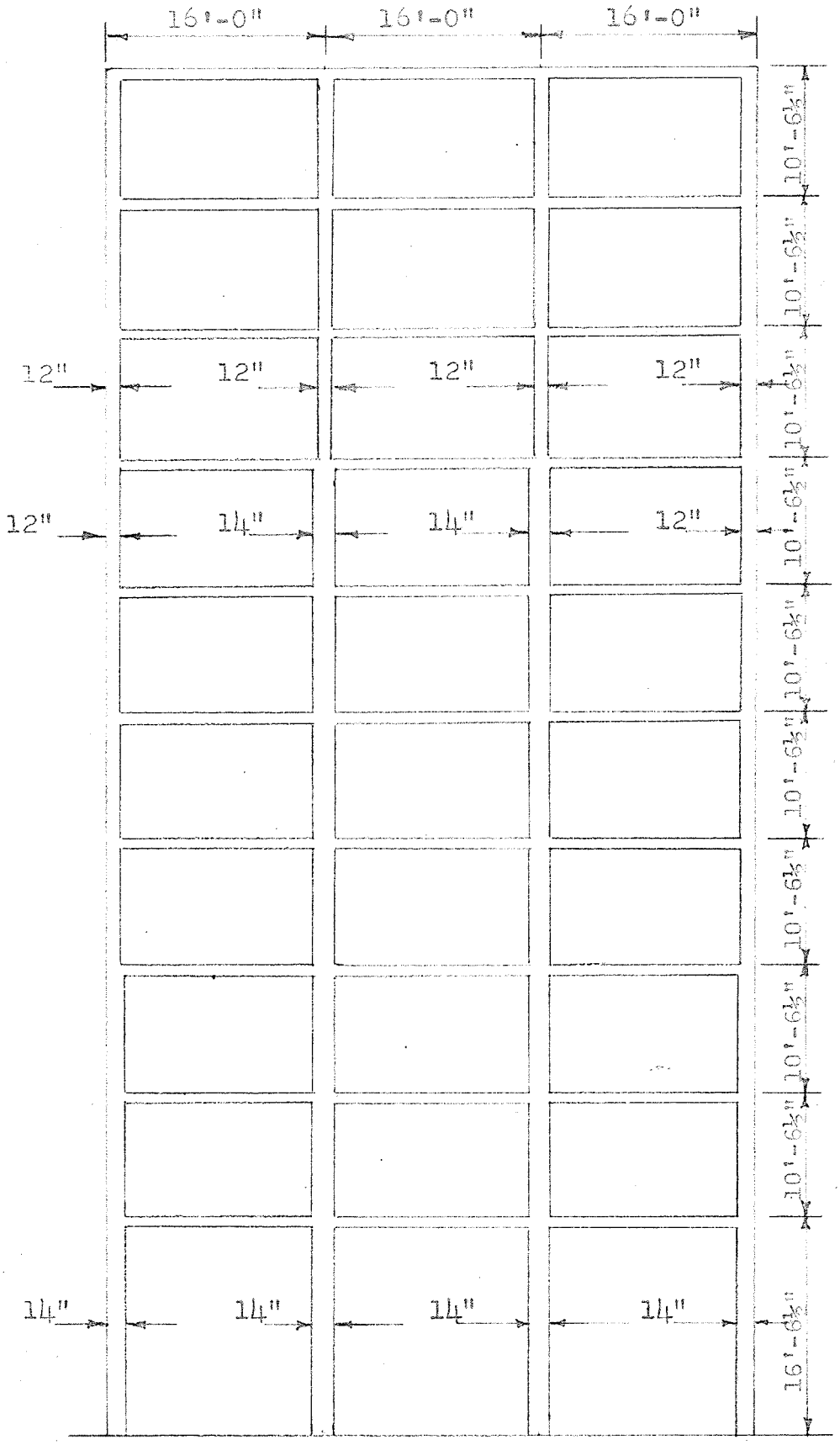

Section Through an Exterior Frame

Figure 2.

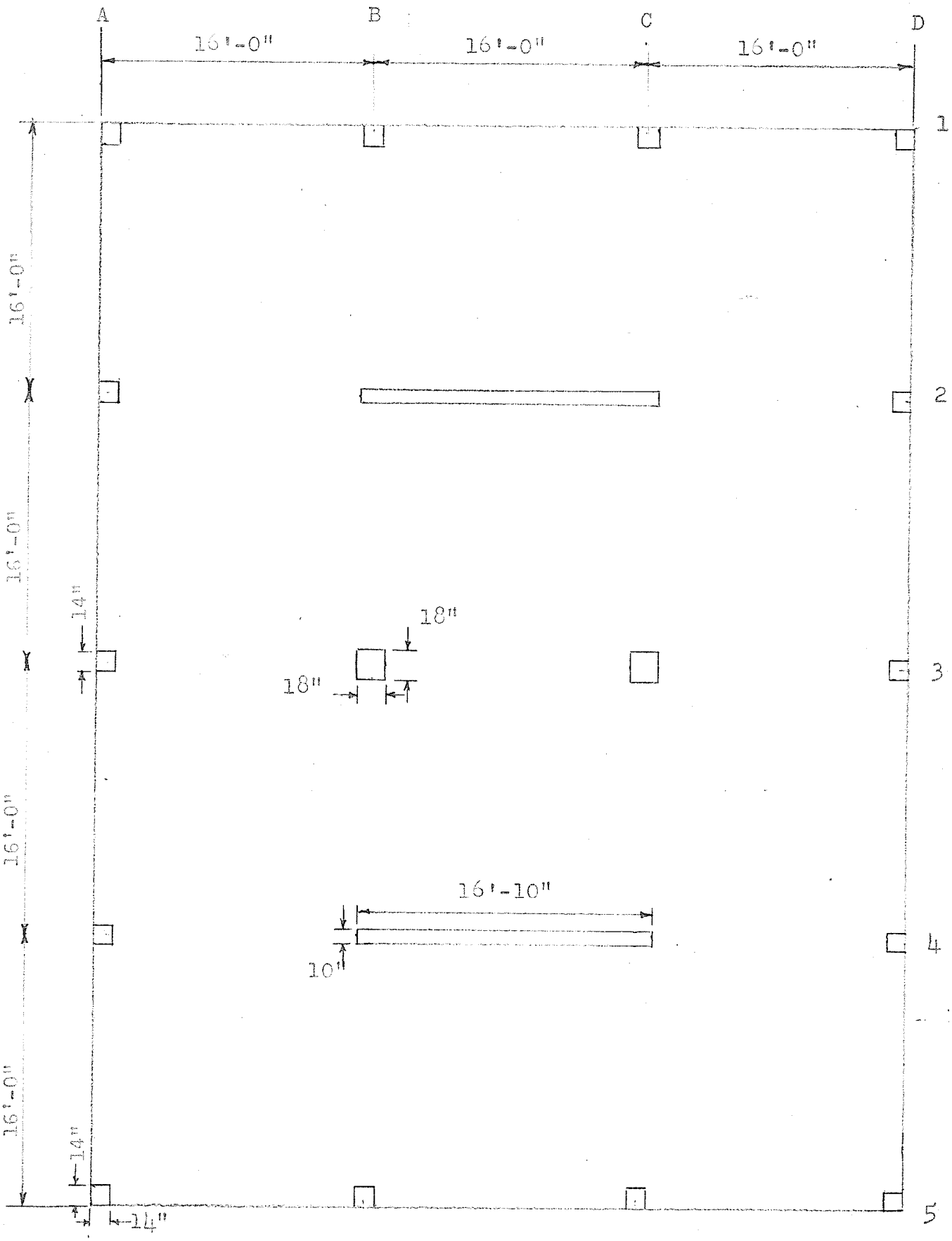

Floor Plan for First, Second, & Third Floor

Figure 3.

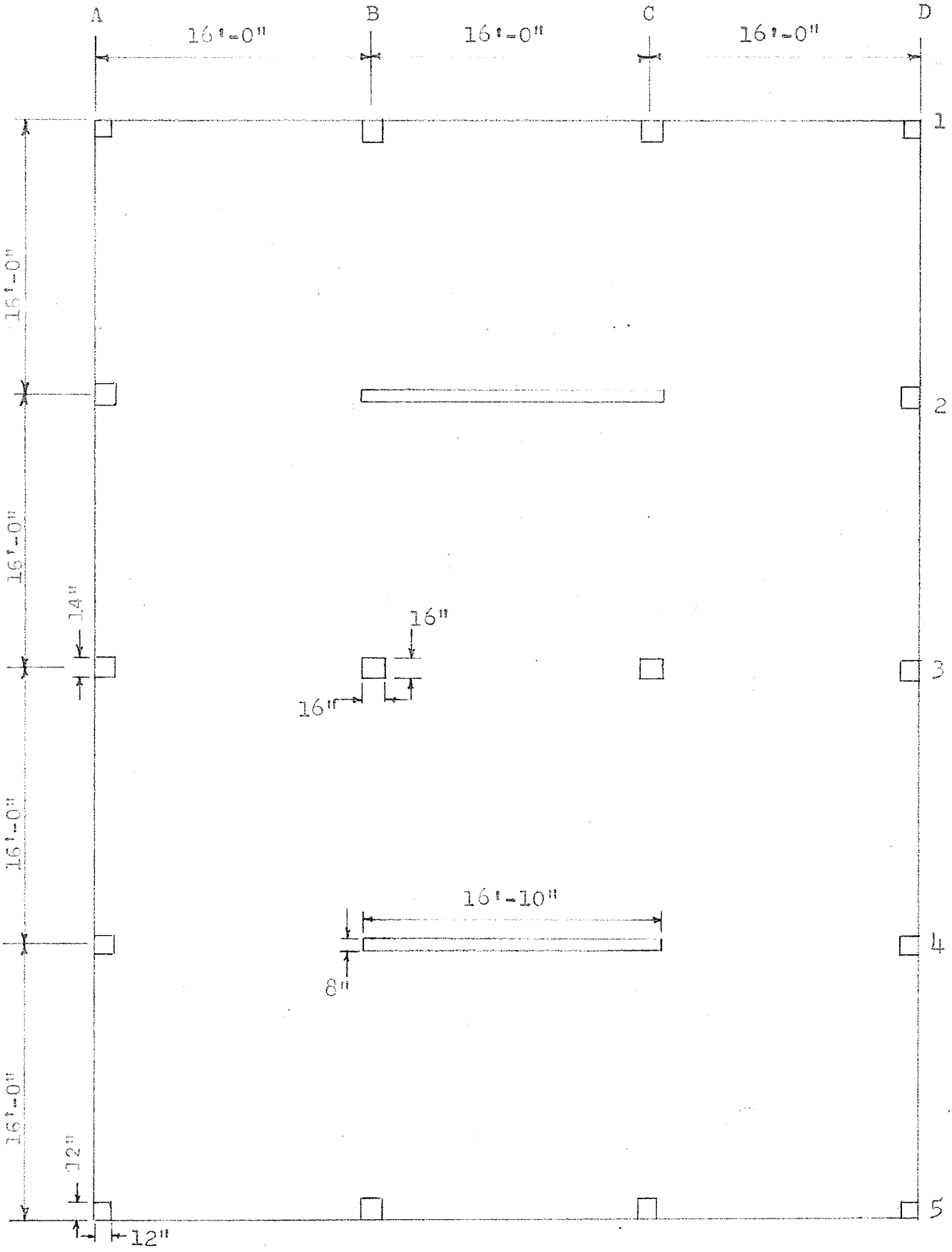

Floor Plan for Fourth, Fifth, Sixth & Seventh Floors

Figure 4.

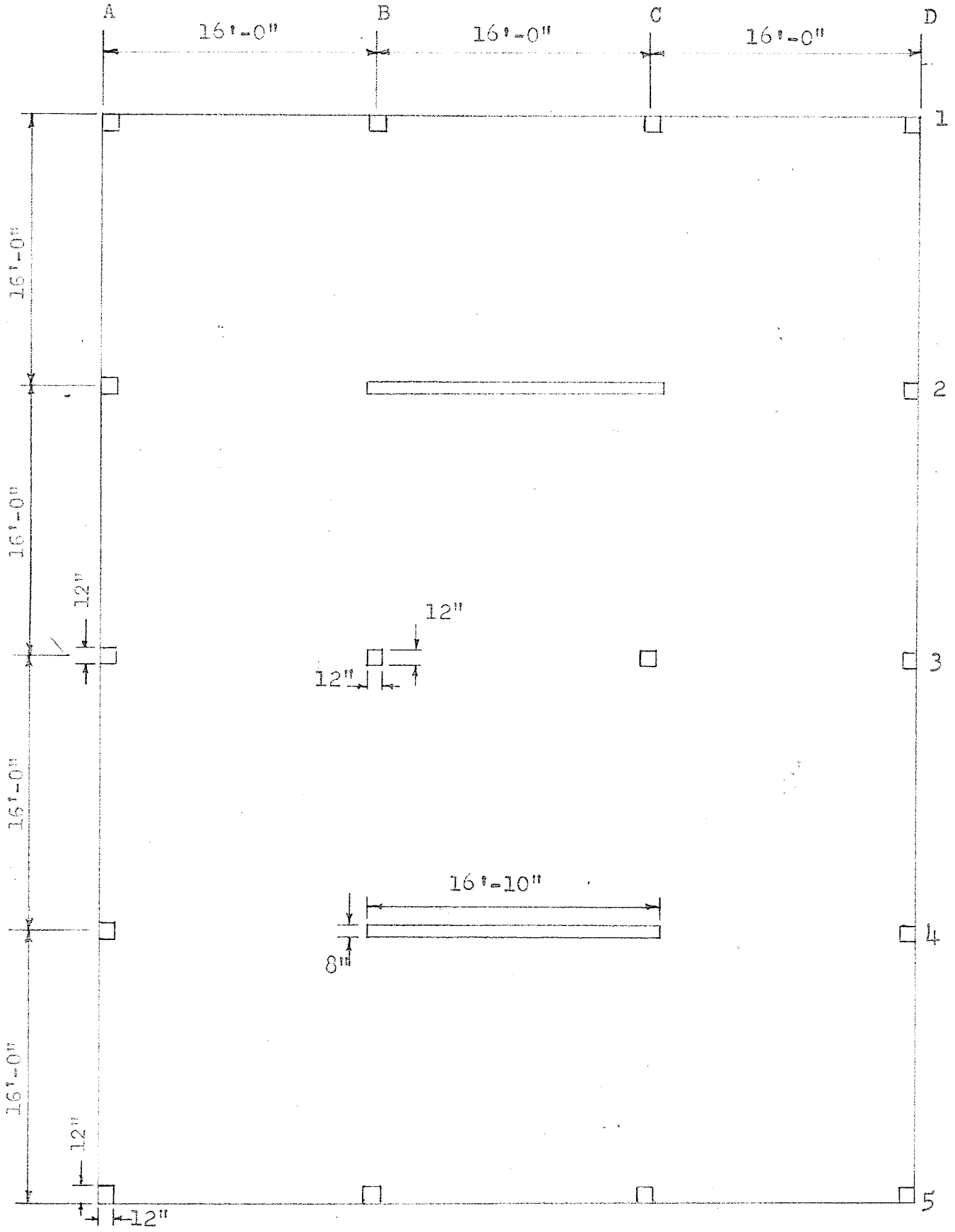

Floor Plan for Eigth, Ninth & Tenth Floors

Figure 5.

Chapter III

MATERIALS

In order to obtain a model to prototype relationship as described in Chapter I, it was necessary to find building materials which have the required mechanical properties. This became a difficult problem as few of these materials were likely to be used on a commercial basis. This creates two problems, one of locating the material and one of being assured of a continuous supply with consistent properties. The second problem proved the more difficult. Since these materials were manufactured for purposes other than model studies, there was often no reason for the manufacturer to keep a close check on their mechanical properties. As a result methods had to be developed in the laboratory for assuring consistent and accurate material properties.

i. Mortar.

There were several requirements for the model material to represent concrete. First, it was hoped to obtain a scaled down concrete of 3,000 psi. Secondly, this concrete had to have the proper slump and workability in order to eliminate air pockets and voids. At the same time excessive shrinkage had to be avoided. It was also important to keep the individual components of the mortar consistent in proportion and moisture content. Thus because of the small sizes and quantities involved it was necessary to be exact in all proportioning and to have materials of consistent properties.

The model aggregate and sand was obtained from the Selkirk Silica Co. Ltd. It was 100% silica sand and was obtained from Black Island on Lake Winnipeg, Manitoba. A similar graduation of particle size as used by the University of Illinois*1 was used here. The sand particles were rounded, the % moisture content was 0, the specific gravity of the sand was 2.65, and the finess modulus of the complete aggregate was 2.20. The finess modulus of that part which was considered sand was 0.88 and the maximum aggregate size was 0.08". The following was the sieve analysis of the model aggregate used:

TABLE IIIa

U.S. Standard Sieve Sizes	% Retained	% of Each Size
#10		
		2.1
#18	2.1	
		46.3
#30	48.4	
		28.1
#50	76.5	
		18.2
#100	94.7	
		4.3
#200	99.0	
		1
pan	100.0	

The sand was obtained from Selkirk Silica in 3 sizes (passing #16 held on #30; passing #30 held on #60; passing #60 held on #100). On further inspection in the laboratory it was found that these sieve sizes were not accurate. It was also found that in buying sand on different days meant obtaining sand of different sieve sizes yet labeled the same size. Therefore it was found necessary to re-sieve the entire batch and re-combine in the proper proportions. This way the above gradation was obtained to a high degree of accuracy.

* See Bibliography.

One point here was of prime importance. It was felt that the above procedure of re-sieving the sand to obtain a definite proportion was unnecessary. However, it was found that in arbitrarily choosing any sand for different tests, using the same w/c ratio and % aggregate, that similar strengths were not obtained. Therefore it would seem reasonable that if a sand of consistent particle size and graduation were used for all tests that consistent strengths should be obtained. A suggested size by the author would be #16 to #30 (U.S. standard sieve sizes) Selkirk Silica sand for 1/16 scale model work. This would represent, for the model, both the sand and gravel or total aggregate for the mix. The actual laboratory sieve analysis of #16 to #30 is shown below in Table IIIb.

TABLE IIIb

U.S. Standard Sieve Sizes	% Retained	% of Each Size
#10		
		1.5
#18	1.5	
		40
#30	41.5	
		49.5
#50	91	
		7
#100	98	
		2
pan	100	

TABLE IIIc

U.S. Standard Sieve Sizes	% Retained	% of each Size
#10	0	
		15
#18	15	
		0
#30	15	
		72
#50	87	
		10
#100	97	
		3
pan	100	

In preliminary testing the sieve analysis of Table IIIa represented the model aggregate. In conjuction with this sand a more uniform Selkirk Silica sand having the sieve analysis of Table IIIc was used in one test in order to compare the ultimate strength values. For both tests (2 cylinders per test) a w/c ratio of 0.75 and % aggregate of 70 was used. In the case of the well graded sand (Table IIIa) the concrete strength was 2,450 psi. In the case of the uniform sand (Table IIIc) the concrete strength was 1,370 psi. This difference could be explained by the fact that a well graded sand needs less paste content (water & cement) than a poorly graded aggregate. Here the w/c ratio does not necessarily govern, but the distribution of the sand particles and resulting arrangement of void spaces to be filled by paste and air is the main cause of different strengths. In order to obtain better dispersion an admixture (pozzolith) was used in both tests and in all mortar used in the model. Thus the only safe conclusion to arrive at was that more testing would be required preferably using #16 to #30

sand as total aggregate and working out by experimentation a w/c versus strength curve. Otherwise the same sand as shown in Table IIIa could be used again, but the time and effort required to re-sieve and proportion the sand was not thought worthwhile.

High-Early-Strength Portland Cement was used in order to obtain an early strength. This was necessary in order to maintain an efficient construction programme.

Thus the materials used for the model concrete were: the proper sand, High-Early-Strength Portland Cement, pozzolith, and water. In order that there be as little shrinkage as possible it was necessary to keep the % paste low. However, one other criteria in direct conflict with this was the requirement of a high slump in order to ensure proper placing of the mortar in confined areas. Several tests (see Table IIId) with past content varying from 40 to 23% and w/c ratio from 0.40 to 0.89 were carried out. Mortar strengths and workability were recorded. Using the lowest % paste that would give the required workability and strength a mix of 70% paste and w/c ratio of 0.70 was selected (see Graph IIIa).

The admixture (pozzolith) appeared to have a very pronounced effect on the results. It was a dispersing agent and its advertisers claim it will increase the strength and workability of the concrete with no increase in cement or water. The proportion of pozzolith used (¼# to 100# of cement) was suggested by the supplier, Master Builders Co. Ltd. Its effect can readily be deduced from the results as shown on Graph IIIa.

Without pozzolith and a low paste content of 24%, it was found that as the w/c ratio decreased the strength decreased. This is

the opposite to what would be expected. However, because of the fine material used it is necessary that there would be sufficient fluid available to disperse the cement throughout the mortar. Therefore an increased w/c ratio was one source, pozzolith was another, and the third and most successful solution being a combination of both a higher paste content and admixture. Once sufficient means of dispersing the cement was available the relationship of w/c ratio versus strength appeared to function properly, as illustrated in the third curve (30% paste with pozzolith). All the mixing of the model concrete was carried out in a $\frac{3}{4}$ cu. ft. capacity electric mixer (see Plate 6). Measurements by weight of all materials were taken on a balance scale to the nearest ounce.

Different compositions for model concrete have been used successfully in different parts of the world. Table IIIe is a list of some of the model concrete in use at present.*(2)

* See Bibliography.

TABLE IIId

Preliminary Mortar Design (See Graph IIIa)

Test cylinder size - 3" x 6"

Trial	% Agg.	w/c	Pozz.	Curing Procedure	Curing Time in Days	f'c	Avg. f'c	Workability	Vibration
#1	76	.82	No	Hum. Room	7	2120	1960	-	Rodding + Tamping
	76	.82	No	Hum. Room	7	1800			"
#2	76	.76	No	Hum. Room	7	1230	1470	-	"
	76	.76	No	Hum. Room	7	1710			"
#3	76	.89	No	Hum. Room	7	2010	2085	-	"
	76	.89	No	Hum. Room	7	2160			"
#4	76	.85	No	Hum. Room	7	2170		-	"
	76	.85	No.	Hum. Room air dried 2 days	12	2690			"
#5	77	.40	Yes	Hum. Room	7	1085	1072	Impossible	"
	77	.40	Yes	Hum. Room	7	1060		"	"
#6	77	.50	Yes	Hum. Room air dried 1 day	7	2350		Impossible	"
#7	77	.70	Yes	Hum. Room air dried 1 day	7	2340		Fair	"
#8	77	.85	Yes	Hum. Room air dried 1 day	7	2330		Excellent	"
#9	70	.70	Yes	Hum. Room air dried 1 day	7	3180		High Slump	"
#10	70	.60	Yes	Hum. Room air dried 1 day	7	3820		High slump	"

TABLE IIId (Cont'd).

Trial	% Agg.	w/c	Pozz.	Procedure	Curing Time in Days	f'c	Avg. f'c	Workability	Vibration
#11	70	.50	Yes	Hum. Room air dried 1 day	7	4070		Reasonable	Rodding + Tamping.
#12	72	.75	Yes	Curing Comp. Applied	7	2290		Stiff	External vibration with hand vibrator.
	72	.75	Yes	Curing Comp. Applied	7	3110		Stiff	External vibration with large hand vibrator
	72	.75	Yes	Curing Comp. Applied	7	2800		"	"
	72	.75	Yes	Curing Comp. Applied	7	3330		"	"
#13	61	.59	Yes	Curing Comp. Applied	7	3470	3350	Excellent	Rodding + Ramping
	61	.59	Yes	Curing Comp. Applied	7	3230		Excellent	"

Graph IIIa

w/c RATIO VERSUS STRENGTH

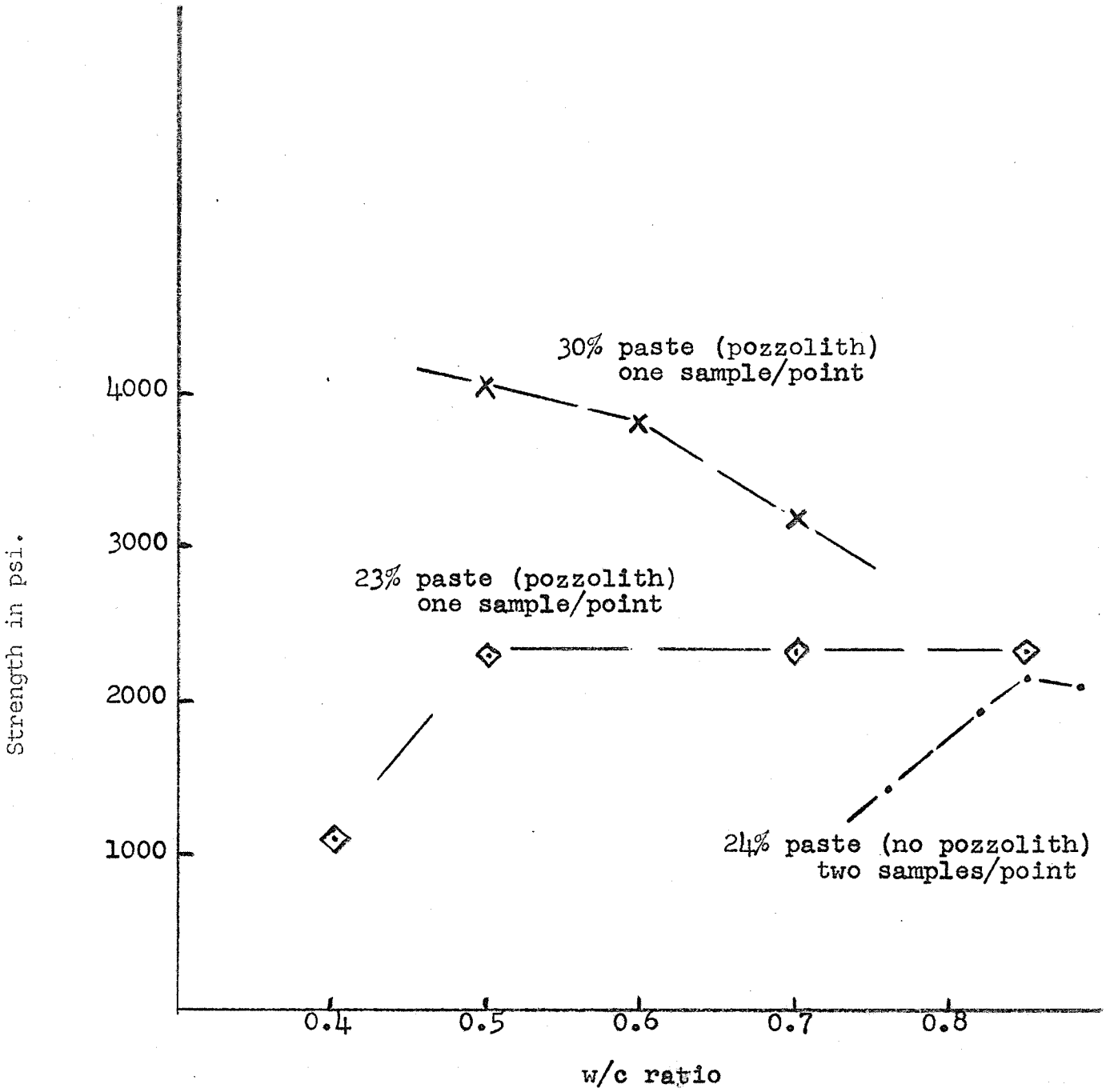

Laboratory	Imperial College London	M.I.T. U.S.A.	M.I.T. U.S.A.	I.S.M.E.S. Italy	I.S.M.E.S. Italy	I.S.M.E.S. Italy	U of Manitoba, Canada.
Water	0.3	0.65	0.80	1.25	1.50	2.50	0.70
Cement	1.00	1.00	1.00	1.00	1.00	1.00	1.00
Aggregate	sand passing 0. inch mesh sieve	concrete sand passing 0.093 inch mesh sieve	concrete sand passing 0.093 inch mess sieve	pumice stone from Lipari less than 0.275 inch	pumice stone from Latium less than 0.275 inch.	pumice stone from Latium less than 0.275 inch.	silica sand, less than 0.08 inch.
	3.00	3.50	4.50	2.22	2.77	5.29	3.96
Admixtures		Pozzolith	Pozzolith	Diatomacious Earth	Diatomacious Earth	Diatomacious Earth	Pozzolith
		0.003	0.003	0.15	0.19	0.36	.0023
				Bentonite	Bentonite	Bentonite	
				0.030	0.025	0.024	
f'_c (psi)	13,000	4,500	3,200	2,000	1,100	700	2,200

TABLE IIIe Typical Mortar Mixes (by weight) Used in Different Laboratories.

ii. Reinforcing Steel:

There were three types of model reinforcing steel used. One type for the column and shear wall reinforcing steel, one for the slab steel, and another for the lateral column ties. All three types were obtained in any hardware store of various gages. However it was found important to buy all the material of a required size at one time to ensure consistent size.

Black annealed wire, more commonly referred to as stovepipe wire, was used as the model material for the column and shear wall reinforcing steel and for the tension steel used in the test beams. The sizes used with the appropriate gage number are shown listed in Table IIIe. The prototype steel and theoretical model steel required are also listed.

TABLE IIIf

Sizes of Black Annealed Wire

Prototype	Theoretical Model	* Actual Model
#5 bar 0.625"	0.0390"	19 gage 0.0395" ± 0.0005"
#6 bar 0.750"	0.0469"	18 gage 0.0472" ± 0.0005"
#8 bar 1.000"	0.0625"	16 gage 0.0628" ± 0.0015"

*The gage referred to is the "British Imperial or English Legal Standard Wire Gage." The diameter recorded in this column is the diameter of the wire after cold working of the wire.

The original black annealed wire was tested to determine the yield point and ultimate strength. The wire used in this test was

19 gage obtained in small 8" diameter rolls. In order to free the wire from any kinks it was first loaded to 35# or about 30,000 psi (see Plate 1). The original yield strength was approximately 35,000 psi and the ultimate strength approximately 47,000 psi. Cold working of the steel was carried out for two reasons. It was necessary to have perfectly straight wire for fabrication of the column steel. Secondly, it was important to have a consistent yield strength for all the column and shear wall steel. The desired yield strength was chosen as 40,000 psi to be consistent with ACI design. The resultant ultimate strength after cold working was 55,000 psi. Table IIIf gives the mean value of a number of tests carried out to determine the yield strength of column and shear wall steel.

TABLE IIIg

Yield Strength of Column and Shear Wall Steel

Gage	Yield Strength	Mean of Each Test.
19 gage	40,750 psi	
	38,300 psi	39,420 psi
	39,200 psi	
16 gage	41,500 psi	
	40,300 psi	40,470 psi
	39,400 psi	
14 gage	40,300 psi	
	39,500 psi	39,980 psi
	40,150 psi	
14 gage	39,400 psi	
	39,400 psi	
	40,400 psi	40,500 psi
	41,000 psi	

Mean value of all tests = 40,090 psi

The reinforcing steel for the slabs (See Plate 5A) was a $\frac{1}{2}$" galvanized screen mesh of 19 gage wire. The required model steel to assimilate the prototype design was 19 gage wire at $\frac{3}{4}$" o.c. spacing for the bottom mat. The 19 gage steel spacing required over the columns varied from $\frac{3}{4}$" o.c. spacing to $\frac{1}{2}$" o.c. spacing. Therefore the use of the mesh steel, although in some cases overdesigned, was felt justified. The $\frac{1}{2}$" galvanized screen mesh was obtained in one roll three feet wide. Small sections were cut for over each column. One solid mat was cut for the bottom steel. Samples of the mesh were cut in the form of single strands and tested to determine the yield strength and ultimate strength. The ultimate failure always occured with fracture at a soldered joint. In each case ultimate failure occured before the yield point was reached, indicating the weakening effect of the soldered joint. The average of the three tests carried out gave an ultimate strength of 67,000 psi.

The lateral column ties were all fabricated from 24 gage brass wire. The diameter was 0.022" which corresponds to a #3 bar in the prototype design. The brass wire was chosen because of its ease in fabrication. The black annealed wire could not be obtained in sizes smaller than 19 gage (which corresponds to a #5 bar in the prototype design). This size was impossible to fabricate accurately into column ties. The yield strength of the brass wire was approximately 24,000 psi and its ultimate strength 58,000 psi.

Chapter IV

CONTROL OF MATERIAL PROPERTIES

It was quite evident that if adequate control of the material properties was not carried out the model to prototype relationship could not be relied upon. Therefore certain goals were attempted in keeping the properties of the different materials uniform and accurate. It was attempted to keep dimensions of columns, shear walls, and slabs to within $\pm 5\%$. That is, for columns and shear walls this would be in the range of $\pm .08$" and for slabs $\pm .02$". Similarly the properties of mortar and steel were also carefully checked and recorded. The methods of construction were arrived at with the aim of ease and rapidity of construction, accuracy of dimension, and uniformity of procedure.

i. Mortar Test Cylinders.

A number of 3" x 6" test cylinders were cast and tested (See Plate 2) with varying mixes and curing procedures before a final design and curing procedure was chosen. The main purpose of casting test cylinders for this project was to be able to predict the properties of the mortar actually placed in the model. The method of curing the mortar placed in the model would therefore have to be the same method applied to the test cylinders. After careful consideration, it was felt that application of a standard curing compound immediately after initial set of the concrete or removal of forms was best adapted to this project. Thus the top of the floor slabs were sprayed before initial set of the

mortar. All other surfaces were first sprayed with water on removal of forms and then with curing compound approximately five minutes later. The same method of curing was applied to the test cylinders. Although this may not be considered as the most ideal method for obtaining maximum strength of concrete, it was felt that this method of curing would give a material of more uniform strength. That is, since the construction period carried on from March 17th to May 22nd, approximately 2 months, the curing period varied from 78 days to 21 days. However, because of the curing procedure adopted, the average strength did not change within this time period. Graph IVa will illustrate this more clearly.

Two test cylinders for each floor and 4 test cylinders for each set of columns and shear walls were normally cast. A total of 71 test cylinders were cast and tested for control purposes. (See Table IVa). A statistical analysis gave an average strength of 2,210 psi and standard deviation of $\pm$ 367 psi or $\pm$ 16.6%. A cumulative probability curve was shown on Graph IVb. A comparison can be drawn between probability curves published by the Massachusetts Institute of Technology showing a concrete having "good" and "poor" control.* (2)

Six test cylinders were instrumented with mechanical dial gages and stress-strain curves were plotted. The stress-strain curves indicate an average value of $E_c = 3.2 \times 10^6$ psi. (See Graph IVc). The average ultimate strength of these six cylinders was 1970 psi.

* See Bibliography

Graph IVa

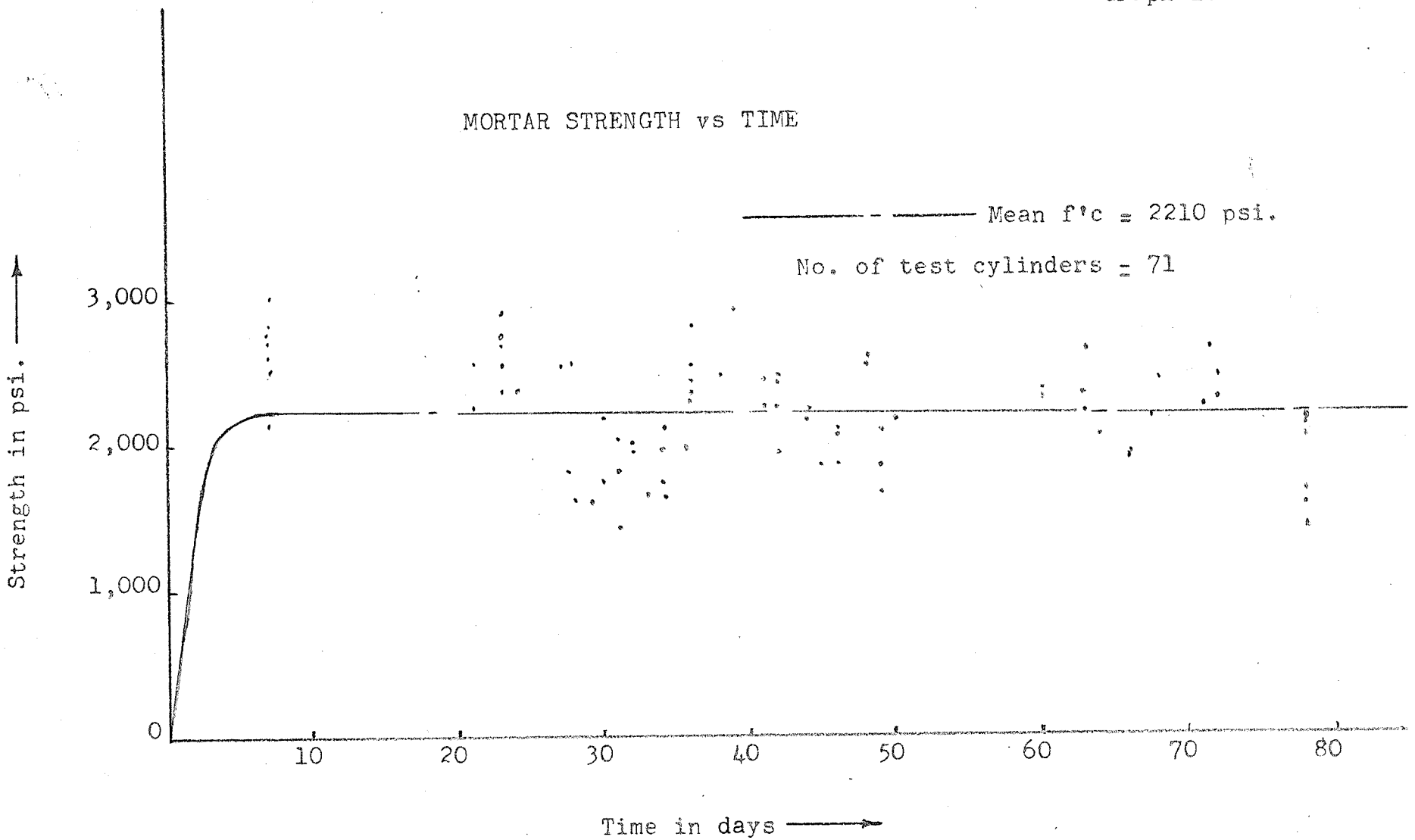
MORTAR STRENGTH vs TIME
Mean f'c = 2210 psi.
No. of test cylinders = 71
Strength in psi.
3,000
2,000
1,000
0
10
20
30
40
50
60
70
80
Time in days

Graph IVb

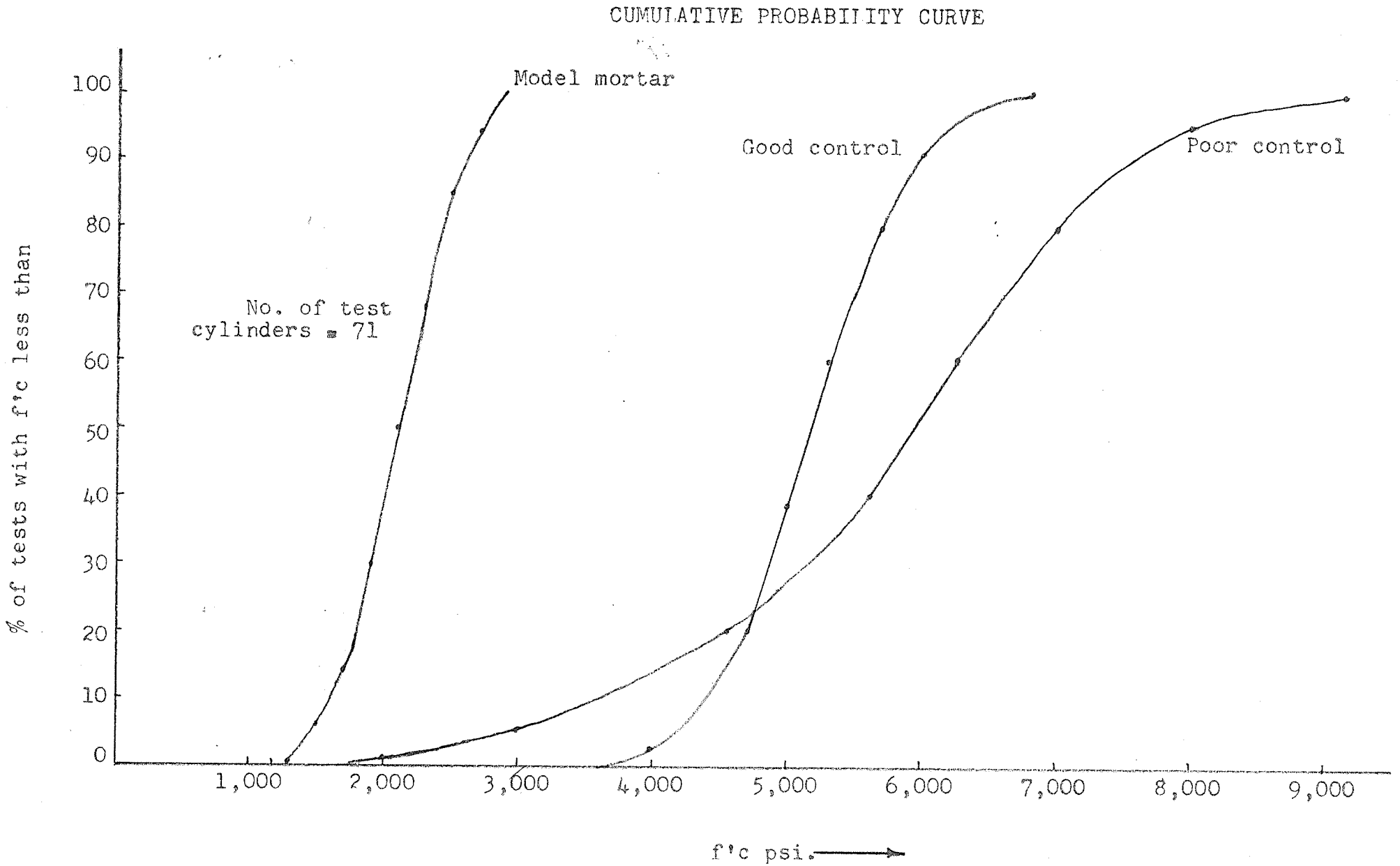
CUMULATIVE PROBABILITY CURVE
Model mortar
Good control
Poor control
No. of test cylinders = 71
% of tests with f'c less than
100
90
80
70
60
50
40
30
20
10
0
1,000
2,000
3,000
4,000
5,000
6,000
7,000
8,000
9,000
f'c psi.

Graph IVc

MORTAR STRESS vs STRAIN CURVE

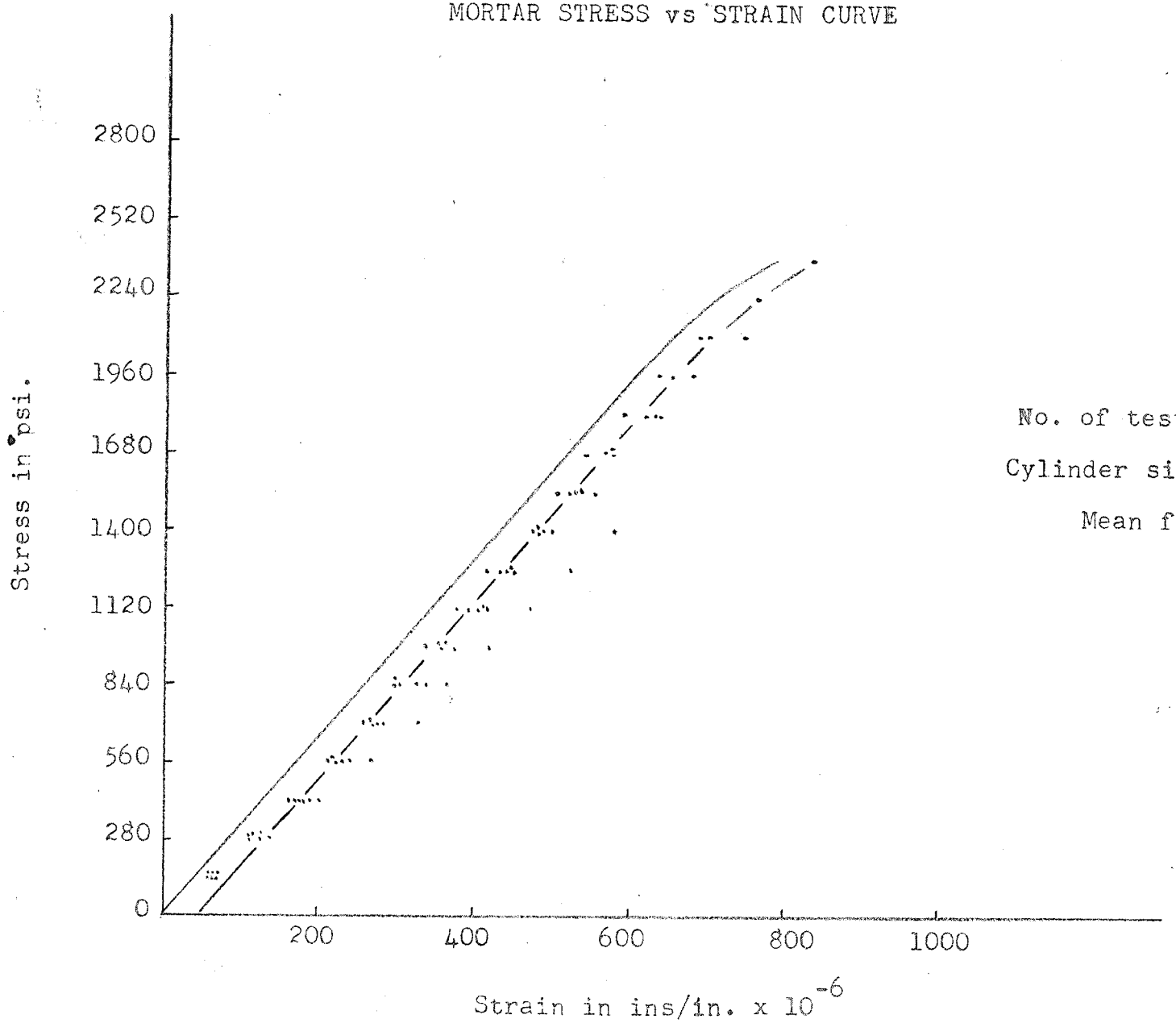

No. of tests = 6

Cylinder size = 3" x 6"

Mean f'c = 1970 psi.

E = 3.2×10^{6} psi.

TABLE IVa

Mortar Test Cylinders

Size = 3" x 6"
w/c = 0.70
% aggregate = 69 to 70%
Admixture = pozzolith

Location	Date Cast	Date Tested	Curing Time	f'c	Workability
1st floor	March 18	March 25	7 days	2575	Excellent
1st floor	March 18	March 25	7 days	3030	Excellent
Cols. 1st to 2nd	March 25	June 11	78 days	1410	Excellent
Cols. 1st to 2nd	March 25	June 11	78 days	1630	Excellent
Cols. 1st to 2nd	March 25	June 11	78 days	1570	Excellent
Cols. 1st to 2nd	March 25	June 11	78 days	2070	Excellent
Cols. 1st to 2nd	March 25	June 11	78 days	2130	Excellent
Cols. 1st to 2nd	March 26	June 11	77 days	2150	Excellent
2nd floor	April 1	June 12	72 days	2450	Stiff
2nd floor	April 1	June 12	72 days	2290	Stiff
2nd floor	April 2	June 12	71 days	2660	Excellent
2nd floor	April 2	June 12	71 days	2250	Excellent
Cols. 2nd to 3rd	April 5	June 12	68 days	2430	Excellent
Cols. 2nd to 3rd	April 5	April 28	23 days	2900	Excellent
Cols. 2nd to 3rd	April 5	April 28	23 days	2680	Excellent
Cols. 2nd to 3rd	April 5	June 11	67 days	2190	Excellent
3rd floor	April 7	June 12	66 days	1910	Excellent
3rd floor	April 7	June 12	66 days	1900	Excellent
Cols. 3rd to 4th	April 9	June 11	63 days	2660	Excellent
Cols. 3rd to 4th	April 9	June 11	63 days	2220	Excellent
Cols 3rd to 4th	April 9	June 12	64 days	2060	Excellent
Cols. 3rd to 4th	April 9	June 11	63 days	2350	Excellent
4th floor	April 13	June 12	60 days	2310	Excellent
4th floor	April 13	June 12	60 days	2350	Excellent
Cols. 4th to 5th	April 23	June 11	49 days	1650	Excellent
Cols. 4th to 5th	April 23	June 12	50 days	2180	Excellent
Cols. 4th to 5th	April 23	June 11	49 days	1860	Excellent
Cols. 4th to 5th	April 23	June 11	49 days	2100	Excellent
5th floor	April 25	June 12	48 days	2570	Excellent
5th floor	April 25	June 12	48 days	2600	Excellent
Cols. 5th to 6th	April 27	June 12	46 days	1860	Excellent
Cols. 5th to 6th	April 27	June 12	46 days	2100	Excellent
Cols. 5th to 6th	April 27	June 12	46 days	2100	Excellent
Cols. 5th to 6th	April 27	June 11	45 days	1840	Excellent
6th floor	April 29	June 12	44 days	2250	Excellent
6th floor	April 29	June 12	44 days	2170	Excellent
Cols. 6th to 7th	May 1	June 12	42 days	1940	Excellent
Cols. 6th to 7th	May 1	June 12	42 days	2240	Excellent
Cols. 6th to 7th	May 1	June 12	42 days	2470	Excellent
Cols. 6th to 7th	May 1	June 12	42 days	2440	Excellent

TABLE IVa (Cont'd)

Mortar Test Cylinders

Size = 3" x 6"
w/c = 0.70
% aggregate = 69 to 70%
Admixture = pozzolith

Location	Date Cast	Date Tested	Curing Time	f'c	Workability
7th floor	May 4	June 12	39 days	2930	Excellent
7th floor	May 4	June 11	38 days	2720	Excellent
Cols. 7th to 8th	May 6	June 11	36 days	2430	Stiffer
Cols. 7th to 8th	May 6	June 11	36 days	2820	Stiffer
Cols. 7th to 8th	May 6	June 11	36 days	2820	Stiffer
Cols. 7th to 8th	May 6	June 11	36 days	1950	Stiffer
8th floor	May 7	June 12	36 days	2290	Excellent
8th floor	May 7	June 12	36 days	2330	Excellent
Cols. 8th to 9th	May 9	June 12	34 days	2120	High slump
Cols. 8th to 9th	May 9	June 12	34 days	1735	High slump
Cols. 8th to 9th	May 9	June 12	34 days	1950	High slump
Cols. 8th to 9th	May 9	June 11	33 days	1660	High slump
9th floor	May 11	June 12	32 days	1950	Excellent
9th floor	May 11	June 12	32 days	2000	Excellent
Cols. 9th to 10th	May 12	June 12	31 days	2020	Excellent
Cols. 9th to 10th	May 12	June 12	31 days	1420	Excellent
Cols. 9th to 10th	May 12	June 12	31 days	1815	Excellent
Cols. 9th to 10th	May 12	June 11	30 days	2190	Excellent
10th floor	May 13	June 12	30 days	1735	Stiffer
10th floor	May 13	June 11	29 days	1600	Stiffer
Cols. 10th to roof	May 19	June 11	23 days	2350	Excellent
Cols. 10th to roof	May 19	June 11	23 days	2530	Excellent
Cols. 10th to roof	May 19	June 12	24 days	2750	Excellent
Cols. 10th to roof	May 19	June 12	24 days	2370	Excellent
Roof	May 22	June 12	21 days	2260	Excellent
Roof	May 22	June 12	21 days	2540	Excellent

ii. Beam Tests.

Several beam tests were carried out in order to arrive at some conclusion as to the scale effect, if any, in going from full scale to 1/16 scale. Part of the 4th year Civil Engineering course involved testing 12" x 14" x 60" concrete beams having different types of steel reinforcing. Beam #4 of this series was used as the prototype and five tests arbitrarily chosen from the past 10 years were recorded for comparison. The structural details of the prototype beam and corresponding 1/16 scale model beam are shown in Table IVb.

Preliminary beam tests were first attempted in order to arrive at an efficient and accurate method of loading and recording deflections. It was found necessary to use scaled down bearing plates for load and support points as shown in the following sketch (also see Plates 3 and 5b).

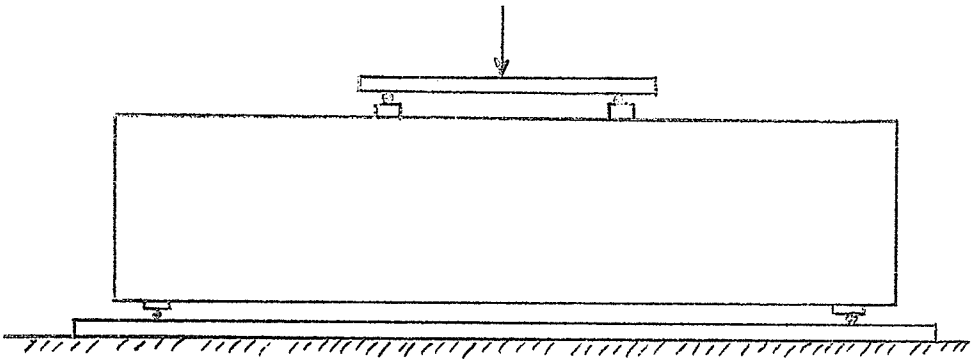

With this method of loading two test series were carried out. The first test series involved 5 model beams with physical properties as listed in Table IVb. The prototype failed due to an initial tension

TABLE IVb

Structural Properties of Prototype and Model Beams

Properties	Prototype	Model Prop. Req'd.	Actual Model Properties	
			Test Series I	Test Series II
Length	60"	3.75"	3.75"	3.75"
D	14"	.875"	.862"	.862"
d	12"	.750"	.736"	.736"
b	8"	.500"	.505"	.500"
As in tension	1.49 sq in	.0058 sq. in	(4-19 gage wires) .00700 sq. in.	(3-19 gage wires) .00525 sq. in.
Stirrups	9 - #3 bars at each end	9 - 21 gage wires at each end	21 gage brass wires at 1/8" spacing.	21 gage brass wires at 1/8" spacing
f_y	55,000 psi	55,000 psi	40,000 psi	40,000 psi
f'_c	2,876 psi	2,876 psi	2,420 psi	2,570 psi
p_u	84,600 #	330 #	332 #	395 #

TABLE IVc

Test Results of Model Beam Series 1

Load in #	Stress	Centre line deflection in inches						Strain
P	M/b d^2	1	2	3	4	5	Average	Δ/L
0	0	0	0	0	0	0	0	0
25	57	---	.0019	.0019	.0012	0	.0012	.00032
50	114	.0019	.0030	.0030	.0020	.0007	.0021	.00056
75	171	.0030	.0040	.0039	.0028	.0010	.0029	.00077
100	229	.0029	.0051	.0047	.0038	.0018	.0037	.00099
125	286	.0038	.0059	.0049	.0042	.0028	.0043	.00115
150	343	.0039	.0060	.0058	.0052	.0037	.0049	.00131
175	400	.0048	.0070	.0070	.0062	.0037	.0057	.00152
200	458	.0058	.0088	.0087	.0071	.0040	.0069	.00184
250	572	.0080	.0120	.0121	.0088	.0057	.0093	.00248
275	629	.0097	.0149	.0151	.0112	.0068	.0115	.00307
300	687	.0108	.0260	.0261	.0120	.0088	.0167	.00446
325	744	.0118			.0190	.0101		

Beam No.	Ultimate Load
1	362 #
2	310 #
3	303 #
4	347 #
5	340 #
mean	332 #

TABLE IVd

Test Results of Model Beam Series 11

Load in # P	Stress M/b d^2	Centre line deflection in inches			Strain Δ/L
		1	2	Average	
0	0	0	0	0	0
25	57	.0015	.0010	.0013	.00035
50	114	.0020	.0019	.0020	.00053
75	171	.0025		.0025	.00067
100	229	.0029	.0035	.0032	.00085
125	286	.0034	.0040	.0037	.00099
150	343	.0039	.0049	.0044	.00117
175	400	.0044	.0059	.0052	.00139
200	458	.0046	.0070	.0058	.00155
225	515	.0055	.0080	.0067	.00178
250	572	.0064	.0082	.0073	.00195
275	629	.0075	.0088	.0081	.00216
300	687	.0081	.0095	.0088	.00235
325	744	.0090	.0101	.0095	.00254
350	801	.0100	.0110	.0105	.00280
375	858	.0110	.0119	.0115	.00306

Beam No.	Ultimate Load.
# 1	397 #
# 2	393 #
mean	395 #

TABLE IVE

Test Results of Prototype Beams

Load in kips P	Stress M/b d^2	Centre line deflection in inches						Strain
		1	2	3	4	5	Average	Δ/L
0	0	0	0	0	0	0	0	0
5	43	.017	.015	.022	.010	.010	.015	.00025
10	87	.028	.028	.031	.024	.016	.025	.00042
15	130	.038	.039	.038	.032	.025	.034	.00057
20	174	.048	.051	.047	.044	.036	.045	.00075
25	217	.059	.065	.060	.055	.048	.055	.00092
30	261	.070	.079	.074	.077	.060	.072	.00120
35	304	.080	.091	.086	.083	.073	.083	.00138
40	347	.091	.095	.099	.095	.086	.093	.00155
45	390	.106	.120	.112	.105	.101	.109	.00182
50	434	.119	.135	.125	.121	.122	.122	.00203
55	477	.131	.149	.136	.134	.126	.135	.00025
60	520	.146	.162	.150	.145	.139	.148	.00247
65	563	.159	.179	.164	.160	.152	.163	.00272
70	606	.170	.195	.178	.172	.166	.176	.00294
75	649	.188	.235	.193	.201		.204	.00340
80	693	.275	.330	.208			.271	.00450
85	736	.338					.338	.00565

Beam No.	Ultimate Load	f'c
#1	85.4^k	2730 psi
#2	82.2^k	3080 psi
#3	85.8^k	2340 psi
#4	81.0^k	3440 psi
#5	88.75^k	2790 psi
mean	84.6^k	2876 psi

Graph IVd .

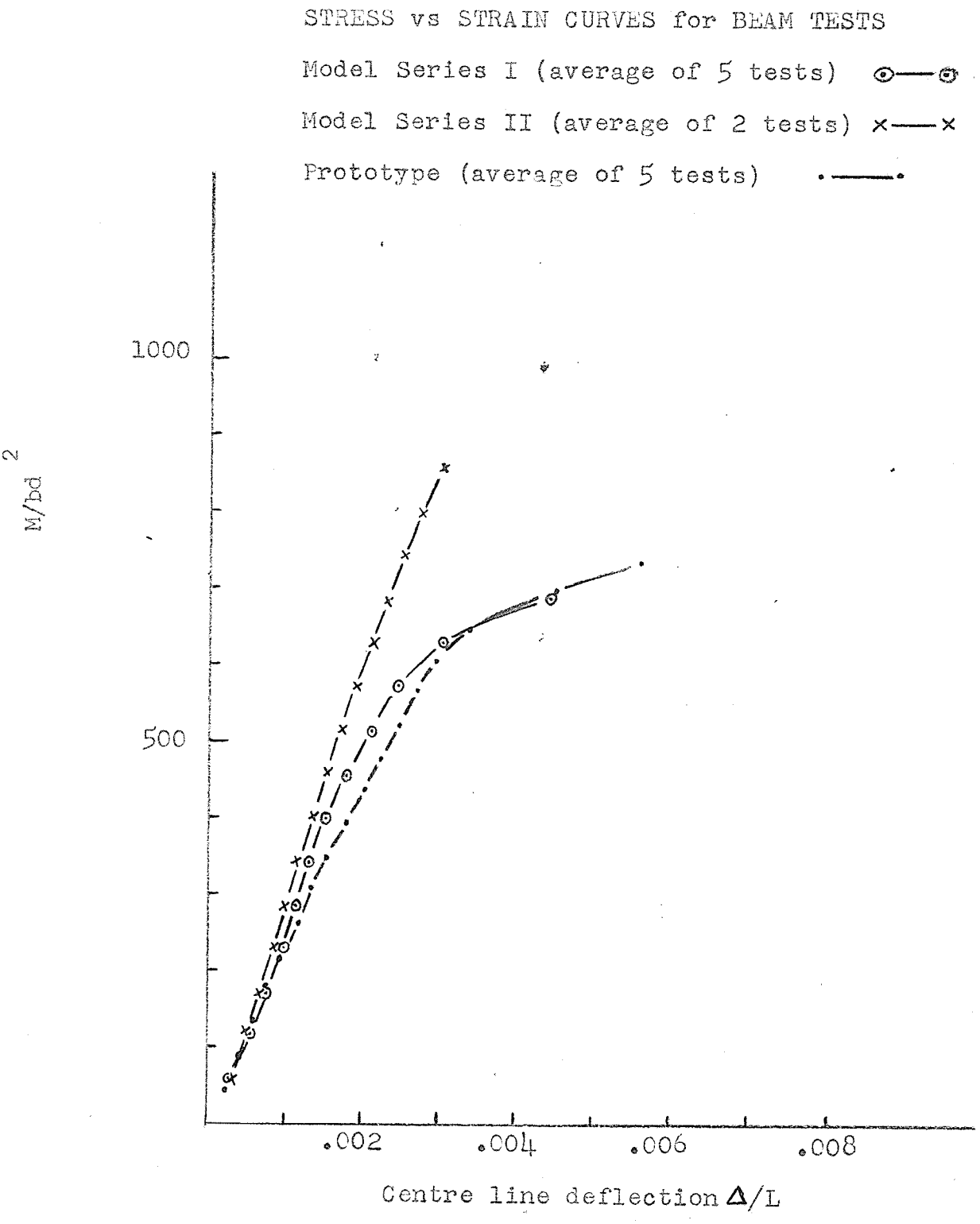
STRESS vs STRAIN CURVES for BEAM TESTS
Model Series I (average of 5 tests)
Model Series II (average of 2 tests)
Prototype (average of 5 tests)
1000
500
M/bd 2
.002
.004
.006
.008
Centre line deflection Δ/L

failure in the concrete and ultimate failure due to compression at the top centre portion of the beam. It is more than adequately designed for shear. However, the results of test series I gave all shear failures. On closer inspection it was found that the stirrups had failed in bond due to the fact that the return hook on both ends of the stirrups were cut short. Thus the bond failure in the stirrup caused diagonal tension cracks to develope. This error in fabrication was corrected in test series II. The return hook on the stirrups was manufactured according to standard specifications. The two model beams of test series II failed initially due to yielding in the steel and ultimately due to crushing in the concrete (identical failure to the prototype). The physical properties of test series II were also recorded in Table IVb.

For test series I and II centre line deflection was recorded with increase in loads. Stress vs strain was recorded in the form M/bd^2 vs Δ/L for test series I and II and for the prototype beam. Tables IVc, d and e gave the results of the individual tests and the average for each test. The average values for each of the two test series and the average value for the prototype series are illustrated in Graph IVd.

A comparison between ultimate load capacity of prototype to model to theory has been worked out for model test series II and also two preliminary beam tests which did not have a premature bond failure. The ratio of failure load to ultimate design load for these three model tests is compared to the ratio of failure load to ultimate design load for the prototype. This allows a true comparison of model to prototype as all discrepancies between the theoretical model and

actual model would be considered in this ratio.

Preliminary Model Test Beam #1

No. of beams = 1

A_s = .00500 sq. ins. b = .500"

f'c = 1960 psi d = .736"

f_y = 40,000 psi

P_u = 350#

failure = initial tension failure, ultimate compression in concrete

$$q = \frac{A_s f_y}{bd\ f'c} = \frac{.005 \times 40{,}000}{.500 \times 0.736 \times 1960} = .277$$

Ultimate Moment = $bd^2\ f'c\ q\ (1 - 0.59q)$

$= .500\ (.736)^2\ 1960\ (.277)\ (1 - .163)$

$= 123$ "#

$$P_u = \frac{123}{.625} = 197\#$$

Ratio of failure load to ultimate design load = $\frac{350}{197} = 1.78$

$$p = \frac{.00500 \times 100}{.500 \times .736} = 1.36\%$$

Preliminary Model Test Beam #2.

No. of beams = 1

A_s = .00704 sq. ins. b = .500"

f'c = 2450 psi d = .736"

f_y = 40,000 psi

P_u = 470#

failure = initial tension failure, ultimate compression in concrete.

Theoretical P_u = 272#

ratio of failure load to ultimate design load = $\frac{470}{272}$ = 1.73.

p = 1.92%

Model Test Series II:

No. of beams = 2

A_s = .00525 sq. ins. b = .500"

f'c = 2570 psi d = .736"

f_y = 40,000 psi

P_u = 395#

failure = initial tension failure, ultimate compression in concrete.

Theoretical P_u = 216#

ratio of failure load to ultimate design load = $\frac{395}{216}$ = 1.83.

$p = \frac{.00525 \times 100}{.500 \times .736} = 1.43\%$.

Prototype.

No. of beams = 5

A_s = 1.49 sq. ins. b = 8"

f'c = 2476 psi d = 12"

f_y = 55,000 psi

P_u = 84,600#

failure = initial tension failure, ultimate compression in the concrete.

Theoretical P_u = 81,000#

ratio of failure load to ultimate design load = $\frac{84,600}{81,000}$ = 1.04.

p = 1.55%

THE UNIVERSITY LIBRARY OF MANITOBA

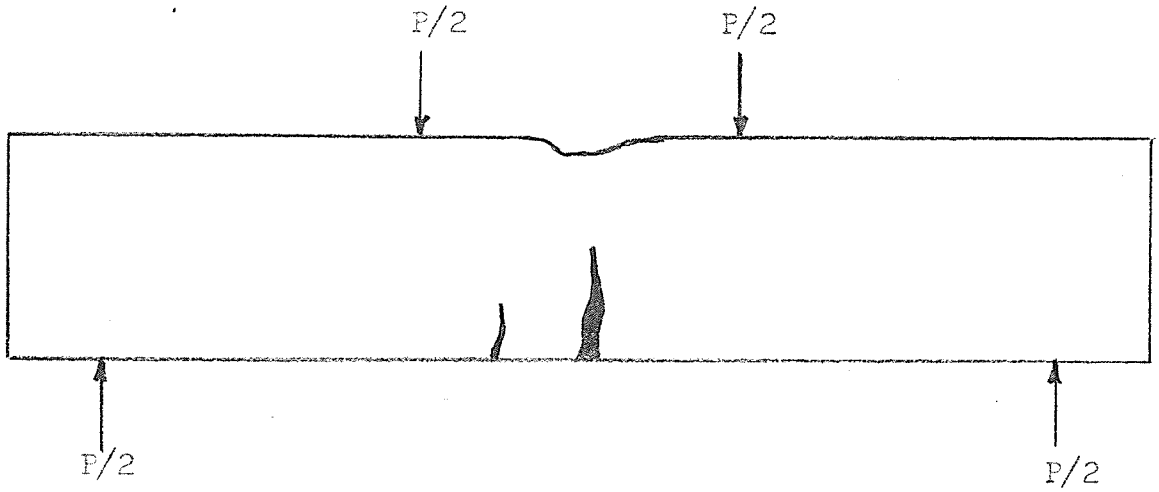

Typical crack distribution on failure of model beams

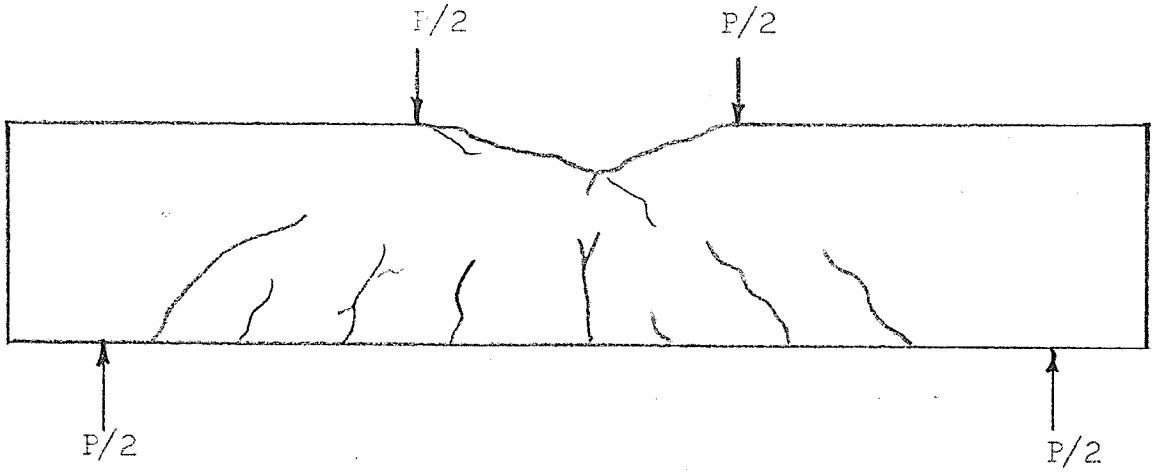

Typical crack distribution on failure of prototype beams

Figure 6:

The average of the three ratios for the model beams was 1.78 ± 0.05. The ratio for the prototype was 1.04. That is, the prototype compared within 4% of ultimate theory and the model beams had a capacity 78% higher than ultimate theory would predict. There was therefore an increase in flexural strength of 74% due to "scale effects".

There was also a pronounced difference in the crack distribution on failure. This was illustrated in figure 6 which showed the model and prototype beams after failure. In the prototype (see Plate 5c) the tension cracks were distributed throughout the beam in the form of numerous small cracks. However, in the model all beam failures developed one and at most two large tension cracks and no further crack distribution.

iii. Column Tests.

Model mortar columns were designed and tested with the purpose of establishing a relationship between full scale and 1/16 scale columns. In this case there was no prototype to relate back to. A comparison has been worked out between model results and theoretical design methods.

One type of column was tested. It has a similar design to the upper lifts (columns 8th floor to roof). Eleven tests were carried our for this design. All model columns are in the short column category. Six columns of column test series 1 were tested to failure using the 30,000 pound Baldwin testing machine (see Plate 4). Deflection readings were taken and one SR4 gage was placed on each column. However, the method of testing proved not too satisfatory

as the columns appeared to fail prematurely due to unsymmetrical loading and bond failure of the column steel in the upper or lower portions of the column. Thus most of the columns failed by a corner shearing off with little or no load being transferred to the steel. For the results of column test series 1 see Table IV G. These errors in testing were corrected in column test series 2. Five columns of the previous test series were cut shorter using a diamond saw from the Geology Department. Thus the length was cut from 7" to approximately $4\frac{1}{2}$". As the 7" column was within the short column category an increase in strength should not be expected due to the shorter column. This time, however, the surfaces of the columns were ground smooth top and bottom and the concrete was flush with the steel. No sulfur cap or spherical head were used. The testing procedure appeared satisfactory and typical column failures occurred. For the results of this column series and a comparison with a theoretical analysis see Table IV h.

The properties of the mortar model columns are given as follows for the different series:

Column test series 1:

$f'c = 2420$ psi

size of columns = $\frac{3}{4}$" x $\frac{3}{4}$" x 7"

Ag = 0.58 $\pm$ .01 sq. ins.

fy = 40,000 psi

As = 0.0124 sq. ins. (4-16 gages wires)

no. of cols. tested = 6

average ultimate load = 1123#

ties = 2k gage brass wire ties @ $\frac{3}{4}$" spacing.

$p_g = 2.1\%$

Column test series 2.

$f'c = 2420$ psi

size of columns = $\frac{3}{4}$" x $\frac{3}{4}$" x $4\frac{1}{2}$"

$Ag = 0.58 \pm 0.01$ sq. ins.

$fy = 40{,}000$ psi

$As = 0.0124$ sq. ins. (4 - 16 gage wires)

no. of cols. tested = 5

average ultimate load = 1270#

ties = 21 gage brass wire ties @ $\frac{3}{4}$" spacing.

$p_g = 2.1\%$

In column test series 2 the theoretical strain readings were arrived at by the following simple derivation:

$$P_t = P_c + P_s$$

$$= S_c A_c + S_s A_s$$

$$= \epsilon (E_c A_c + E_s A_s)$$

$$\epsilon = P_t / E_c A_c + E_s A_s$$

where E_c = modulus of elasticity of concrete = 3.2×10^6 psi

$A_c = 0.58 - .01 = 0.57$ sq. ins.

E_s = modulus of elasticity of steel = 30×10^6 psi

$A_s = 0.0124$ sq. ins.

P_t = total load applied to the column.

There seemed to be little correlation between the three different sets of values for strain. The theoretical values were lowest, the SR4 strain readings came next by a factor of approximately 1.7, and the dial gage readings were highest by a factor of approximately 4.5. Further testing would be necessary to give adequate

TABLE IV

Column Test Series 1

	Strain Readings in Micro inches/inch											
	Col. #1		Col. #2		Col. #3		Col. #4		Col. #5		Col. #6	
Load	Dial	SR4	Dial	SR4	Dial	SR4	Dial	SR4	Dial	SR4	Dial	SR4
0	0	0	0	0	0	0	0	0	0	0	0	0
200	1300	0	1575	156	440	15	340	203	585	67	345	230
400	2450	0	1770	277	770	45	585	380	1160	170	615	385
600	3430	155	2140	381	1330	95	1010	520	1430	240	885	510
800	4600		2460	490	2000	185	1730	700	1630	350	1160	530
1000	6720	540	3030	635			2600	287	2030	490	1310	750
1200											1590	866
1400											1740	983

Column No.	Ultimate Load
#1	1120#
#2	985#
#3	830#
#4	1065#
#5	1175#
#6	1560#
Average	1123#

TABLE IVg

Column Test Series 11

	Strain Readings in Micro inches/inch										
	Col. #1		Col. #2		Col. #3		Col. #4		Col. #5		
Load	Dial	SR4	Dial	SR4	Dial	SR4	Dial	SR4	Dial	SR4	Design
0	0	0	0	0	0	0	0	0	0	0	0
200	267	180	432	318	265	275	238	23	650	234	91
400	444	316	886	448	707	487	475	53	1088	424	182
600	511	453	1340	571	1100	670	1535	165	1390	621	273
800	733	593	1990	640	2210	744	1970	273	1960	769	364
1000	975	730	2590	693		772	2250	405		824	455
1200	1380	840	3110	785			2680	560	5070	824	546
1400			3760	900							

Column No.	Ultimate Load
#1	1303#
#2	1430#
#3	1000#
#4	1325#
#5	1285#
Average	1270#

reasons for the variation.

However, the ultimate failures was typical of lateral tied reinforced concrete columns. All failures occured due to buckling of vertical steel between the lateral ties. Also the ultimate failure checked reasonably close to ultimate theory.

The average of the results of test series 2 was 1270# $\pm$20% (see Table IV h). By ultimate design theory the column capacity was:

$$P_u = \phi (0.85 f'c (A_g - A_s) + A_s f_y)$$

where $\phi = 0.70$, a reduction factor for unavoidable eccentricity,

$$P_u = 0.70 (0.85 (2420)(0.580 - 0.012) + 0.0124 \times 40{,}000)$$

$$= 1165\#$$

Thus the test results were approximately 10% higher than theoretical results.

iv. Slab Tests

Four slab tests were carried out in order to give an indication of the increase in strength with the use of 19 gage wire mesh. All slabs were loaded at the third points as two-way slabs although reinforcing steel was placed running in both directions. Two slabs were reinforced with black annealed wire on a $\frac{3}{4}$" grid and two slabs were reinforced with the $\frac{1}{2}$" wire mesh. (See Plate 5a) However the same size of slab and area of reinforcing steel (in the direction of maximum stress) were used in all 4 slabs. The structural properties of these slabs are listed as follows:

TABLE IVh

Structural Properties of Test Slabs

Properties	Test 1	Test 11
No. of samples	2	2
Size	.513" x 1.99" x 5.00"	.523" x 2.02" x 5.00"
Type of steel	black annealed wire	½" 19 gage wire mesh
d	.414"	.424"
b	1.99"	2.02"
As in tension	.00375 sq. ins.	.00379 sq. ins.
f_y	40,000 psi	67,000 psi
f'_c	1960 psi	2450 psi
P_{u_1}	95#	184#
P_{u_2}	95#	191#
P_u	95#	188#
p	.45%	.44%

Reinforcing steel for test 1 consisted of 3-19 gage black annealed wires running in the longitudinal direction and 7 in the transverse direction. All wire was cold worked to 40,000 psi yield. The ultimate design of these two slabs was as follows:

Test 1:

$$q = \frac{A_s f_y}{bd f'_c} = \frac{.00375 \times 40,000}{1.99 \times .414 \times 1960} = .093$$

$$\text{ultimate moment} = bd^2 f'_c q (1 - 0.59 q)$$

$$= 1.99\ (.414)^2\ 1960\ (.093)\ (1-.055)$$

$$= 58.8"\#$$

$$P_u = \frac{58.8}{.833} = 70.4\#$$

ratio of failure load to ultimate load $= \frac{95}{70.4} = 1.35$

Reinforcing steel for test 11 consisted of the $\frac{1}{2}$" wire mesh. Three wires were running in the longitudinal direction and eleven in the transverse direction. The ultimate design of these two slabs was as follows:

Test 11:

$$q = \frac{.00379 \times 67{,}000}{2.02 \times .424 \times 2450} = .121$$

$$\text{ultimate moment} = 2.02\ (.424)^2\ 2450\ (.121)\ (1-.0713)$$

$$= 100"\#$$

$$P_u = \frac{100}{.833} = 120\#$$

ratio of failure load to ultimate load $= \frac{188}{120} = 1.57$

The elastic behaviour of the slabs should be identical but the ultimate load in flexure of the slab reinforced with wire mesh was almost twice that of the slab reinforced with the same area of black annealed wire at 40,000 psi yield. The main reason for the increase in the slab reinforced with wire mesh was the high yield stress (67,000 psi). The fact that a greater area of steel was actually used in the model (mesh is at $\frac{1}{2}$" spacing while design calls for $\frac{3}{4}$" spacing) will also increase the capacity of the

existing model slabs. Thus the model building slabs would fail at $188 \times \frac{.75}{.50} / 70.4$ or 4.00 times the predicted design. The ratio of failure load to ultimate design load for the slab reinforced with black annealed wire and the slab reinforced with wire mesh was 1.35 and 1.57 respectively. Thus there was an increase in flexural strength of the 1/16 scale slabs over ultimate design theory of 35 to 57%. The % of steel in these slabs was less than $\frac{1}{2}$%.

The crack patterns again were outstanding in that there was no crack distribution. All four slabs failed due to the development of one and at most two tension cracks.

v. Discussion on Adequacy of Model Similarity.

The previous tests in Chapter IV were all performed to determine the accuracy of a reinforced concrete model of 1 to 16 scale in predicting prototype behaviour. There were two main questions which had to be answered. The first was whether the model could be built accurately in dimension and the structural properties of all its members accurately controlled. The second was whether there were unexplainable "scale effects" occuring in this scale range and if so what were they and what effect did they have on the ultimate capacity and elastic range of the model.

The first question appeared to be answered. The control on the concrete poured and reinforcing steel placed was adequate. All reinforcing steel in the model (except for the floor slab steel) was maintained at 40,000 psi yield and well within $\pm$5%. The floor slab steel, when the increase in yield strength, grid spacing and "scale effects" were considered, was overdesigned by a factor slightly larger

than four. However, this was not considered serious as the elastic behaviour of the slabs should not be altered. The physical dimensions of the slabs remained within 5% and the small % of reinforcing steel (less than 1/2) would not affect the flexural rigidity of the slab. The ultimate strength of the concrete was determined from an adequate number of concrete test cylinders and found to have a standard deviation from the mean steength of 16.6%. This was believed well within normal control expectations as illustrated by Graph IVb.

The answer to the second question with respect to "scale effects" was more difficult to analyse. There was a definite increase in strength in the model beams as compared to the prototype beams. This increase was again evident in model slab tests. Both of these tests (model beams and slabs) were strictly flexural failures. The increase in strength of model to prototype varied from 35% to 74%. It was exceptionally consistent for the three different model beam tests being an increase of 74% ($\pm$5%). The distribution of tension cracks in the model beams and slabs varied considerably from the pattern developed in the prototype beams. (see Figure 6 and plate 5c) The 1/16 scale model beams developed one or two large cracks while the prototype had a distribution of numerous fine cracks. Within the elastic range the model beams compared quite favourably to the prototype. The model, however, appeared to be slightly stiffer than the prototype. This could be explained by the early development of fine cracks in the prototype and the resulting deviation from the load deflection curve of the model (see Graph IVd).

The inability of small scale models of reinforced concrete to distribute concrete cracking throughout the length of the member

had been evident for some time. In a series of tests carried out by Massachusetts Institute of Technology in conjunction with the Universidad Central in Caracas, Venesuala on model beams*(2) it was found that an increase in flexural strength was evident with increase in scale factor. Also, this increase in strength was related directly to the % of reinforcing steel used. If large percentages of steel were used (in the order of 4%) there were significant increases in strength for small scale models. As the percentage of steel decreased the increase in strength was not as pronounced. The percent of reinforcing steel in the model slabs was less than ½% and the increase in strength varied from 35% to 57%. The percent of reinforcing steel in the model beams was 1.6% and the increase in strength was consistent at 74%. This would appear to be comparable with the experiments stated above. These tests deal only with flexural behaviour. The model columns tested in Section iii of Chapter IV indicated an increase in strength over ultimate design theory of 10%. Thus in straight compression there appeared to be a less significant increase in strength due to "scale effects".

It would be reasonable to expect excellent comparison of the 1/16 scale model with full scale results within the elastic range. However, at ultimate failure there would be a pronounced increase in capacity of the 1/16 scale model (depending on the percent of reinforcing steel) in the order of 75% for flexural failures. Bond failures were not analysed extensively but from experience in testing and printed literature bond defects could be a problem. The expected

* See Bibliography.

increase in strength for compression failures would be in the order of 10%. These figures of increase of strength due to "scale effects" would be used as a guide only as not enough testing had been carried out in each case to justify an exact statement.

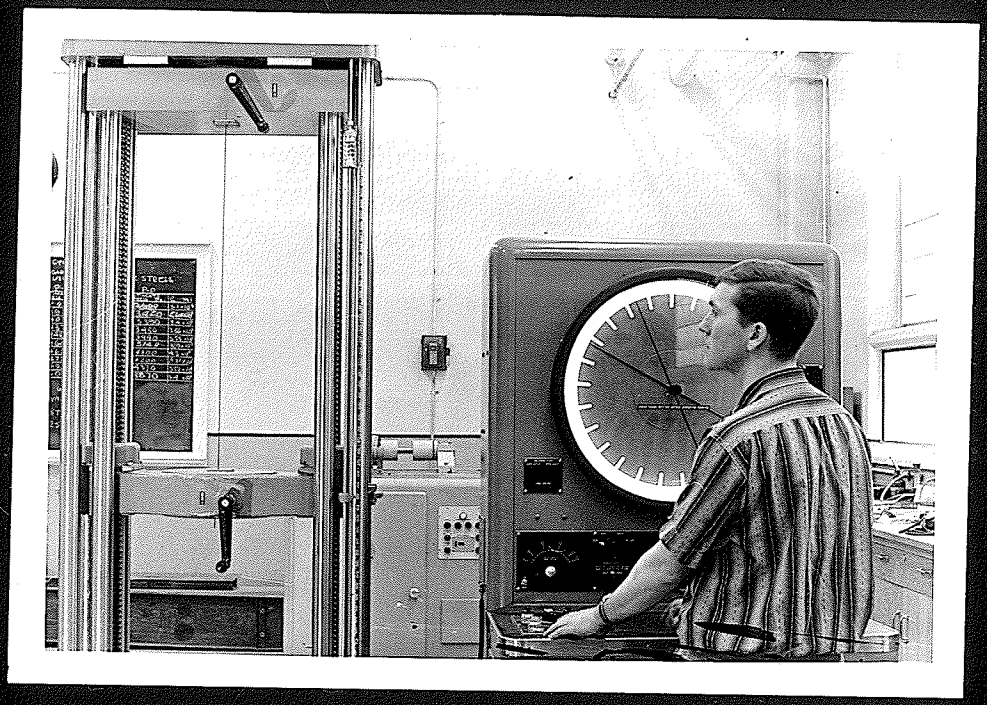

Plate 1. Use of 30,000# testing machine for cold - working of reinforcing steel

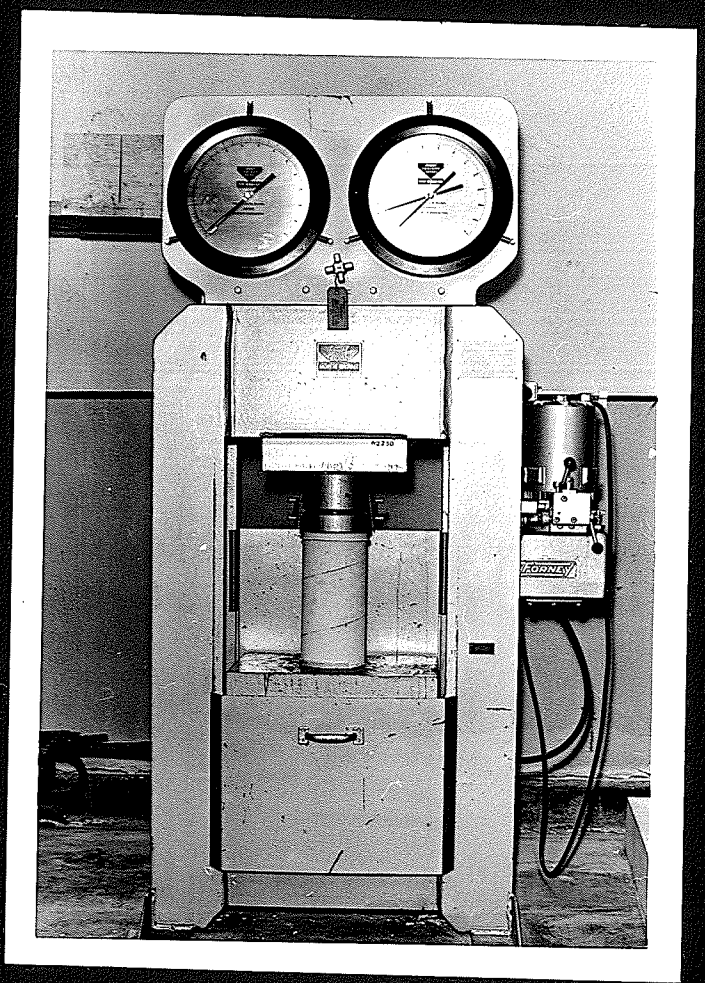

Plate 2. Testing of model concrete cylinders in 300,000# testing machine

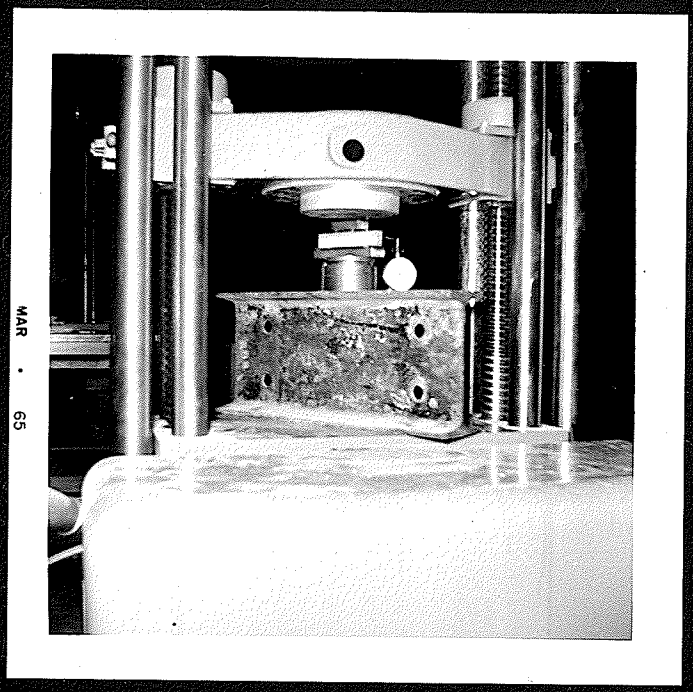

Plate 3. Testing of model beams in 30,000# testing machine

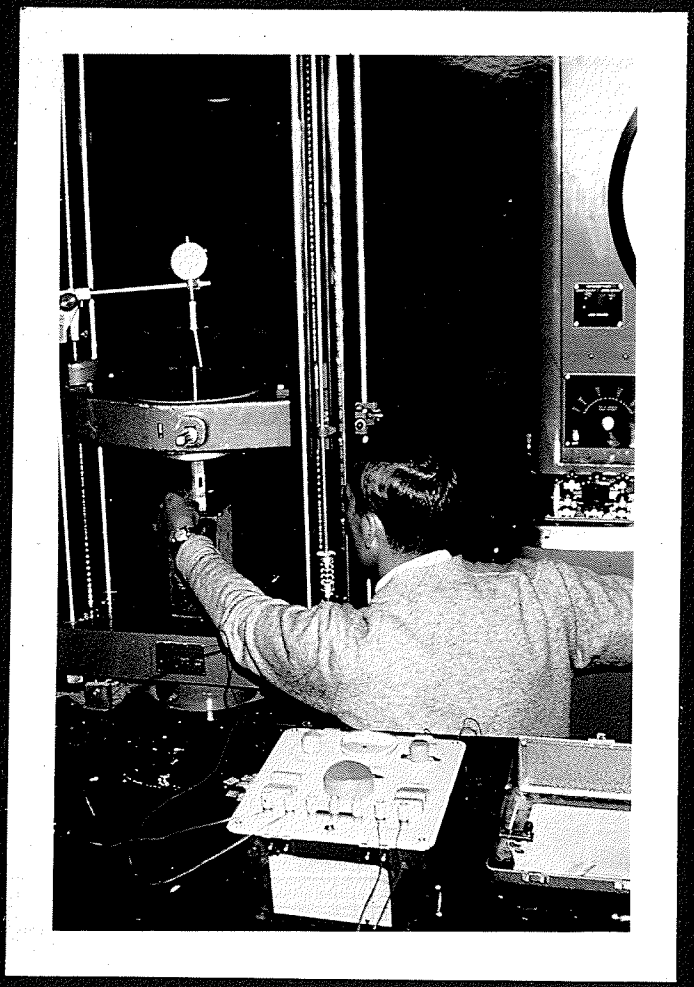

Plate 4. Testing of model columns in 30,000# testing machine

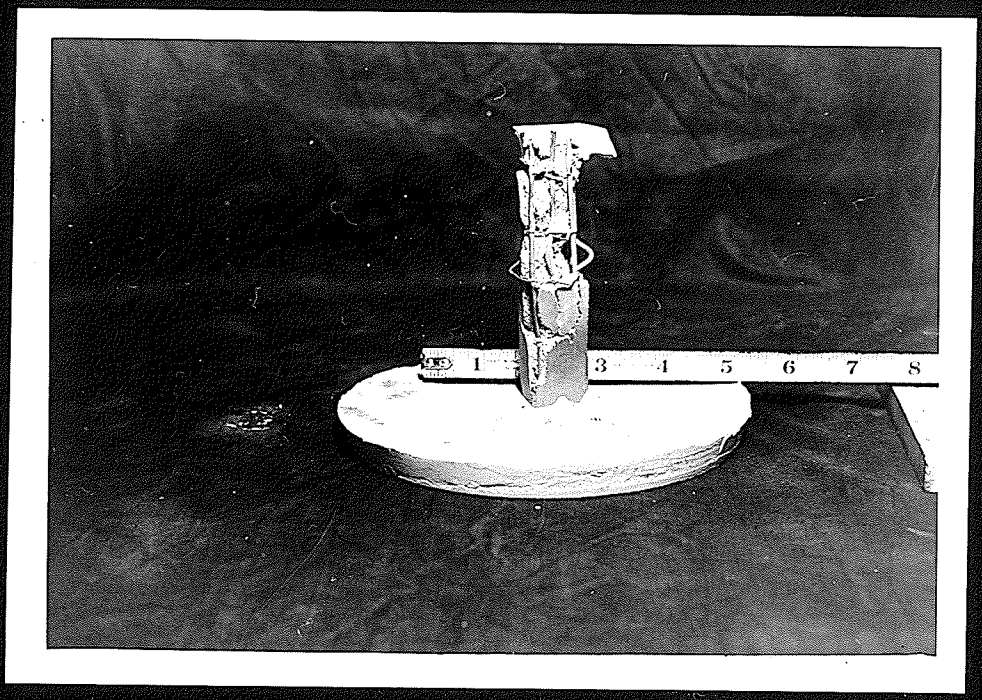

Plate 5. Model column test specimen after failure

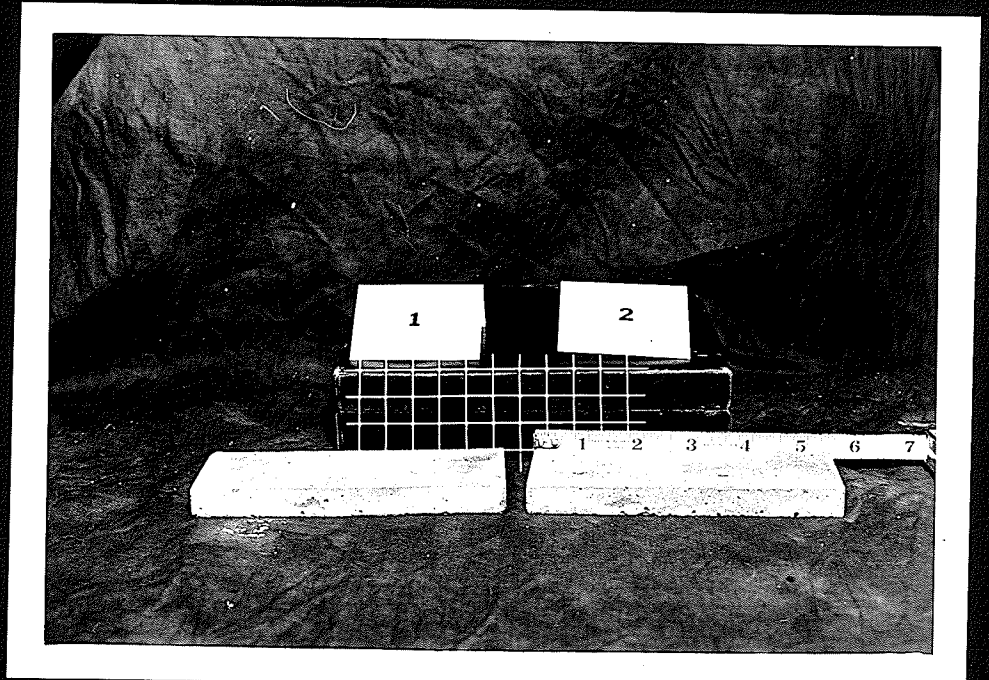

Plate 5a. Model slabs

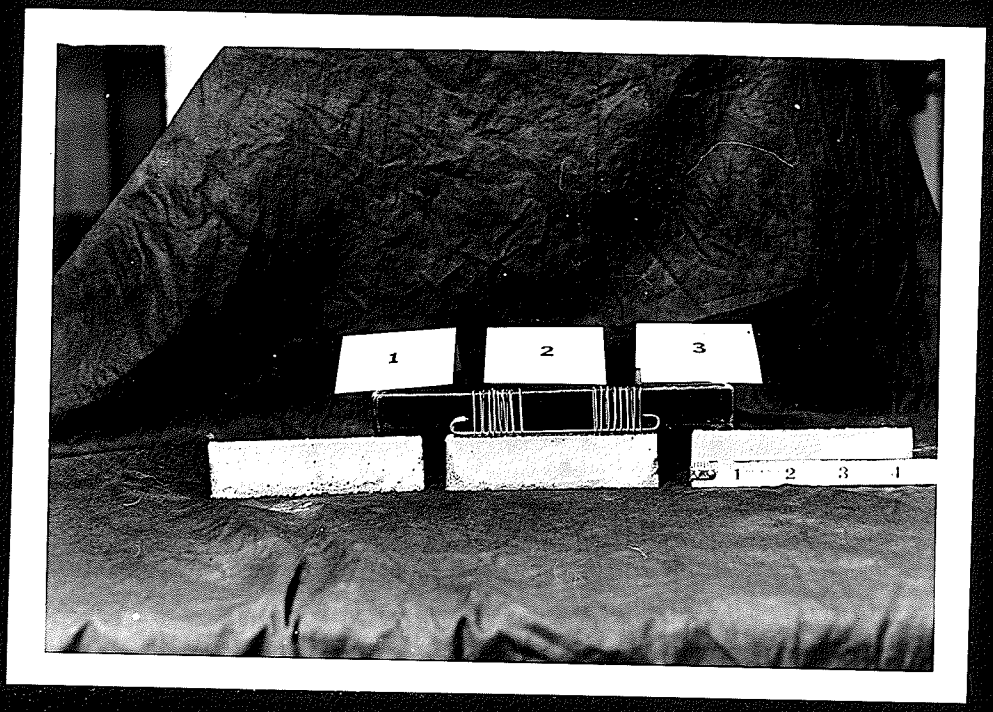

Plate 5b. Model beams

Plate 5c. Crack distribution of prototype beams

Chapter V

METHODS OF CONSTRUCTION

i. Placing and Fabrication of Column and Shear Wall Steel.

All steel was placed according to the American Concrete Institute Building Code, 1956 edition. The lateral ties for column and shear wall steel were soldered in position with the use of All-State Paste Solder (see Plate 12 and 13). Before the solder would adhere to the metal the protective coat of paint on the wire had to be removed. This was carried out by dipping the wire, after cold working, in a 1 to 4 hydrochloric acid bath for approximately five minutes. This removed the paint giving a clear surface for proper soldering. The wall steel for the shear walls was soldered together in the form of a vertical mat. All column steel and shear wall steel was fabricated in three lengths. The first fabrication was continuous for the first three stories, the second fabrication for the next four stories, and the third fabrication for the top three stories. Dowels were placed at the fourth and eighth floor levels for adequate bond. The first fabrication of column and shear wall steel is shown in place in Plate 7. To determine the effect of the acid bath and heat due to soldering on the yield point the wire was tested after cold working, after the acid bath and then after soldering. The results of these tests indicated a negligible change in the yield strength.

ii. Placing of Slab Steel.

The slab steel consisted of the $\frac{1}{2}$" galvanized screen mesh

as described in Chapter III. It was necessary to place two layers of steel in a slab having a total depth of $6\frac{1}{2}/16$ inches. Small pieces of the 19 gage wire mesh were placed under the mat to assure the proper cover of concrete on the bottom steel. Small staples were then used to hold the bottom mat down on top of these spacers. The staple was driven into the slab forms and small pieces of balsa wood wedged between the staple and the bottom steel. Plate 8 shows the bottom steel for one floor in place and being poured. The top steel was placed immediately after the slab was poured and trowelled. Small mats were placed over each column and shear wall according to the empirical design procedure set out in the American Concrete Institute code. Figure 7 shows the placing of the top steel for all slabs.

iii. Fabrication of Forms.

The slab forms were made from square foot panels of $\frac{3}{4}$" plywood with a 1/8" birch cover. The 1/8" birch sheet was glued to the plywood in order to give a smooth finish. The proper notches were cut from each corner of the panel to allow the column and shear wall forms to be placed in their correct positions. The 12 separate panels were then assembled together. A set of three panels were assembled with two 1" x 3" laths and wood screws. Then the four sets of three were assembled by nailing them to two rigid wooden supports approximately $5\frac{1}{2}$ feet long running parallel to the longitudinal direction of the building. The entire assembly was then supported as shown in plates 15 to 27. The proper depth of slab was maintained by using steel dexion angle iron as the edge forms. These were fastened

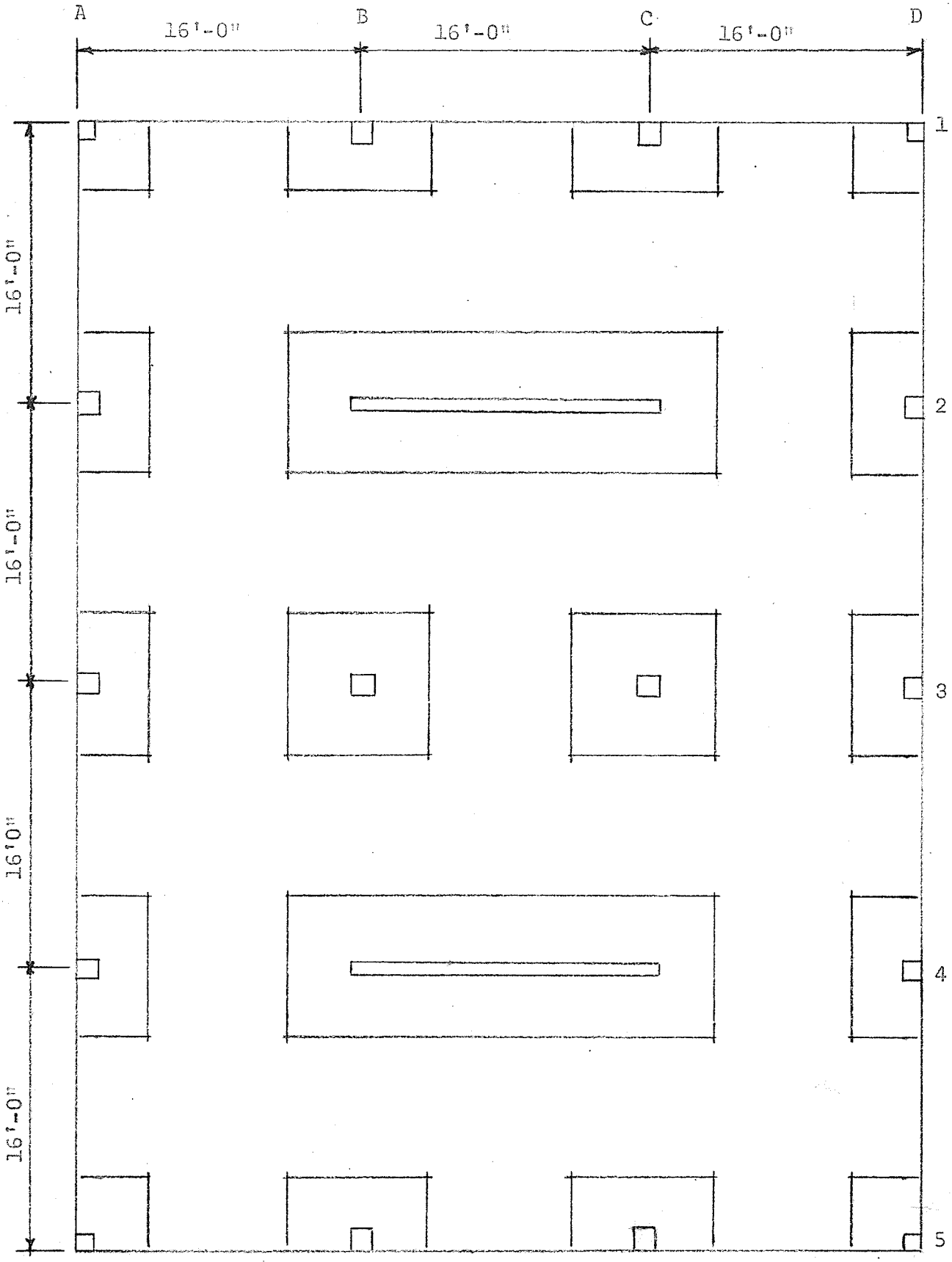

Location of Top Steel Reinforcing Mats

Figure 7.

with screws to the wooden panels. Twenty-four hours after each slab was poured the forms were removed. The same panel forms were reassembled for each of the ten slabs poured.

The column and shear wall forms were all fabricated from plexiglass. They were machined to within 5/1,000" accuracy. Plexiglass was used for several reasons. Since the column and shear walls contained steel in such a confined space it was important to be assured that there were no voids within the forms when the concrete was placed. Since the plexiglass is transparent it made it possible to locate all large air bubbles and vibrate the forms in the proper location to remove them. Also, plexiglass is easily machined and accuracy of dimension was easily maintained. The smooth surface of the plexiglass allows for better flow of the concrete than would be possible with wood forms. Plate 13 shows several of the column forms stacked and one assembled. The column forms were reused for the entire building. (See plates 9, 10, and 11 for method of forming columns). The shear wall forms were replaced with new ones after the fifth storey.

iv. Construction Procedure.

Table V gives the construction timetable from beginning to end of construction. Plate 7 illustrates how the grid system for the first lift of columns was originally set out. The position of the columns was marked out on the concrete base and a lath grid supported approximately two feet above the base. The column and shear wall steel all had a one inch 90° bend in the steel at the base. This was to ensure proper anchorage in the $1\frac{1}{2}$" first floor slab. The top of

the column steel was then anchored to the lath grid in the proper position. The first floor slab was then poured. The column forms were then placed and the floor panel assembly dropped over the column steel and anchored in place with the use of the corner supports. The columns were then poured and twenty-four hours later the slab. The slab was allowed twenty-four hours to cure and then the slab forms removed. The process was repeated in the same sequence until completion. Vibration of the concrete for placing was carried out with the use of a $\frac{1}{4}$" electric drill.

TABLE Va

Construction Timetable

Date	Development	Plate
March 17	Re-bar complete to fourth floor.	7 & 14
March 18	First floor poured.	7
March 25	First to second floor walls poured and columns 2A, 5A, 5B, 5C.	15
March 26	Rest of columns first to second were poured.	15
April 1	One half of second floor poured.	16
April 2	Second floor completed.	17
April 5	Second to third columns completed.	18
April 7	Third floor poured.	19
April 9	Third to fourth columns poured.	--
April 13	Fourth floor poured.	20
April 23	Fourth to fifth columns poured.	21
April 25	Fifth floor poured.	--
April 27	Fifth to sixth columns poured.	22
April 29	Sixth floor poured.	23
May 1	Sixth to seventh columns poured.	--
May 4	Seventh floor poured.	--
May 6	Seventh to eighth columns poured.	--
May 7	Eighth floor poured.	24
May 9	Eighth to ninth columns poured.	---
May 11	Ninth floor poured.	25
May 12	Ninth to tenth columns poured.	--
May 13	Tenth floor poured.	--
May 19	Tenth to roof columns poured.	26
May 22	Roof slab poured.	27

Chapter VI

INSTRUMENTATION AND LOADING PROCEDURES

All readings of direct lateral deflection and local concrete strains were obtained with the use of mechanical dial indicators and SR-4 strain gages. The design of a loading apparatus was required to apply a uniform lateral load to assimulate wind loading.

i. SR-4 Gages.

All wire SR-4 gages were of $\frac{1}{2}$ inch gage length, type A-5, resistance 120 ohms, gage factor 2.01, and manufactured by the Baldwin-Lima-Hamilton Corporation. The SR-4 gages were placed as shown on Figure 8. The gages were positioned on the third floor slab for the purpose of obtaining the point of inflection between the shear wall and exterior columns. Location of the points of inflection were required for a theoretical frame analysis of the building. Gage numbers 9 to 18 were positioned to determine the behaviour of the slab to column joint. From these readings a deflected shape for the exterior column in the plane of the shear wall and column to slab connection could be determined. The range of the readings were from 2 or 3 microinches to 100 microinches. For recording readings the manual SR-4 Strain Indicator Type N manufactured by Baldwin-Lima-Hamilton Corporation was used.

ii. Mechanical Dial Gages.

Mechanical dial indicators were used to obtain lateral deflections at each floor level. They were attached to a rigid

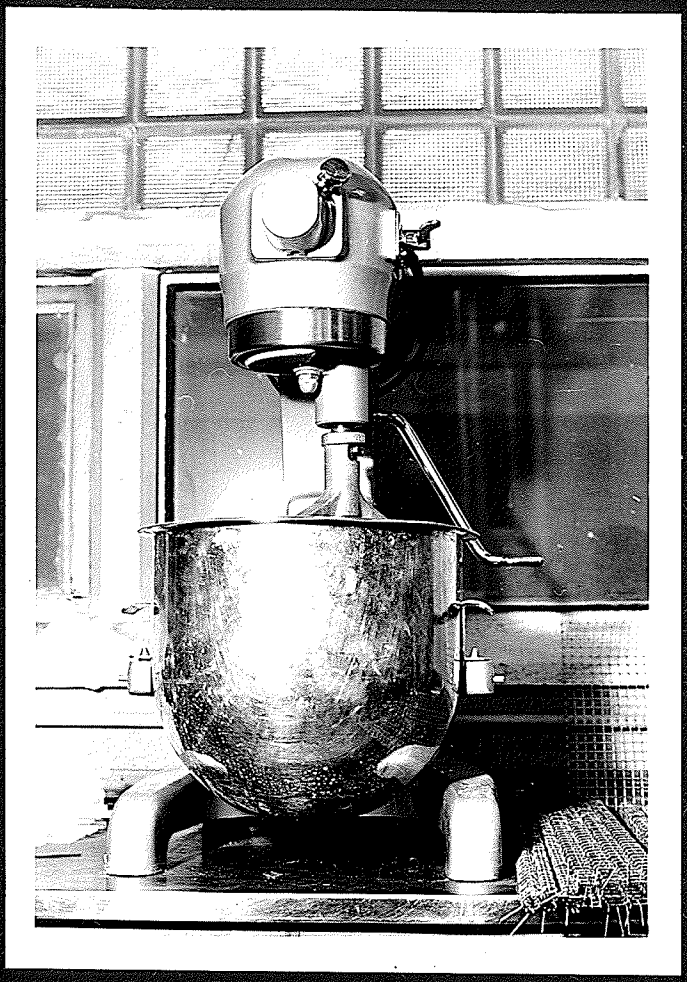

Plate 6. Mortar mixer (capacity 3/4 cubic foot)

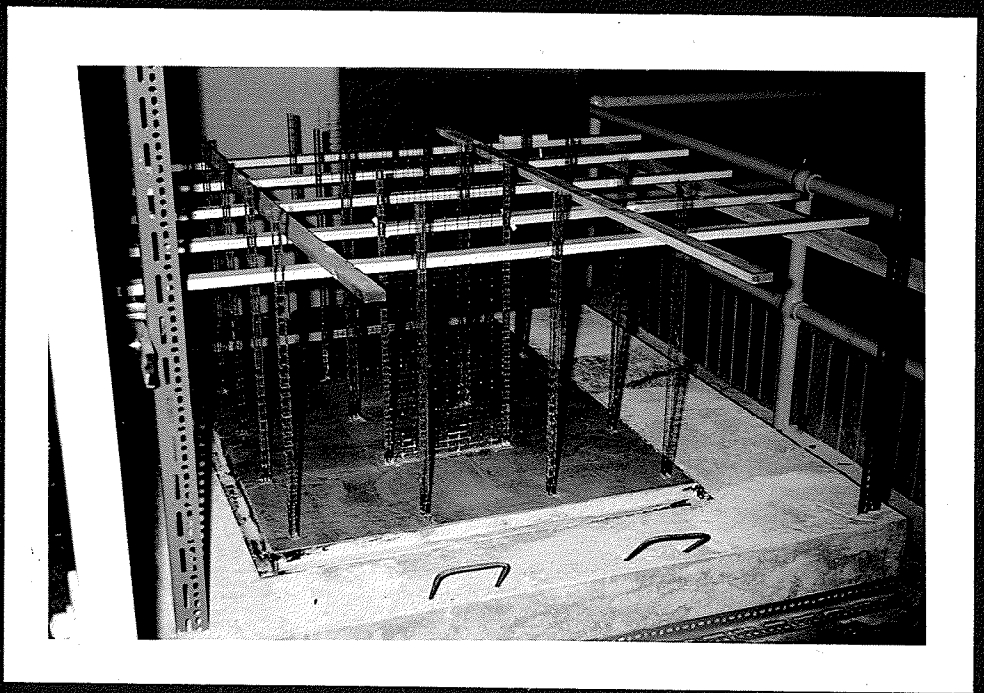

Plate 7. Placing of column steel using a grid system

Plate 8. Method of pouring slabs

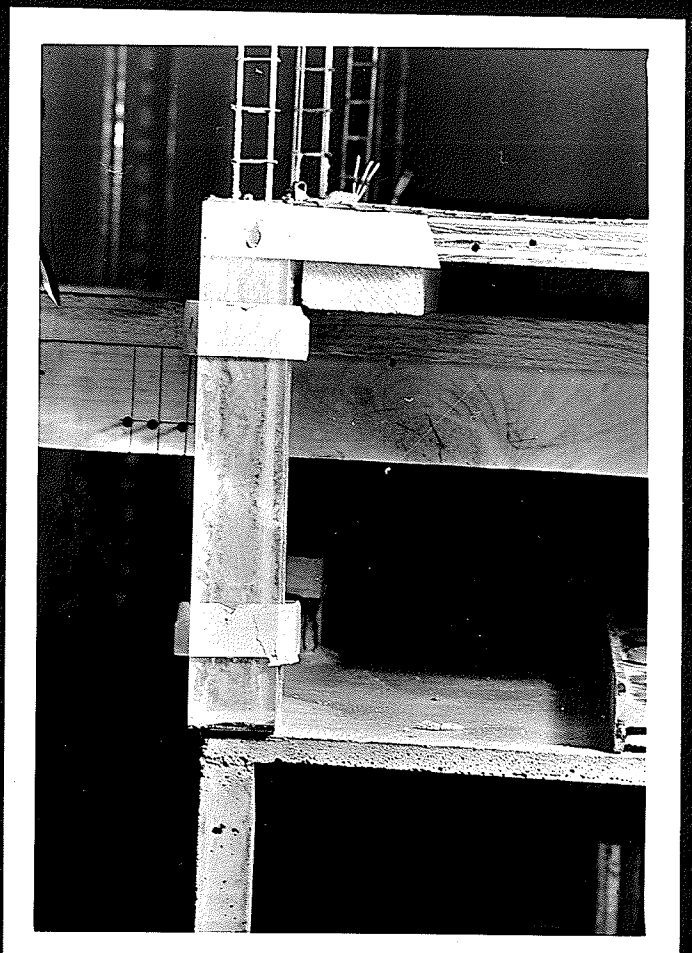

Plate 9. Method of forming columns

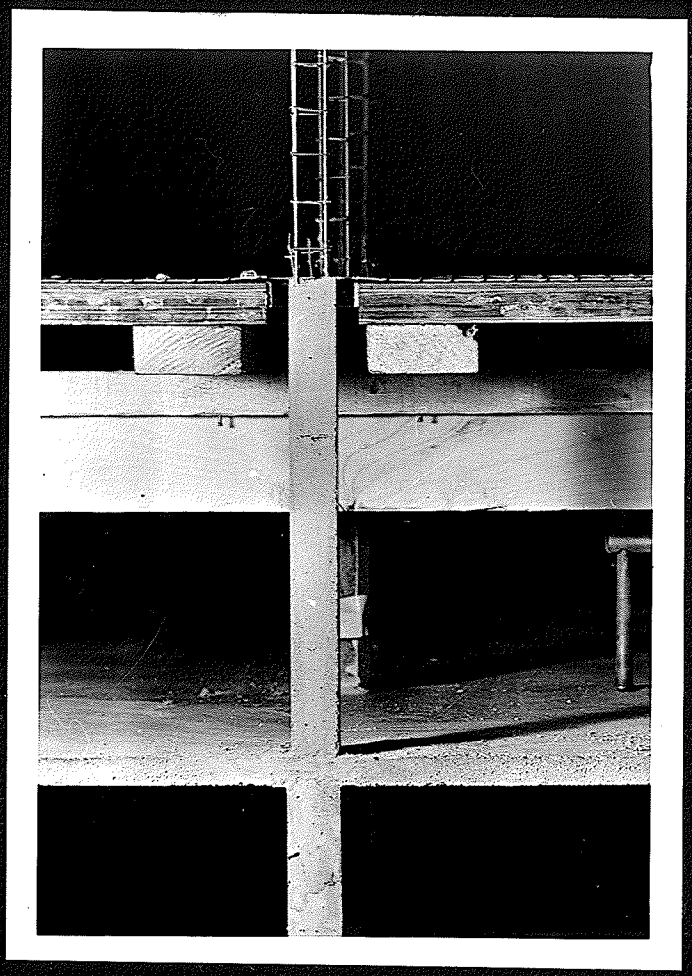

Plate 10. Removal of column forms

Plate 11. Replacing column forms with filler plexiglass pieces

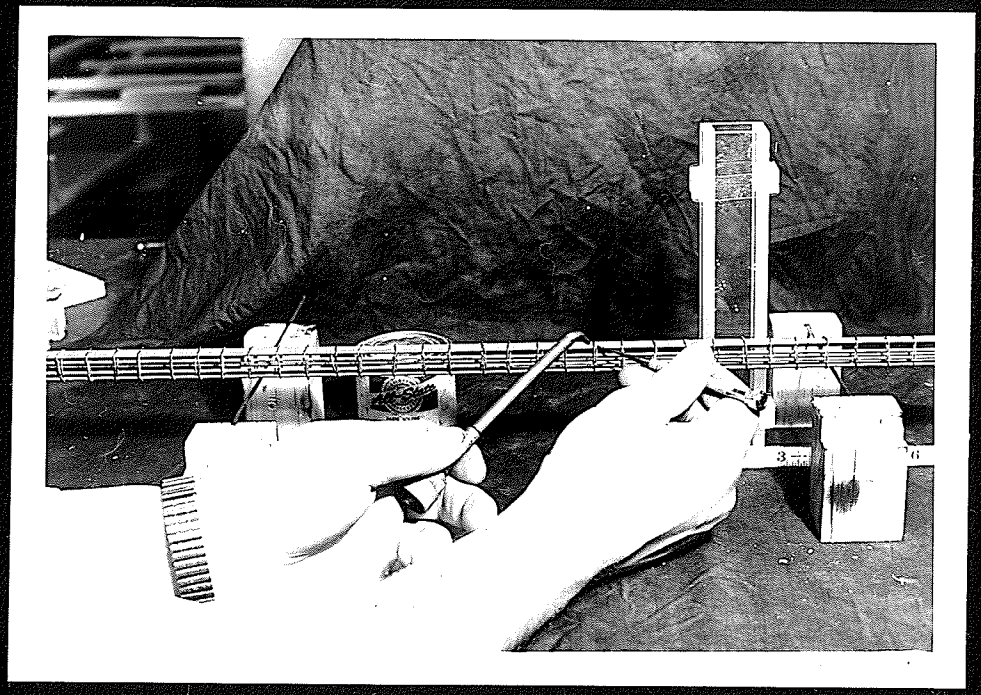

Plate 12. Fabrication of shear wall reinforcing steel

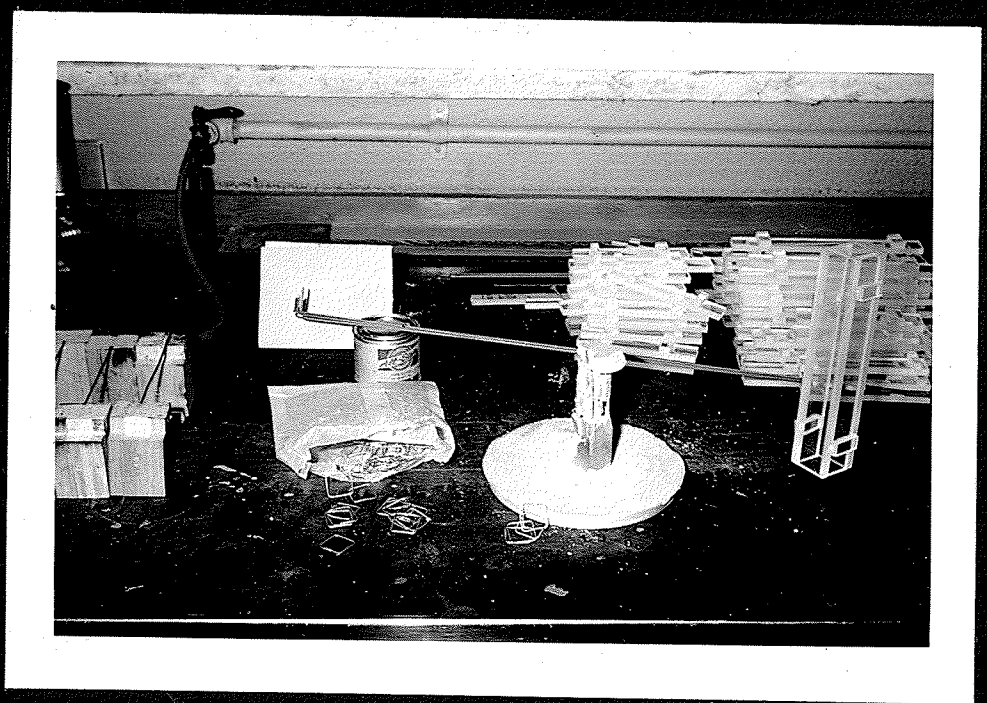

Plate 13. Plexiglass column forms

Plate 14. Base of model

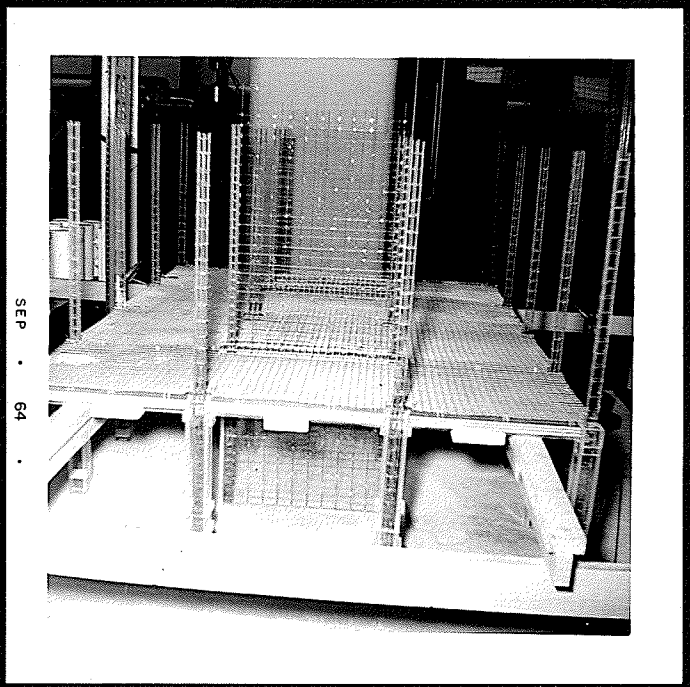

SEP . 64 .

Plate 15. Forming of 1st to 2nd columns

Plate 16. Forming of 2nd floor

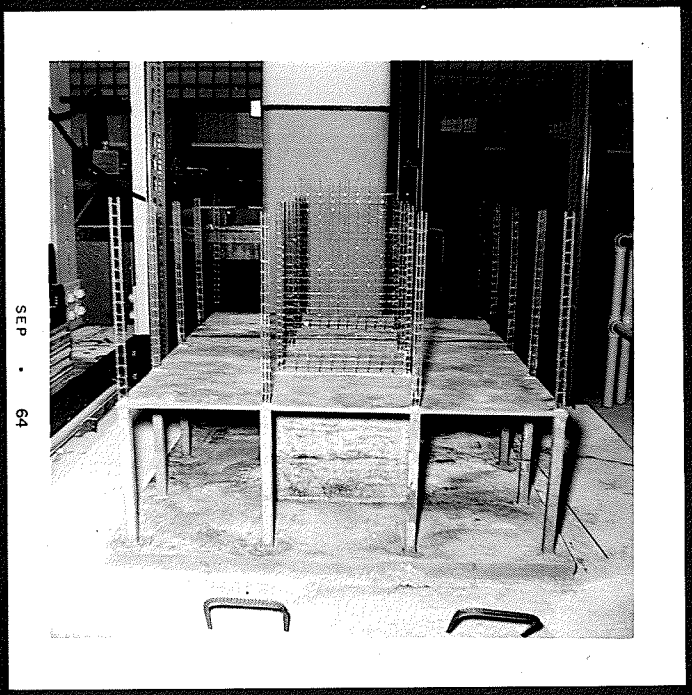

Plate 17. Finished 2nd floor

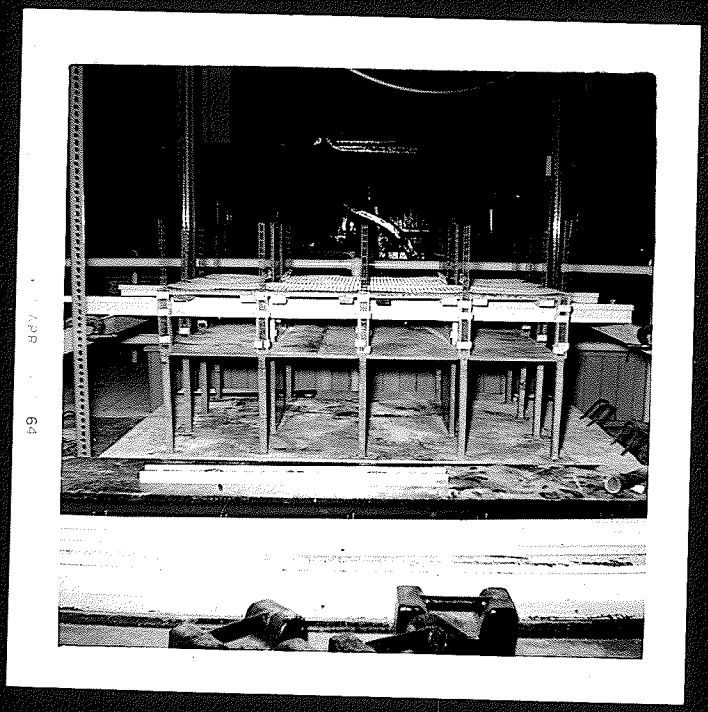

Plate 18. Forming of 2nd to 3rd columns

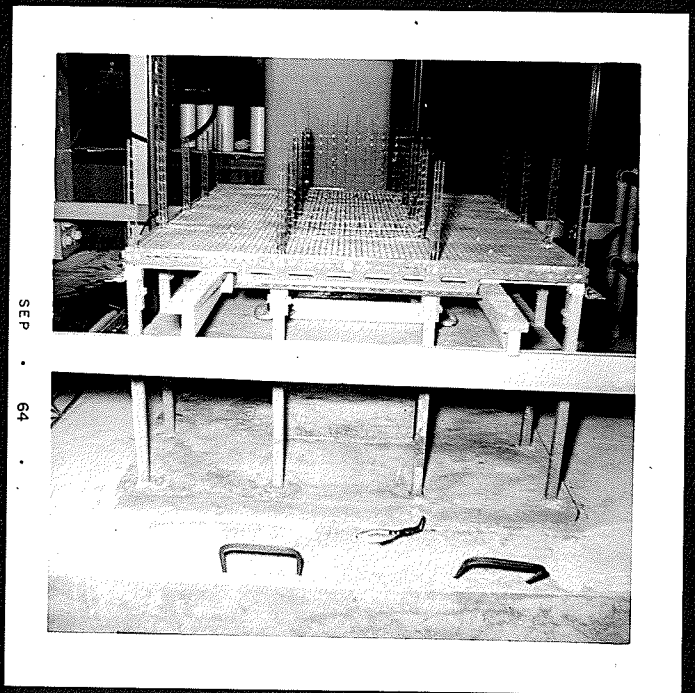

Plate 19. Forming of 3rd floor

Plate 20. Finished 4th floor

Plate 21. Forming of 5th floor

Plate 22. Forming of 5th to 6th columns

Plate 23. Finished 6th floor

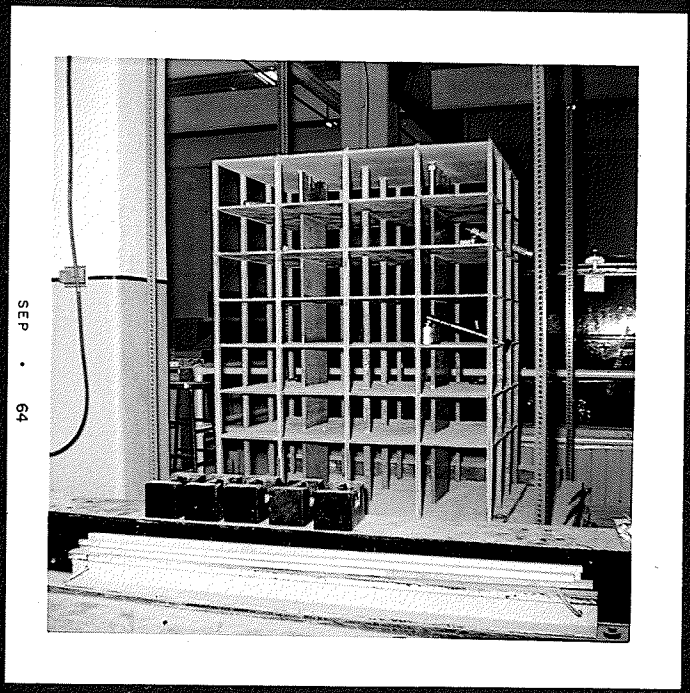

Plate 24. Finished 8th floor

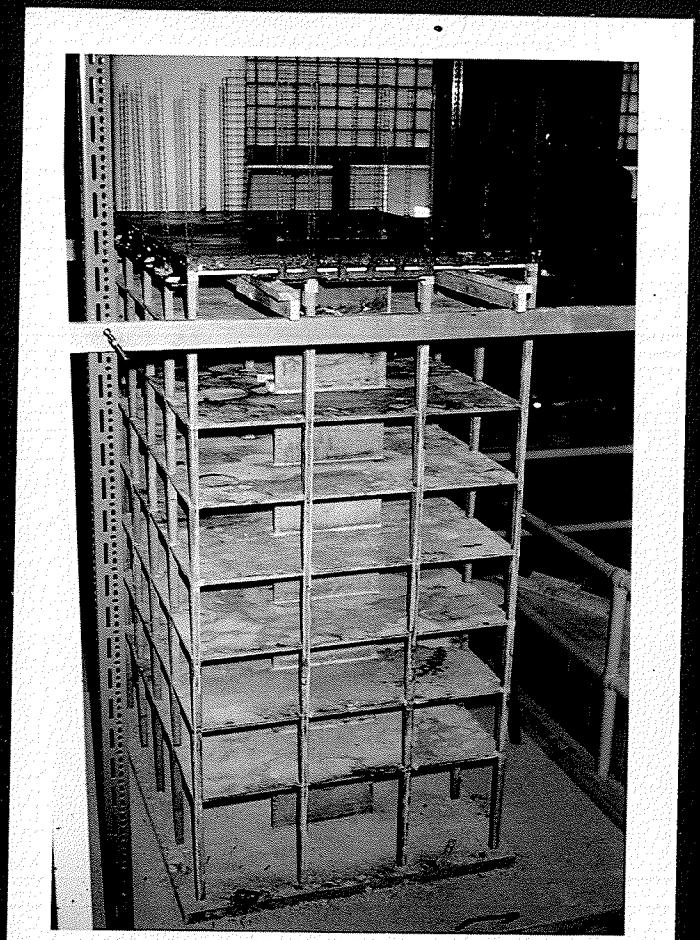

Plate 25. Poured 9th floor

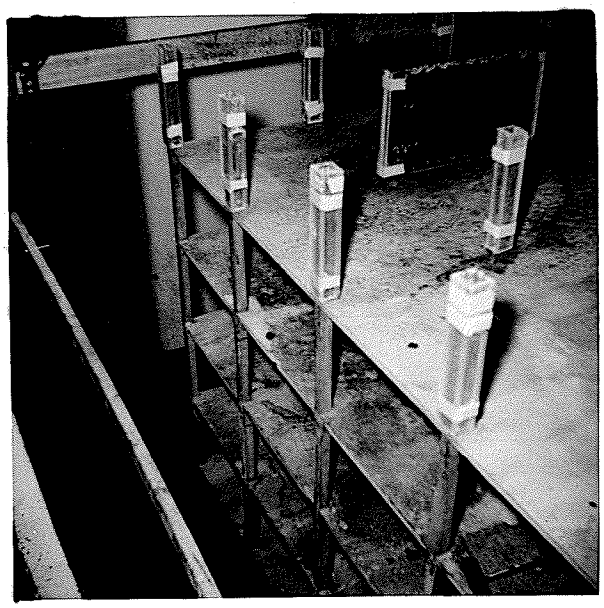

Plate 26. Forming of 10th to roof columns

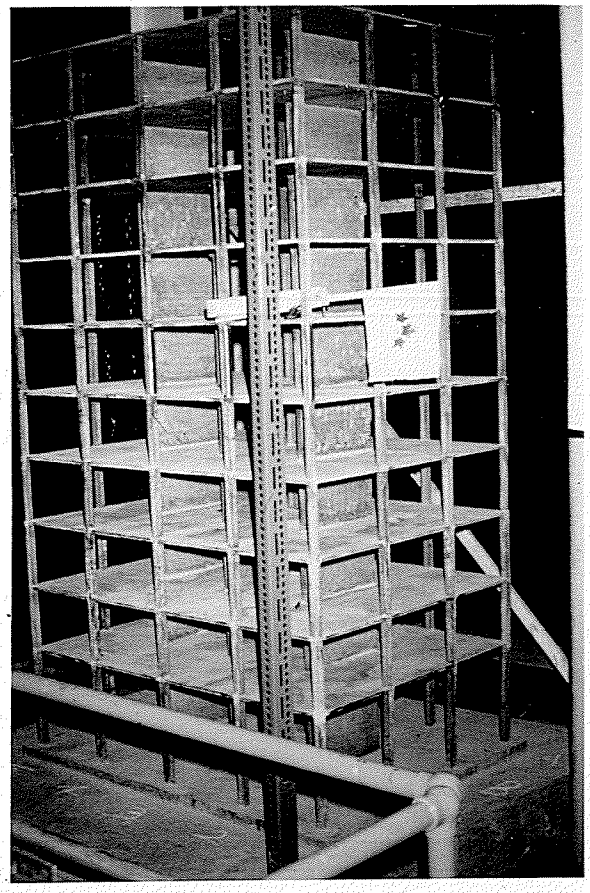

Plate 27. Finished model

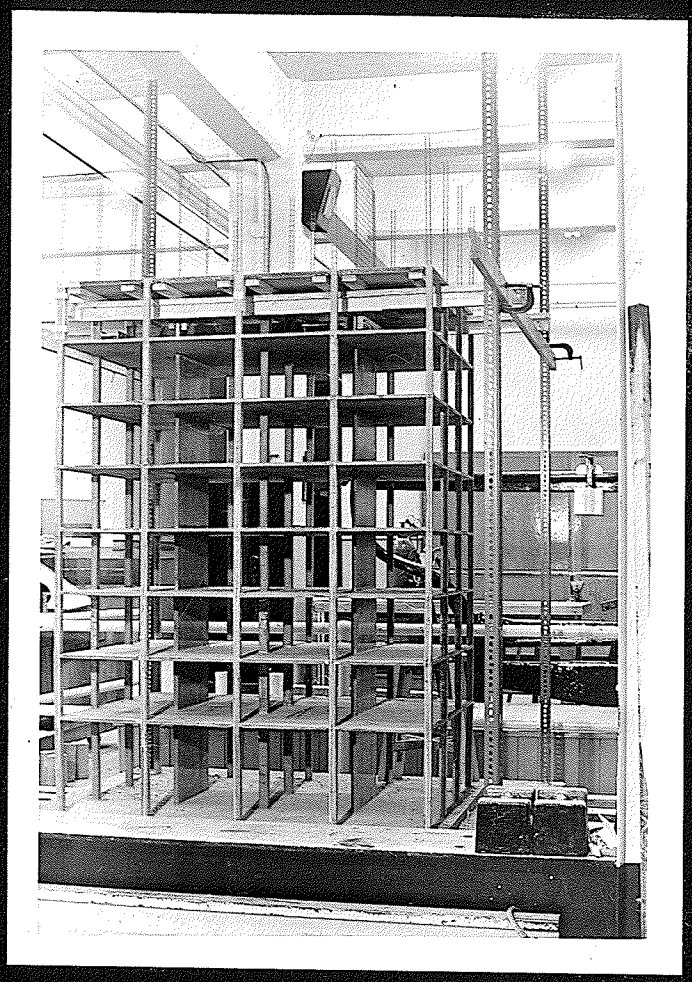

Plate 28. Detail showing supporting frame

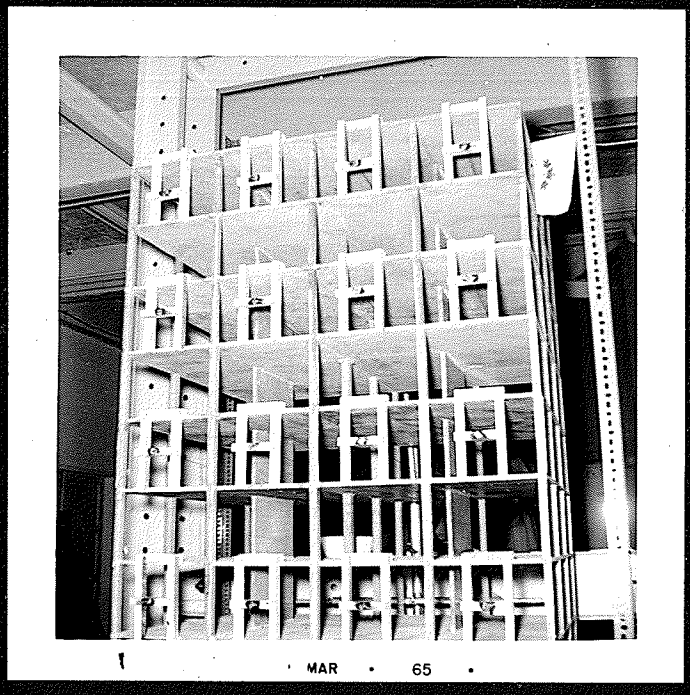

Plate 29. Detail of loading apparatus

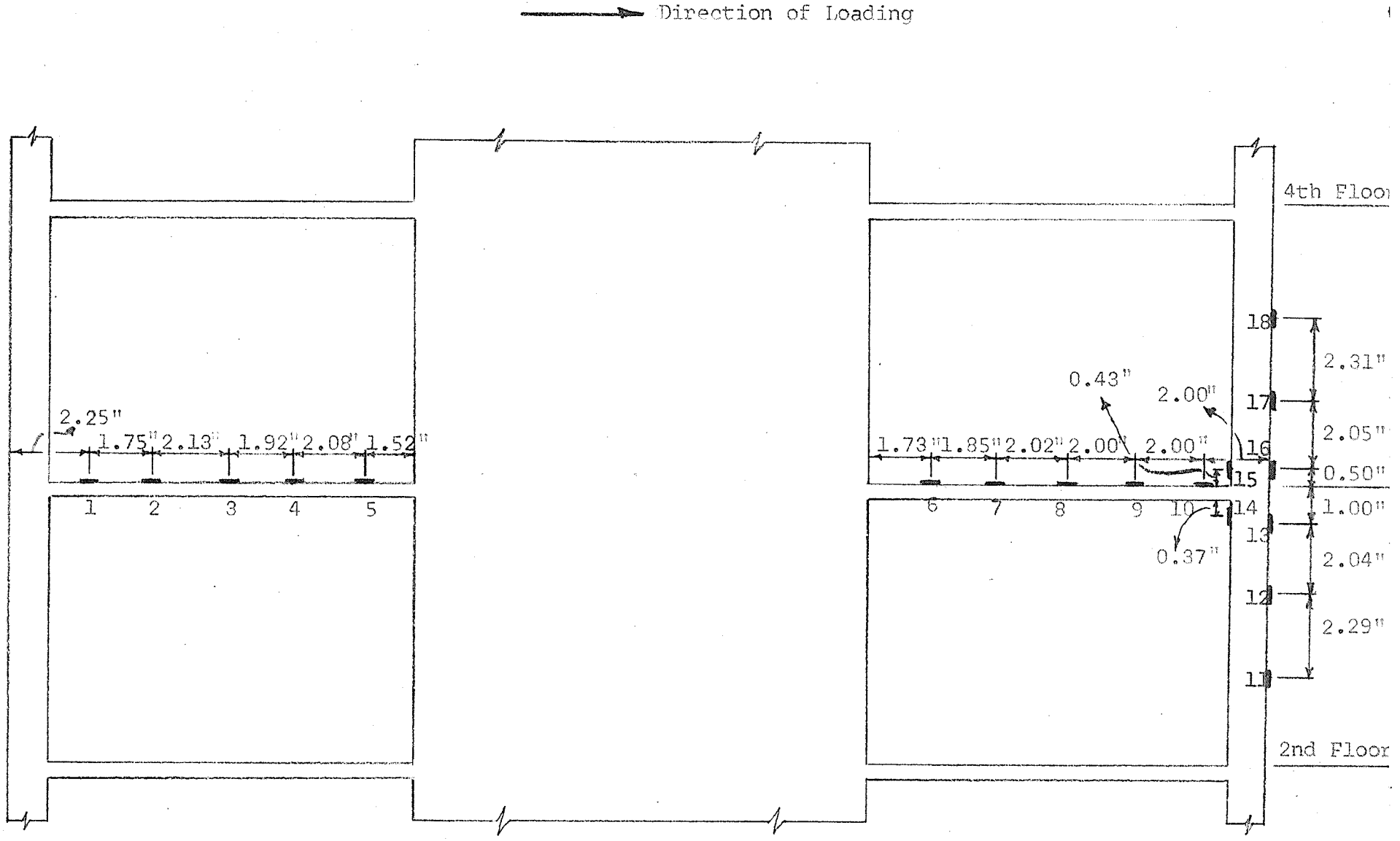

Location of S R-4 Gages

Figure 8.

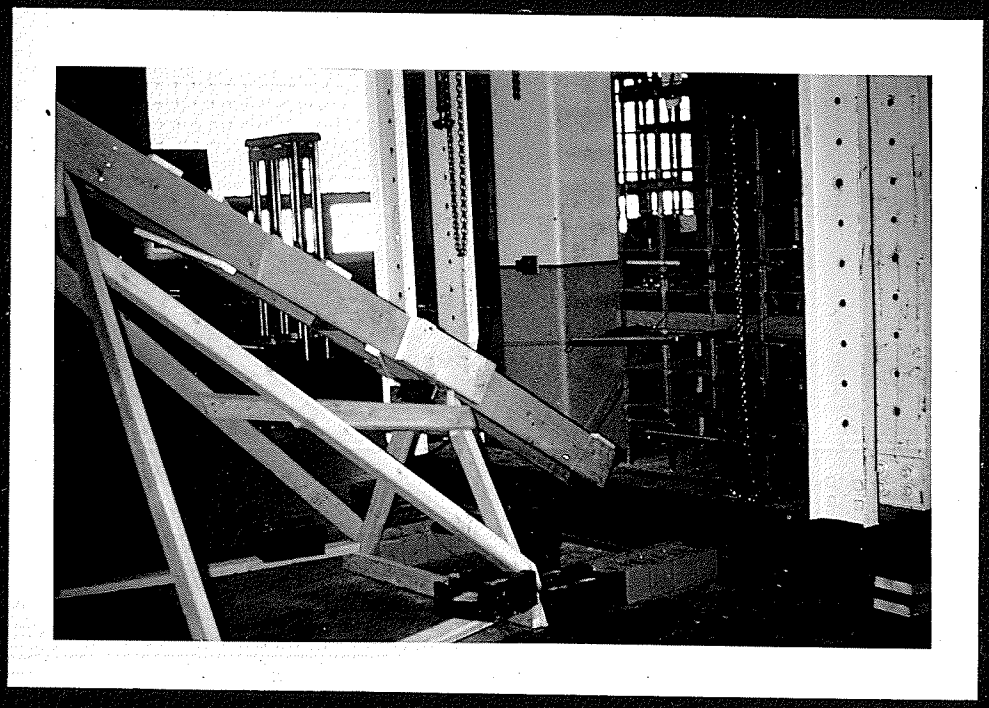

Plate 30. Detail of method of applying lateral loads

frame and gage readings to the nearest 1/10,000 inch were recorded at each floor level (except at the tenth floor level). The gages were numbered from roof to first floor as gages 1 to 9. For lateral loading in the direction of the shear walls the gages were attached so that they read the lateral deflection at the middle of each slab along the centre frame. Thus the deflected shape under various loads could be determined. For lateral loading in the direction perpendicular to the shear walls the same method of fixing the gages was used. Thus lateral deflections were again obtained for each floor level and the deflected shape of the model under different loads could now be obtained for a building frame without shear walls.

iii. Loading Apparatus.

The purpose of the loading method was to apply a uniform lateral load to assimilate wind loading. The loading apparatus for load application in the direction parallel to the shear walls consisted of a wiffle tree system. Two floors were loaded together with the use of wooden slats (see Plate 30). Black annealed wire and aluminum piping were used to assemble the horizontal yoke system. Small pulleys were then used with a loading frame (see Plate 29) for application of dead weights to assimilate uniform loading for two floors. For applying a uniform lateral load for all floors simultaneously a different system was used. Four of the five horizontal yoke systems were again yoked together in a vertical plane. Thus from one load application the applied load would be uniformly distributed to eight floors. This load was applied using a pulley system and turnbuckle

with a dynamometer for recording the load. The top two floors were loaded using the loading frame as before and applying dead weights. The wiffle tree system was arranged so that the proper portion of the load was applied at each floor. For design load this is illustrated in Figure 9. The same horizontal yoke system was used for load application in the direction perpendicular to the plane of the shear walls.

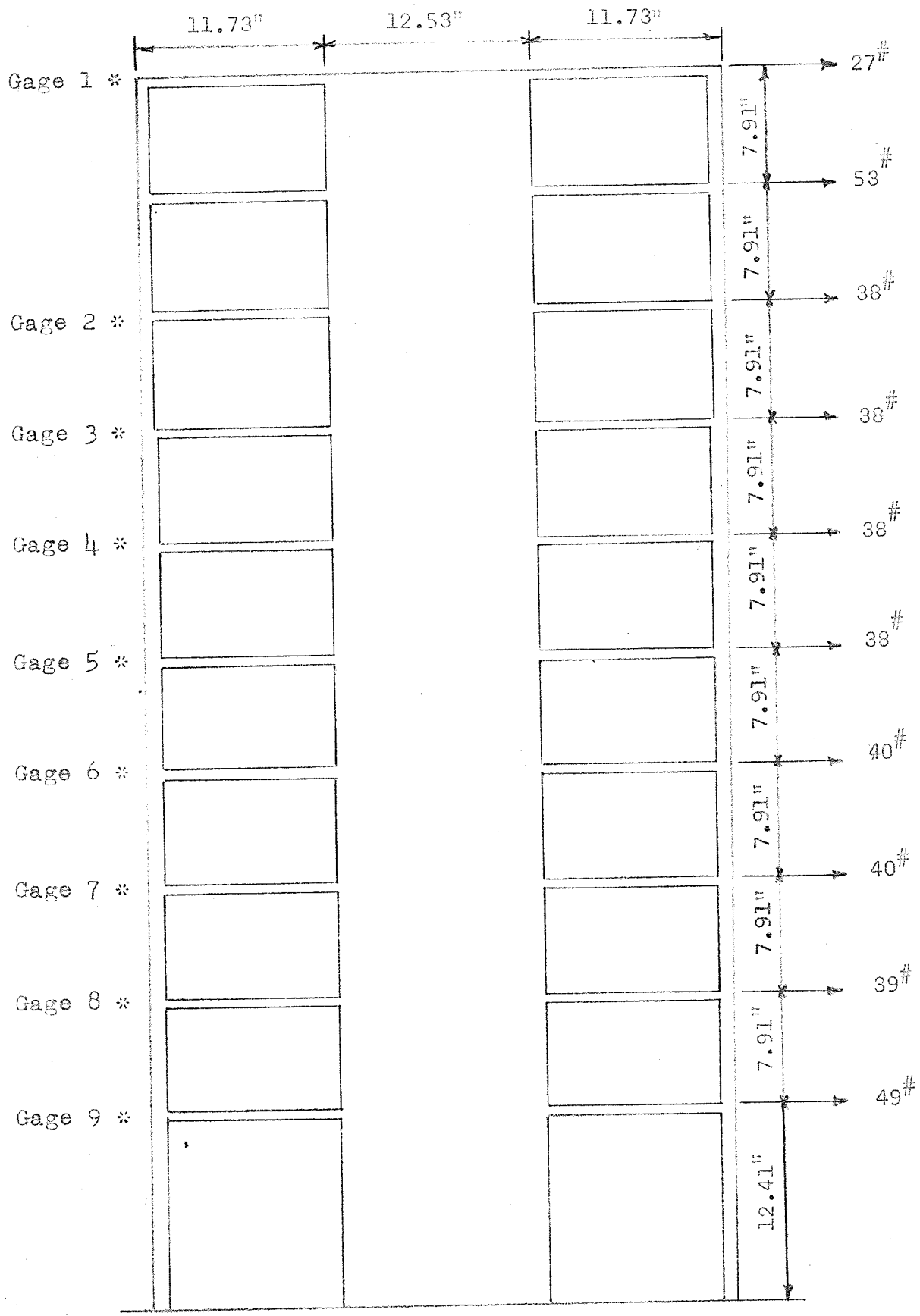

Total Lateral Design Load for the Model

Figure 9

CHAPTER VII

TEST PROCEDURE AND EXPERIMENTAL RESULTS.

The model was loaded in two directions to obtain (a) the deflected shape of the model containing shear walls and (b) the deflected shape when no shear walls were acting. In the shear wall direction two types of loads were applied. One was the application of dead weights, the load being distributed to two floors only. The second was with the application of a turnbuckle at one point, the load being distributed to eight floors and the top two floors being loaded by dead weights. Thus the entire model was loaded simultaneously with a uniform lateral load. The loading of two floors at a time with dead weights was the only method used in the direction perpendicular to the plane of the shear wall.

The test results are divided into three categories: lateral deflections, slab deformations, and joint deformations.

i. Lateral Deflections.

The tests carried out to determine lateral deflection (see Figure 9 for location of gages) was divided into two parts. The first part dealt with lateral deflections and resulting deflected shape of the model in the plane of the shear walls. Three test series were carried out as follows:

Test Series I:

The model was loaded with dead weights two floors at a time and the lateral deflections recorded for each floor level.

This test series involved three trials. The three trials and average values were recorded in Table VIIa. By superposition the deflected shape due to total uniform lateral loading was determined from the average of the three trials. The deflected shapes were shown in Graphs VIIa and VIIc for one half design load increments to twice design load.

Test Series II:

In this series the model was loaded with a total uniform lateral loading applied simultaneously. Again three trial runs were carried out and the lateral deflections recorded in Table VIIb. The lateral loading varied from one half design load to twice design load in one half design load increments. A comparison with test series I and II and with theory were illustrated in Graph VIIc.

Test Series III:

Test series III is identical to test series II except that loading was continued in one half design load increments until failure of the loading mechanism occurred. It was attempted to load the model to failure but successive failures of the loading apparatus prevented ultimate failure of the model being reached in this test series. Thus the model was loaded to a maximum of four times desigr load. This brought the model into the plastic range (see load deflection curve on Graph VIIk) as a definite permanent set was recorded. See Table VIIc for tabulation of the lateral deflections. Graph VIId illustrates the deflected shape of the model under different total load increments and compares them with the theory.

The second part of the test results involving lateral

deflections dealt with the deflected shape of the model when loaded in the direction perpendicular to the plane of the shear wall. This gave a comparison between a structure relying on frame rigidty only (no shear walls) with the previous results. Four test series were carried out as follows:

Test Series IV:

The model was loaded with a 10# lateral load/floor, loading being applied two floors at a time and lateral defledtions being recorded at all floors (except 10th floor). Only one trial was carried out. The deflections were recorded in Table VIId and the deflections due to total lateral loading found by superposition. Graphs VIIe and VIIj show the deflected shape of the model and a comparison with theoretical values.

Test Series V:

Test sries V was carried out identical to test series IV except that a 20# lateral load/floor was used. The deflections are tabulated in Table VIIe and the deflected shape with a comparison to theory were illustrated in Graphs VIIf and VIIj.

Test Series VI:

The loads were again applied two floors at a time but in this test the deflection was set and the load required to produce this deflection found. The purpose of the test was to find the rigidity of the building loaded perpendicular to the shear wall as compared to the rigidity in the direction of the shear wall. Thus the load required to produce the same deflection at roof level would be

proportional to the rigidity of the building. The roof deflections of test series I at twice design were used. The results were recorded in Table VIIf. The deflected shape of the model with a comparison to theory were illustrated in Graph VIIg.

Test Series VII:

This test series was identical to test series VI except that the deflections used were obtained from test series III at four times design load. The results were recorded in Table VIIg. The deflected shape of the model with a comparison to theory were illustrated in Graph VIIh.

Graph VIIa

Deflected Shape of Model due to point loads (Test Series I)

(Direction of loading in plane of shear walls)

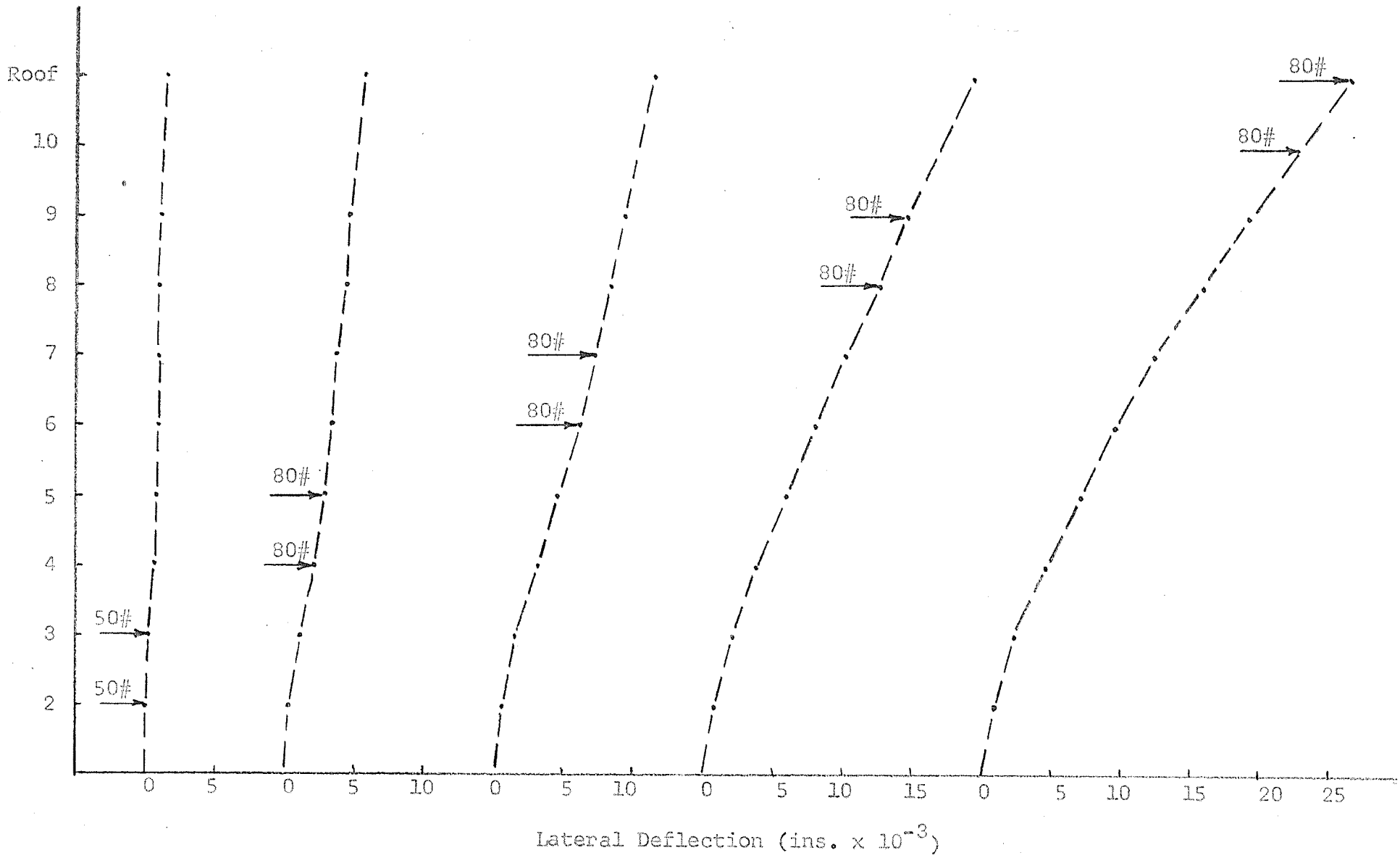

Theoretical derivation of deflected shape of the model due to lateral loading in direction of shear walls.

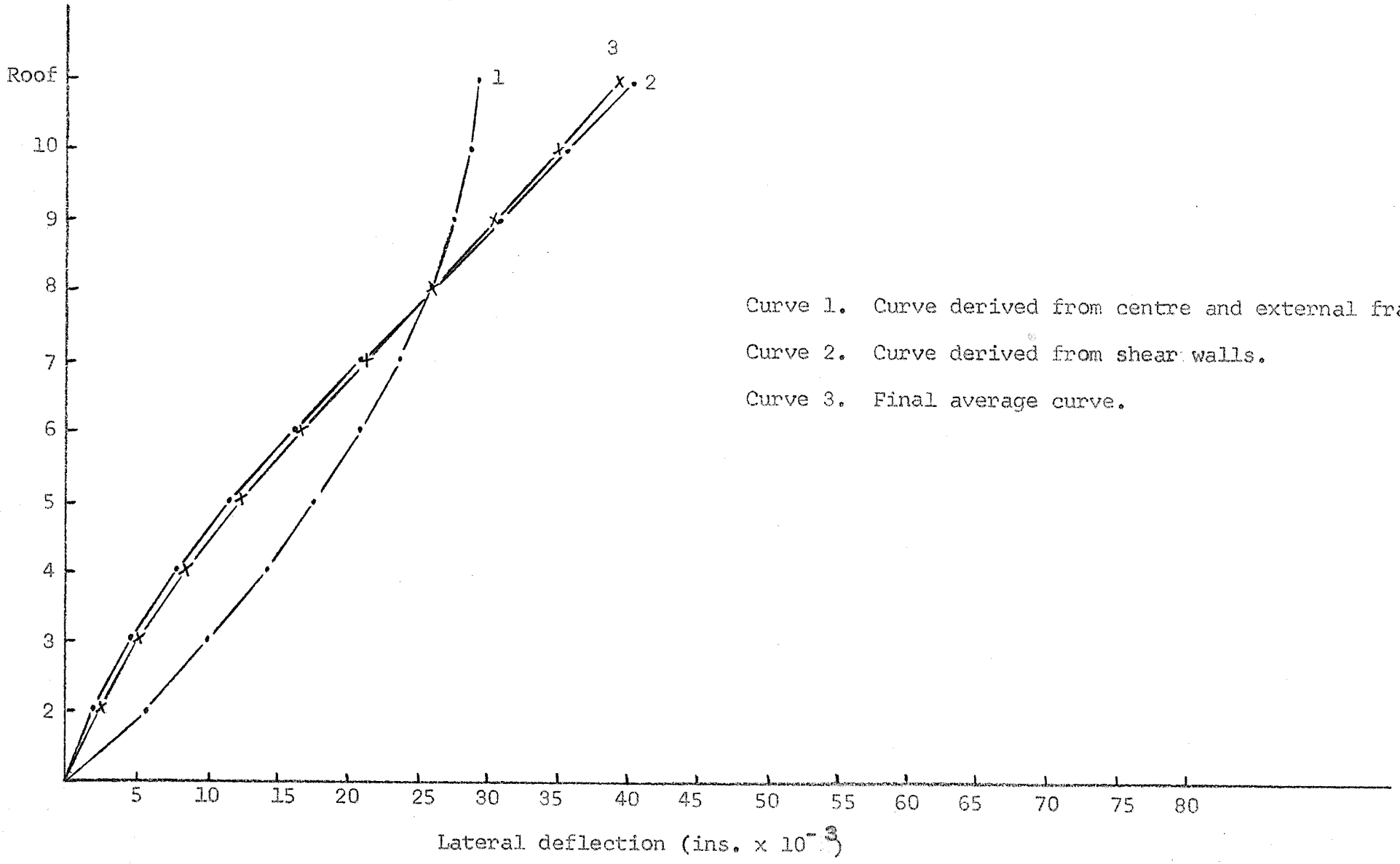

Curve 1. Curve derived from centre and external frames.

Curve 2. Curve derived from shear walls.

Curve 3. Final average curve.

Comparison of deflected shape of the model at design load between test series I, test series II and the theoretical results of Graph VIIb.

(Direction of loading in plane of shear walls)

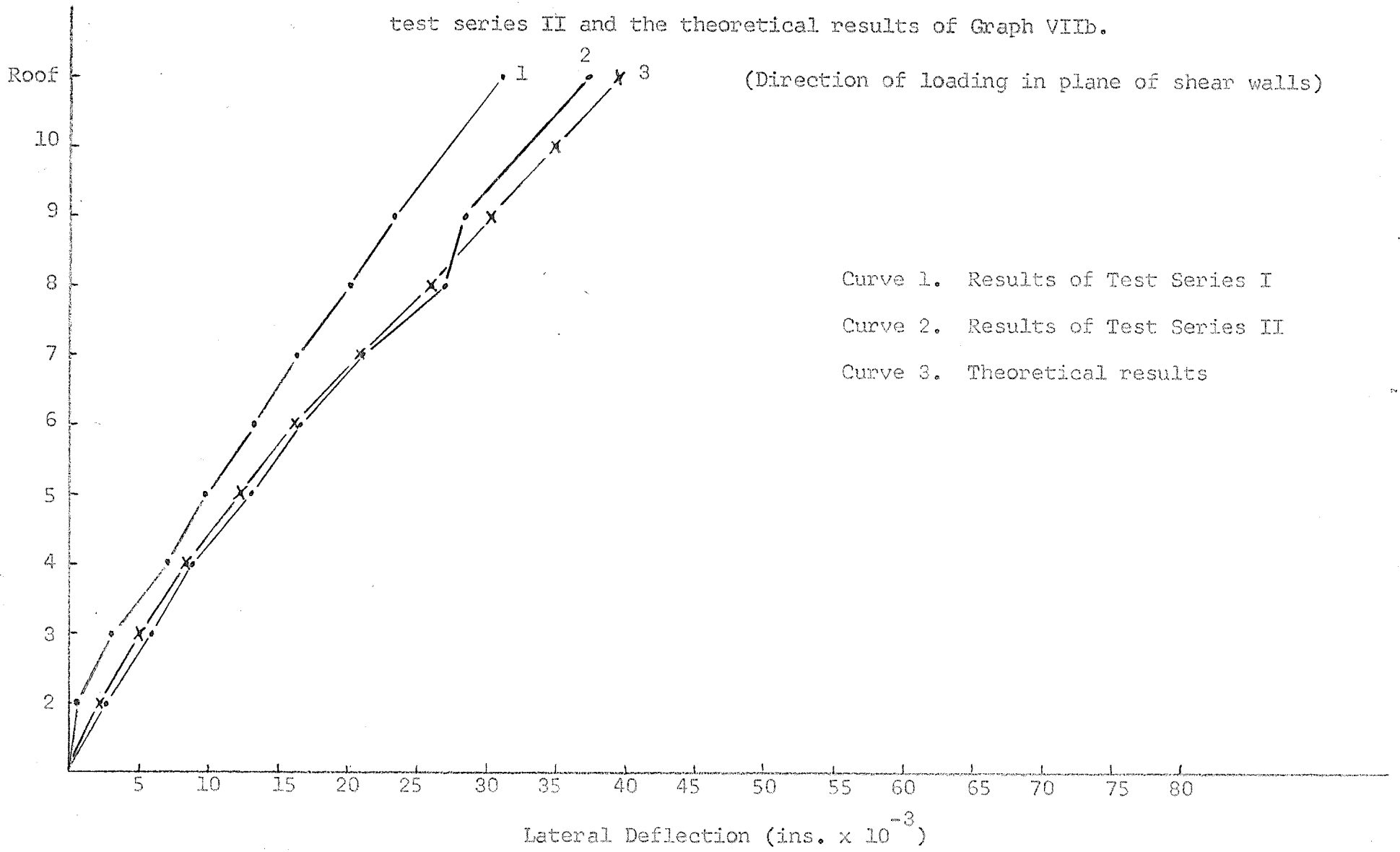

Curve 1. Results of Test Series I

Curve 2. Results of Test Series II

Curve 3. Theoretical results

Graph VIId

Deflected shape of model due to different uniform lateral loads and comparison with theoretical results.

(Direction of loading in plane of shear walls)

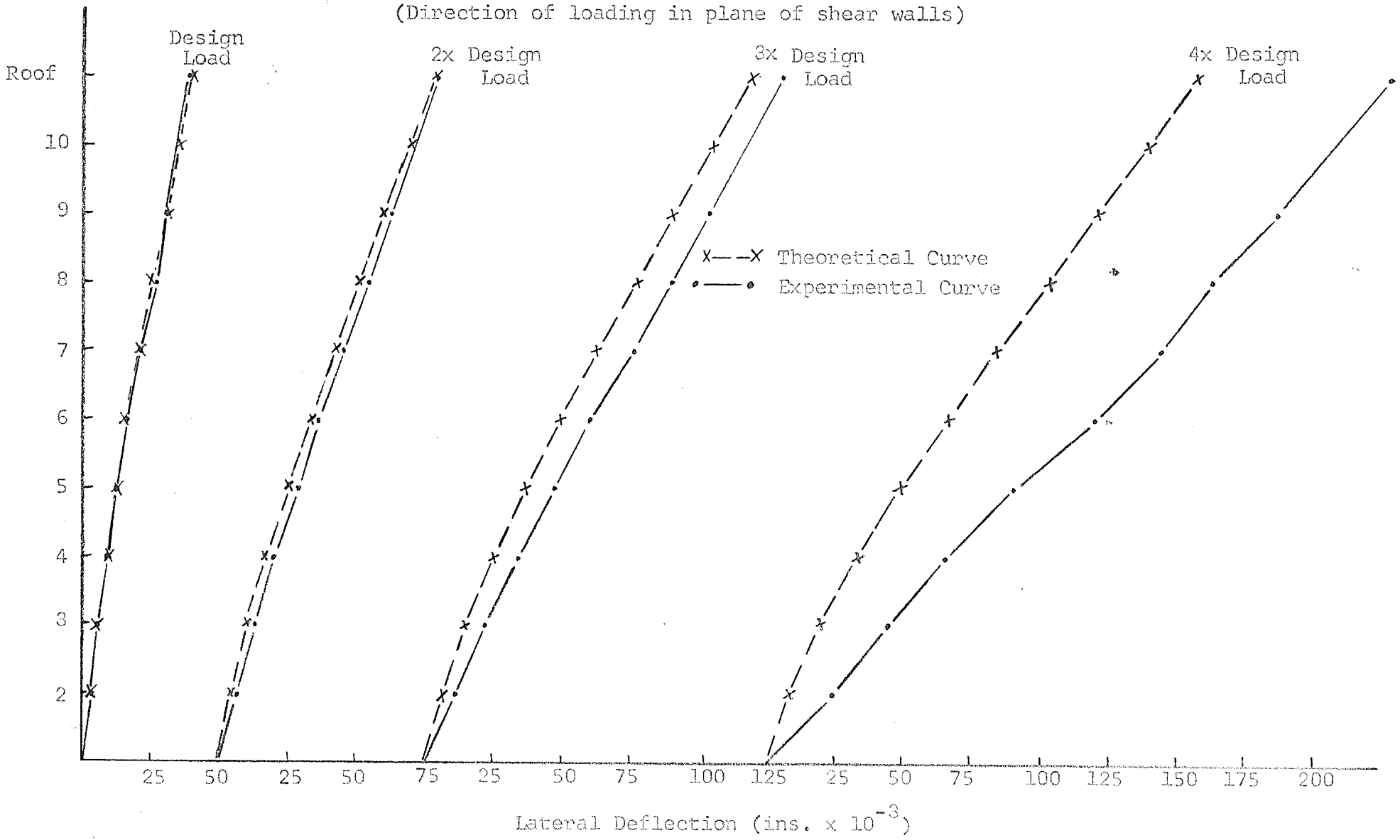

Deflected shape of model due to $10^{\#}$ point loads. (Test Series IV)

(Direction of loading perpendicular to the plane of shear walls)

_____ Theoretical Results . _____ . Experimental Results

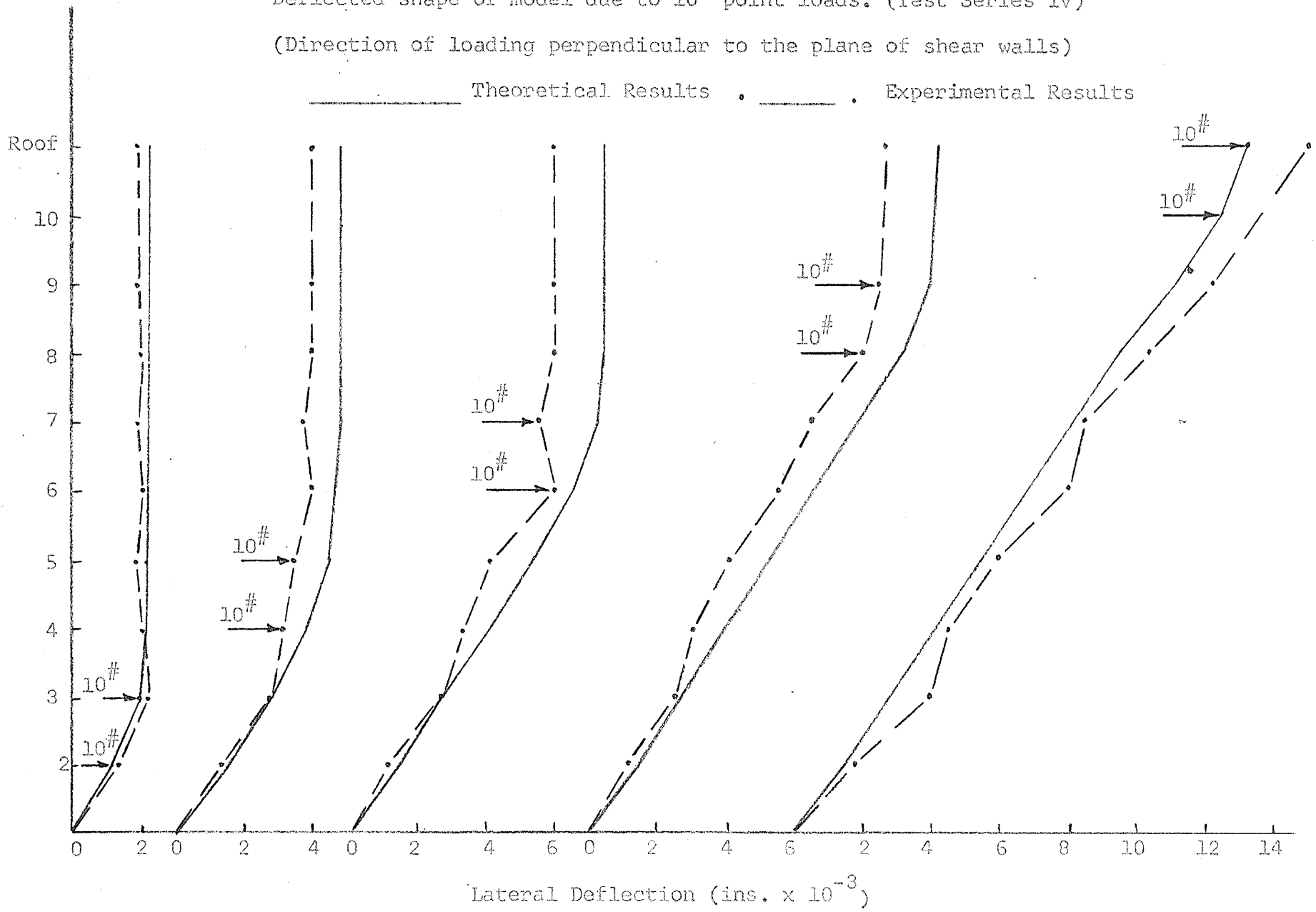

Deflected shape of model due to $20^{\#}$ point loads.(Test Series V)

(Direction of loading perpendicular to the plane of shear walls)

_____ Theoretical Results . _____ . Experimental Results

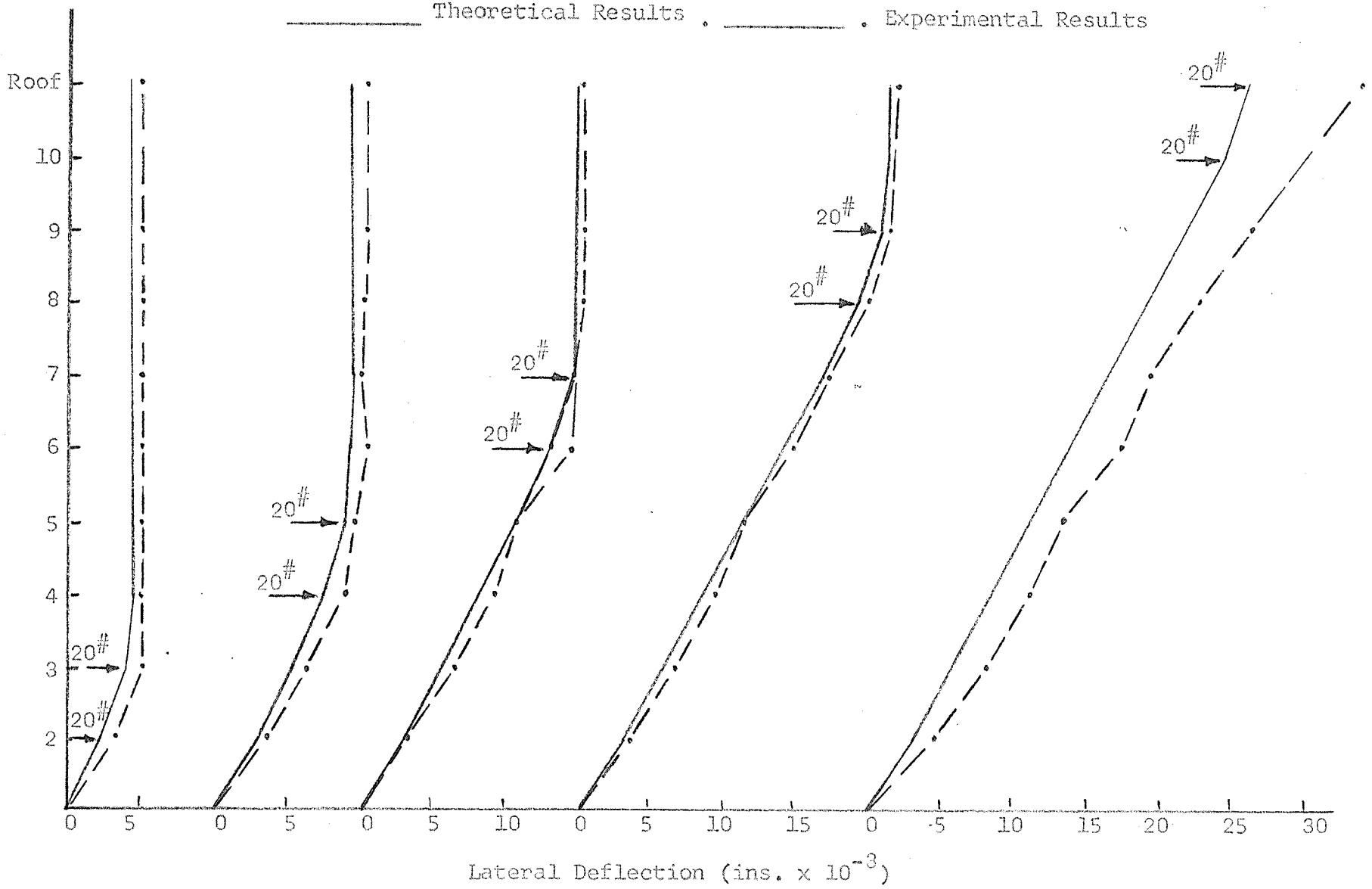

Deflected shape of model due to point loads from Test Series VI. Graph VIIg

(Direction of loading perpendicular to the plane of the shear walls)

Theoretical Results . . . Experimental Results

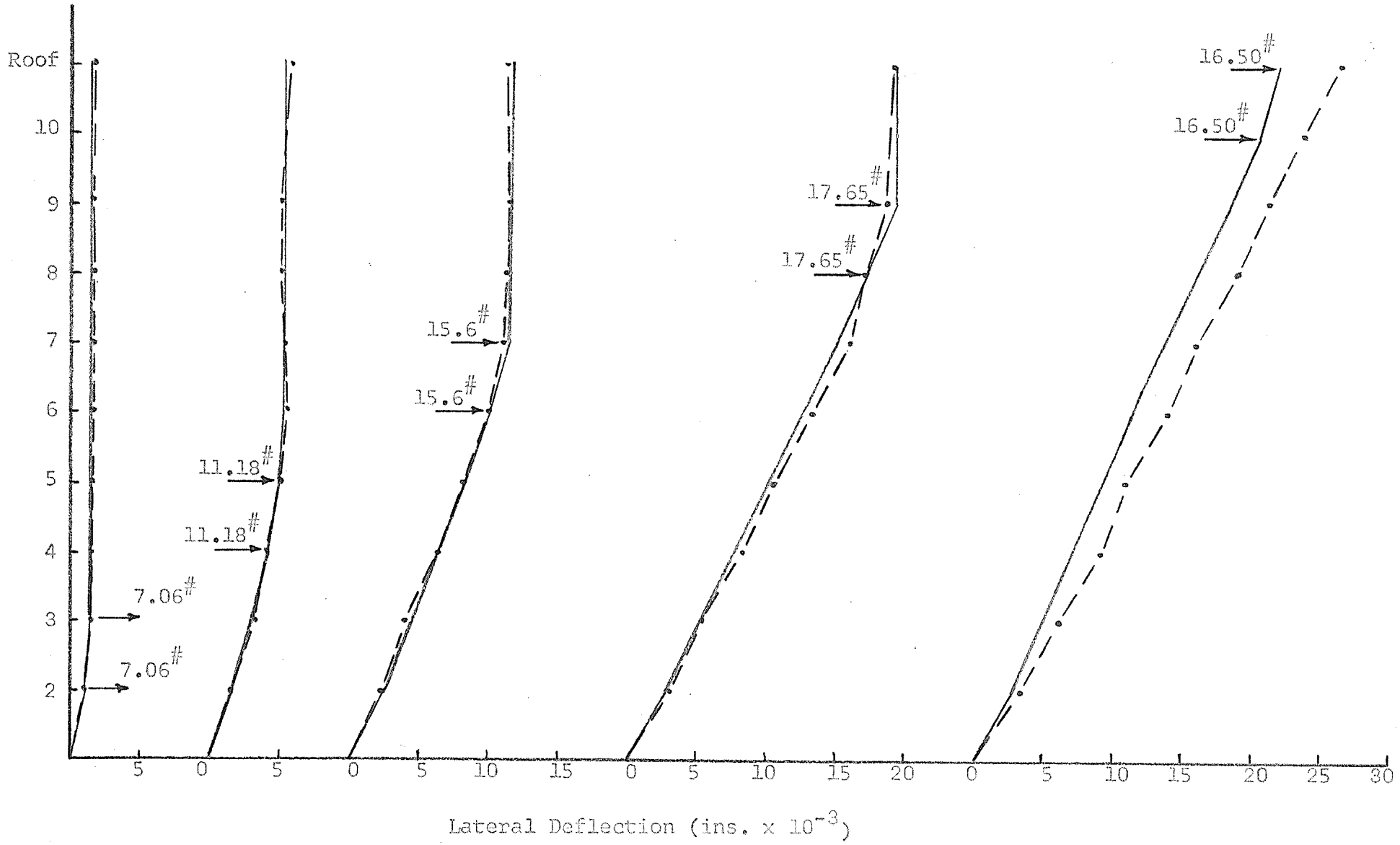

Graph VIIh

Deflected shape of model due to point loads from Test Series VII.

(Direction of loading perpendicular to the plane of the shear walls)

_____ Theoretical Results . _____ . _____ . Experimental Results

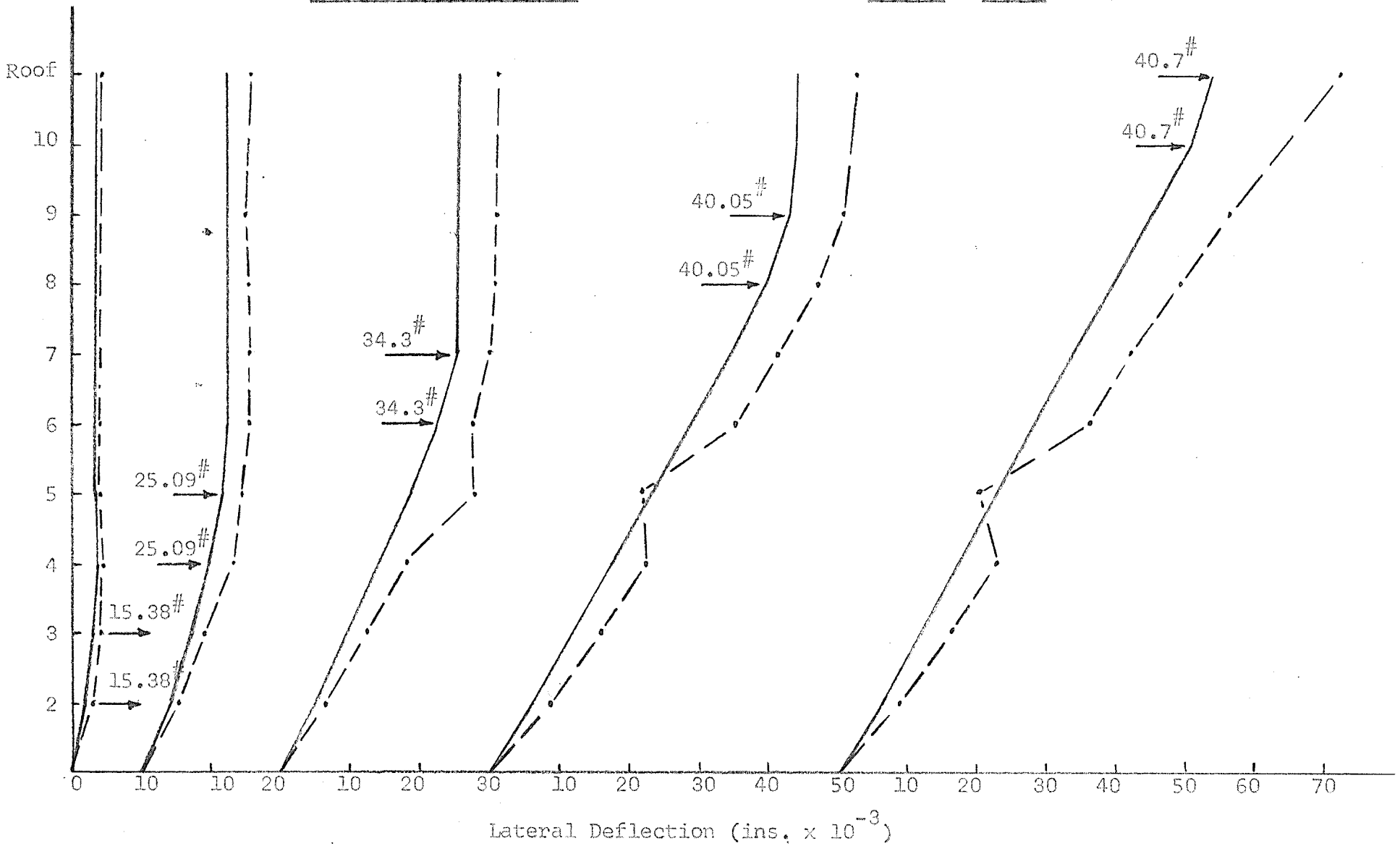

Deflected shape of model due to uniform load application of $10^{\#}$/floor and $20^{\#}$/floor. (Test Series IV and V)

(Direction of loading perpendicular to the plane of the shear walls)

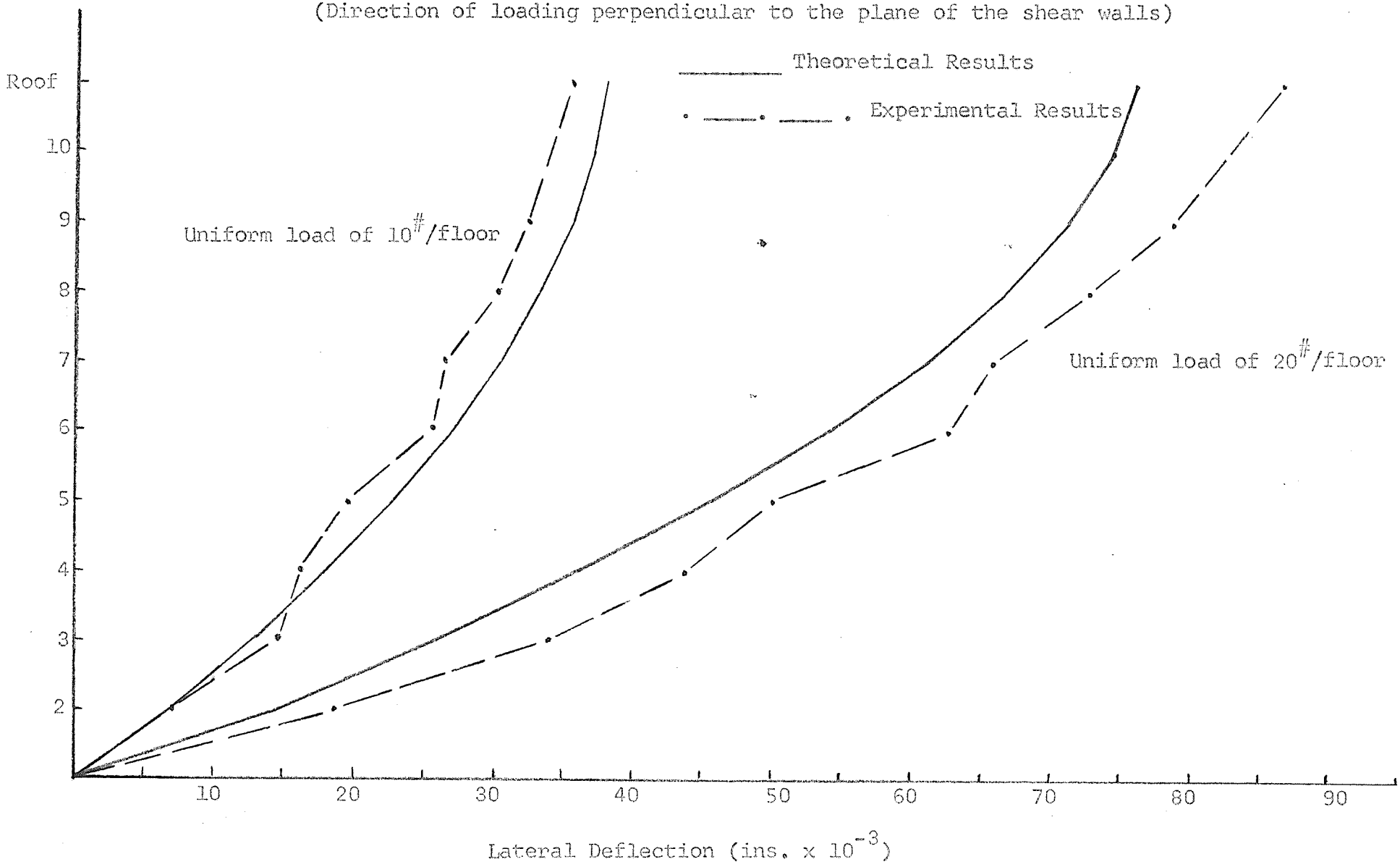

Graph VIIk

Load deflection curve from Test Series III

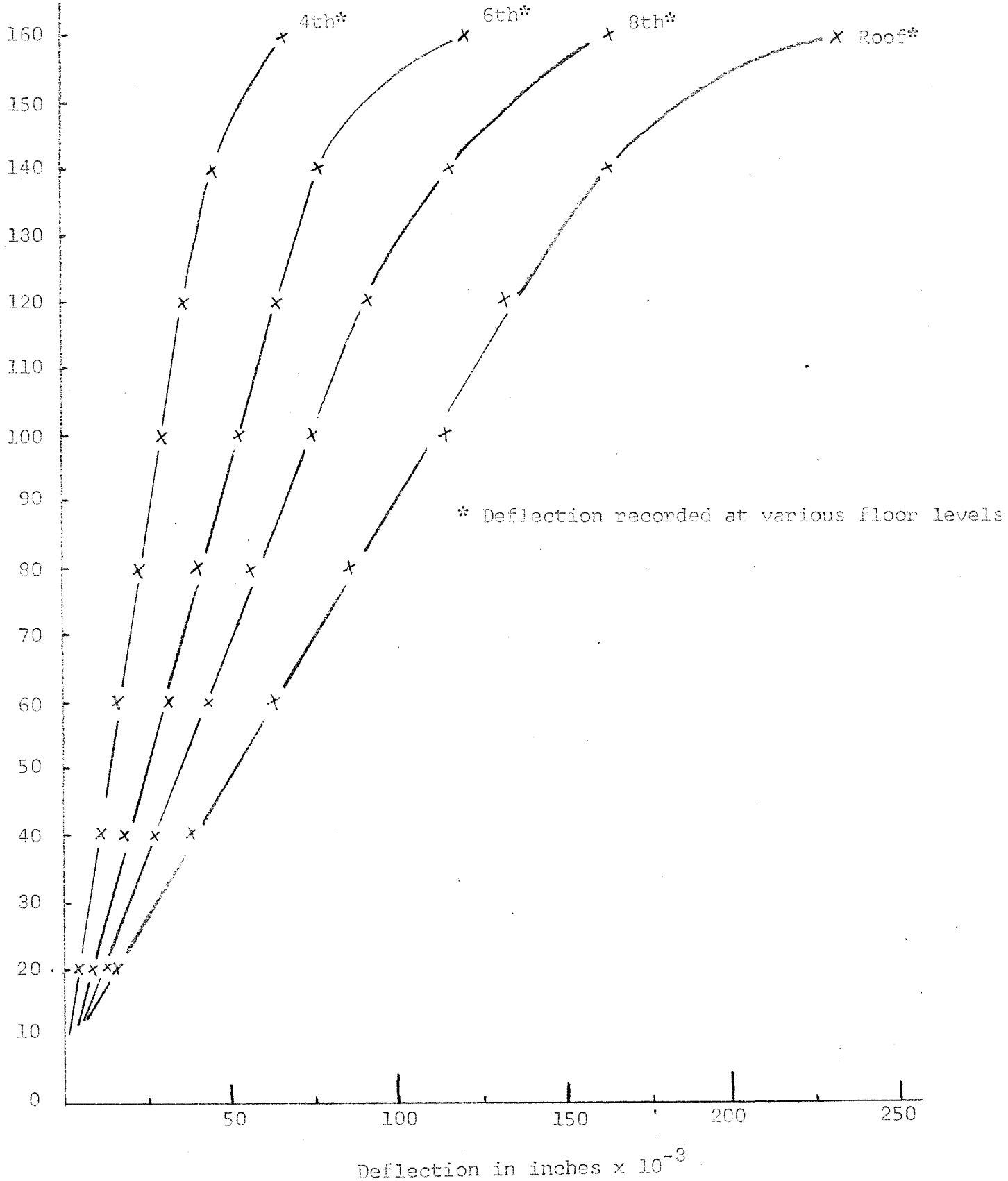

ii. Slab Deformations.

SR-4 gages as described in Chapter VI, part i, were placed on the third floor slab.

The deflected shape of the slab acting as a beam between the shear wall and exterior columns could be determined. Also for further theoretical analysis the location of the points of inflection could be determined. The gages were numbered from one to ten and were placed as shown in Figure 8. Table VIIh gave the average values obtained by superposition from test series I. Table VIIj and VIIk gave the average results of test series II and III respectively. The deflected shape of the model as derived by the gage readings was illustrated in Figure 10.

iii. Joint Deformations.

SR-4 gages were placed on the exterior column in the plane of the shear wall for one storey height above and below the third floor. The exact location of these gages can be obtained from figure 8 (numbers 11 to 18). From the gage readings the deflected shape of the column can be obtained and location of points of inflection determined. Table VIIl gave the average values obtained by superposition from test series I. Table VIIm and VIIn gave the average results of test series II and III respectively. The deflected shape was illustrated in Figure 10.

CHAPTER VIII

DISCUSSION OF RESULTS

The control on material properties and construction quality showed the model to be within the limits of accuracy expected on a full-scale structure (See Chapter III and IV). The following discussion will involve the elastic behaviour of the model. From the discussion on adequacy of model similarity in Chapter IV part v it was concluded that the model would represent accurately a full-scale replica within the elastic capacity of the structure. This has been borne out with the experimental results as illustrated in Graphs VIIa to VIIj and their comparison to theory.

i. Theoretical Results.

Theory in this case refers to the Kani method of analysis*(4) for free frames and an adaptation of this method to include frames containing shear walls. The Kani method of analysis for both free frames and for frames containing shear walls has been programmed for the 1620 computer by Professor G. Morris. The use of this programme has made it possible to compare all lateral deflections determined by experiment to a theoretical analysis. The general principles involved in the Kani method and its adaptation to frames including shear walls has been illustrated in Appendix III. The only assumptions required in this analysis were:

(1) the width of slab which would act in beam action as part of the frame.

(2) Location of the points of inflection in these "beams".

The width of slab used was 5 inches. Reference*(3) was used to arrive

* See Bibliography.

at this figure. The analysis by Khan and Sharounis involved the use of a model to determine the effective width of slab to be used as a beam element. The location of the points of inflection in this beam element was taken as one half the clear span. This was derived from the results of the SR-4 gages placed along the slab in the shear wall frame. All the pertinent data required for the computer analysis was listed in Appendix III. All of this data was either taken directly from the model itself or from tests carried out in conjunction with the model testing.

Graph VIIb was derived from the method mentioned above. The total uniform lateral design load was applied to each of the five frames. The load taken by each frame was found by relating the relative stiffness of each frame to the shear wall stiffness. The relative stiffness was found by comparing the lateral deflection of each frame at the 8th floor. Then the deflected shape of the three frames acting together was compared with the deflected shape of the shear wall frames (Curve 1 and 2 on Graph VIIb). The weighted average of the two shapes was then referred to as the theoretical design curve for the building (curve 3 on Graph VIIb). It was found that the two shear wall frames took 91% of the lateral load and the three free frames took the remaining 9%. Within the shear wall frame itself it was found that the contribution to lateral stiffness of the frame by the exterior columns was negligible (less than 1%). Thus if the resistance to lateral loading was assumed to consist of the two shear walls acting as cantilever beams and the resisting moments due to the interconnected slabs taken into account (see Appendix III) the design would be conservative by 9%. However this model has quite

large shear walls (one full bay length) and it should not be assumed that the cantilever design method would be applicable for lesser shear walls.

The discussion of the results has been divided into three categories; lateral deflections, slab deformations, and joint deformations.

ii. Lateral Deflections:

Graph VIIa shows the deflected shape of the model due to point loads being applied laterally in the plane of the shear wall. These results when combined by superposition to represent the deflected shape of the model due to a uniform lateral load do not compare exactly with the results obtained by test series II in which the same uniform lateral load was applied simultaneously (see curves 1 and 2 in Graph VIIc). The results obtained by simultaneous loading (test series II) were greater by 16 to 18%. It should be noted from the recorded results that as more load cycles were applied the lateral deflection readings increased. Table VIIIa will illustrate this:

TABLE VIIIa

Increase in Flexibility with Increase in Number of Cycles.

Load Cycle	Load	Test Series	Gage No. 1*	Gage No. 2*
1	60#/floor	Preliminary	40.9	27.7
2	"	Preliminary	- -	- -
3	"	Preliminary	- -	- -
4	"	I	47.4	35.8
5	"	I	47.8	35.0
6	"	I	49.8	38.6
7	"	II	55.0	43.0
8	"	II	57.0	45.0
9	"	II	58.4	47.0
10	"	III	61.0	49.5
11	"	III	62.3	50.0
12	"	III	63.0	50.5

* lateral deflection in inches x 10^{-3}

This increase in flexibility with the number of load cycles would explain the difference in test series I and II.

The comparison between the experimental results and theory as illustrated by Graph VIId was excellent. Graph VIIk would indicate that yield of the structure under lateral loading seemed to occur at $3\frac{1}{2}$ times design load. The model was not loaded to ultimate failure.

The results of the tests carried out on the model when loading perpendicular to the shear wall (see Graph VIIe to VIIj) also compared quite well with theory. The results of Graphs VIIe and VIIf by superposition were also used to develop a deflected shape of the structure due to total uniform load as illustrated in Graph VIIj. From the comparison to theory it would seem that the 20#/floor uniform load brought the model into the plastic range.

This was also verified by the larger deflections occurring when the point loads were applied to the top two floors (Graph VIIe and VIIf).

In test series VI and VII it was found that due to the difference in deflected shape of the free frame and shear wall frame the relative rigidities of the two varied with storey height. The free frame would add more rigidity to the structure in the upper stories than in the lower stories. The relative rigidity between the two frames varied as follows:

Location of Point Loads	Relative Rigidity	
	Test Series VI	Test Series VII
2nd and 3rd floor	11.3	10.4
4th and 5th floor	7.2	6.4
6th and 7th floor	5.1	4.7
8th and 9th floor	4.5	4.0
10th and roof	4.8	4.0

Thus when the model was loaded in the plane of the shear walls it was about five times as rigid as when loaded in the plane perpendicular to the shear walls. The value for relative rigidity when the loads were applied to the 10th floor and roof was used because this is the point at which the lateral deflections have been maintained the same. Test series VII involved deflections and loads when the model was suspected of being in the inelastic range for both directions of loading. Therefore the values of relative rigidity would not be as reliable for test series VII as for test series VI.

iii. Slab Deformations.

The SR-4 gages were placed on the slabs to obtain the point of inflection in the beam elements. This location was then required (see Appendix III) to compute the resisting moment contributed by the slabs to the shear wall. It was found that the secondary compression effect caused by the direct lateral loading on the slabs tended to increase the compressive stresses and decrease the tension stresses in the slab. The result was that the point of inflection would be offset in one direction for both beam elements. This is illustrated in the following table:

TABLE VIIIb

Location of points of inflection in the slab

Test Series	Gages #1 to #5*	Gages #6 to #10*
I	3.90"	5.60"
II	4.52"	5.60"
III	4.56"	5.60"
Mean	4.41"	5.60"

*These measurements represent the location of the point of inflection from the edge of the shear wall.

It was noted that in test series III after a lateral loading of 2x design the point of inflection began to creep towards the shear wall. The point of inflection had approached 3.40" (gages #1 to #5) from the shear wall at the maximum load reached in test series III. This would indicate a local concentration of stress

at the column to slab joint. Due to the secondary effects it would seem, as borne out by the experimental readings, that the concentration of stress would be greater at the joint located nearest to gage #1 rather than gage #10. Thus as the lateral load was increased it would seem reasonable to expect an initial failure in the slab at the column to slab joint at gage #1.

The average value of the location of the point of inflection (values for loads up to 2x design) on either side of the shear wall would be 5.00". Since secondary effects like the above were not taken into account in the theoretical design the value for location of points of inflection was taken as 5.00" for every slab for the computer analysis.

iv Joint Deformations

Gages numbered 10 to 18 were used to illustrate the deflected shape of the model at the third floor slab to column joint in the plane of the shear wall. In all three test series run the recorded values of strain readings in the critical areas compared within 3 or 4 micro-inches. It was found that the areas of local stress concentration were immediately around the slab to column joint. The point of highest stress concentration was at gage #16 (See Figure 8 and 10) located on the exterior face of the exterior column at the third floor. Gages placed either side of the column did not compare. This would be due to the "cantilever effect" of the building acting as a unit. Secondary compressive stresses would be developed in the column due to the reaction of the slab or "beam element" at the joint.

Thus in the column itself there would be a rotation and displacement which would produce equal and opposite stresses on either face of the column and a direct compressive stress producing pure compression. This compression effect would be most severe in the lower stories. This was illustrated by the experimental results as it was found that there was no point of inflection below the third floor. That is, the direct compression was greater than any tensile stress developed due to bending. A point of inflection was located 4.86" above the third floor. That is, above the third floor the total compressive stress developed by the reaction of the slabs was not large enough to offset the flexural tensile stress developed due to slab rotation and lateral displacement. The deflected shape is illustrated in Figure 10.

CHAPTER IX

CONCLUSIONS

The conclusions will be divided into two categories: adequacy of model similarity and frame rigidity.

i. Adequacy of model similarity.

(a) The control on material properties and construction quality showed the model to be within the limits of accuracy expected on a full-scale structure.

(b) A 1/16 scale model would be expected to behave accurately under low loads within the elastic behaviour of the structure.

(c) There was a noted increase in ultimate capacity of 1/16 scale model beams and slabs as compared to ultimate design theory or the actual prototype beams. This increase varied from 35% to 74% depending on the percent of steel reinforcing used. All of the above specimens had flexural failures.

(d) There was a noticable difference in the ultimate crack pattern in the flexural failures between model and prototype. The models developed one or two tension cracks while the prototype on failure developed numerous fine diagonal tension cracks.

(e) The model columns showed an increase of only 10% over ultimate design theory.

(f) Except for the difference in crack patterns and a noted increase in ultimate capacity the model beam failures were similar to the prototype behaviour. These two differences

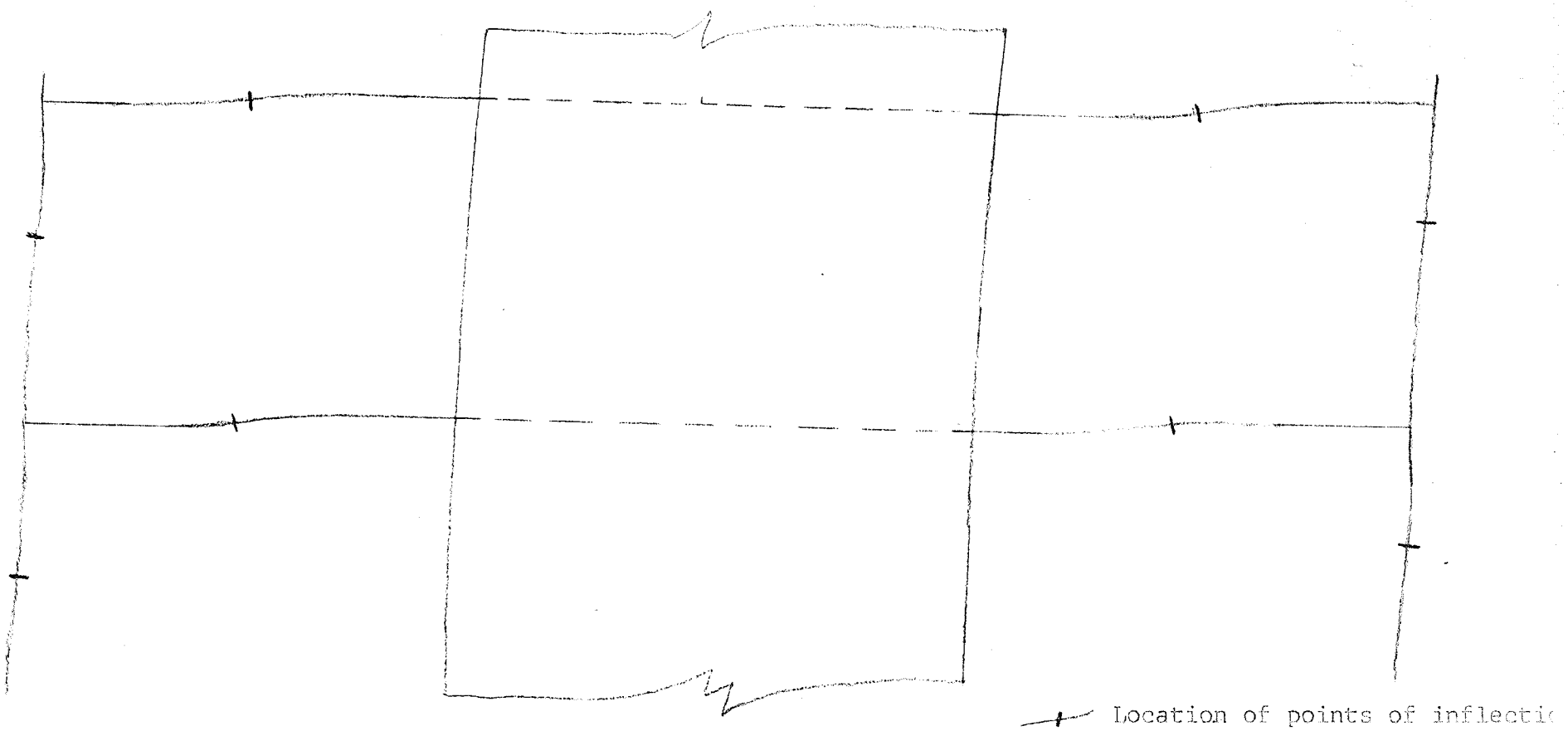

Interaction of Shear Wall, Slab and Columns

Figure 10.

have been noted in other technical literature *(2) and *(4).

ii. Frame Rigidity.

(a) The Kani method of frame analysis and its adaptation to shear wall frames compares excellently with the theoretical results within the elastic range of stress.

(b) Khan and Sbarounis's method of determining effective slab widths for team action applied itself successfully.*(3)

(c) The shear wall frames took up to 91% of the total lateral load applied. The approximate cantilever method of shear wall analysis could therefore be used for this model as the design would be only 9% conservative.

(d) The comparative rigidity of the model when loaded in both directions within the elastic range was approximately 5. This value, due to the different deflected shapes involved in a free frame and shear wall frame, was open to varying interpretations with respect to where to compare the lateral deflections.

(e) The free frame would contribute more to the lateral rigidity of a structure in the upper stories than in the lower stories. The relative rigidity of a shear wall frame to free frame varied accordingly.

* See Bibliography.

(f) It was noted that the model tended to increase in flexibility with an increase in the number of load cycles.

(g) The points of inflection in the "beam elements" within the shear wall frame were offset in the direction of loading due to the compression developed in the slabs from direct lateral loading.

(h) The average value for the location of the points of inflection was 5.00" from the edge of the shear wall.

(i) The compressive stress developed in the exterior column due to slab reactions and dead weight of the model was enough to offset any flexural stress developed by rotation or lateral displacement below the third floor level (in the plane of the shear wall).

BIBLIOGRAPHY

1. R. E. Shewmaker, M. Xanthakis, M. A. Lozen, "Very Small Scale Reinforced Concrete Mult-panel Flat Slabs", University of Illinois. Structural Research Series No. 265, June 1963.

2. 1.52.S "Structural Models", July 1964, Department of Civil Engineering, Massachusetts Institute of Technology.

3. Fazlur R. Khan, John A. Sbarounis, "Interaction of Shear Walls and Frame". Volume 90, No. ST3, June 1964 edition of A.S.C.E. Journal.

4. Zuheir Y. Alami, Phil. M. Ferguson, "Accuracy of Models Used in Research on Reinforced Concrete", A.C.I. Journal, Proceedings Vol. 10, No. 11, November 1963.

5. Gaspar Kani, "Analysis of Multistory Frames".

6. Urquhart, O'Rourke, G. Winter, "Design of Concrete Structures".

7. A.C.I. Building Code (ACI 318-56)

APPENDIX I

Design of Prototype

Appendix I Design of Prototype

Layout of each floor

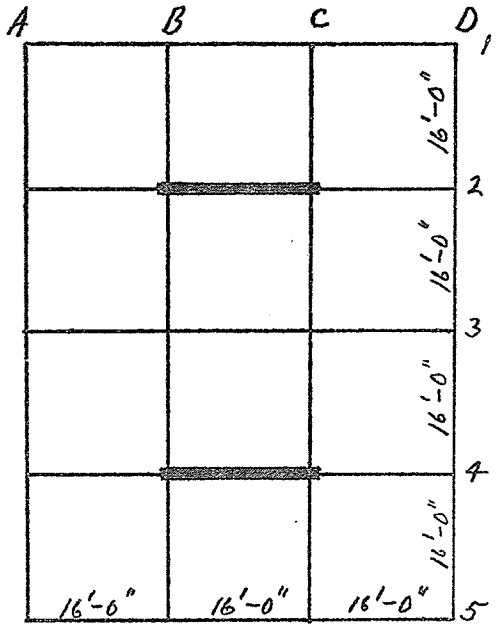

Allowable unit stresses:

$f'_c = 3000$ psi

$f_y = 40{,}000$ psi

$E_s = 30 \times 10^6$ psi

$E_c = 3 \times 10^6$ psi

$n = 10$

The slab design and column design is carried out by the empirical method as set out in the ACI Building Code (ACI. 318-56)

Design of floor (Empirical Method):

L.L. = 50 psf.
D.L. = 75 psf.

Slab thickness:

Least $t = 5''$

Section 1004 (d)1

$$t = L/36 = \frac{16 \times 12}{36} = 5\tfrac{1}{3}''$$

Section 1004 (d)2

$$t_1 = 0.028\, L \left(1 - \frac{2c}{3L}\right) \sqrt{\frac{w'}{f'_c/2000}} + 1\tfrac{1}{2}$$

$$= 0.028(16)\left(1 - \frac{2 \times 1}{3 \times 16}\right) \sqrt{\frac{125}{1.5}} + 1\tfrac{1}{2}$$

$$= 5.41''$$

Section 1004 (d)3

Increase of 15%

$t_1 = 5.41 \times 1.15$

$= 6.22''$

Use $6\tfrac{1}{2}''$ slab, $d = 5''$ ←

Then $W = 50 + 80 = 130$ psf.

Section 1004 (f)1

$$M_o = 0.09\, WLF\left(1 - \frac{2c}{3L}\right)^2$$

$$F = 1.15 - \frac{c}{L} = 1.09$$

$$M_o = 0.09\,(130)\,16\,(1.09)(0.958)^2 \times 16 \times 16$$

$$= 48{,}000^{\#}$$ ←

Check shear for 12" column:

$$v = \frac{V}{bjd} = \frac{16 \times 16 \times 30}{25 \times 4 \times .875 \times 6.5} = 58.5 \text{ psi}$$

Allowable = $.025 f'c$ = 75 psi > 58.5 psi ←

From table 1004 (f) a, compute necessary steel for top and bottom continuous mat for whole area:

by Use 25% M_o top and bottom and design negative steel around each column head individually:

Mat 25% M_o = .25 × 48,000
= 12,000 '#

$$A_s = \frac{M_s}{f_s j d} = \frac{12000 \times 12}{20,000 \times .875 \times 5.0}$$

= 1.65 sq. ins. / 8' width

6 #5 bars = 1.84 sq. ins.

Use #5 bars each way @ 12" spacing ←
(Spacing ≯ 2t)

Reinforcing over columns:

Exterior columns B-1, C-1, A-2, D-2, A-3, D-3, A-4, D-4, B-5, C-5

Use 40% of M_o = 19,200 '#

$$A_s = \frac{19,200 \times 12}{20,000 \times .875 \times 5.0} = 2.64 \text{ sq. ins.}$$

Use 9 #5 bars = 2.76 sq. ins in 8' width

by #5 bars @ 10" ←

Corner columns A-1, D-1, A-5, D-5

Use 20% M_o = 9,600 ft#

$$A_s = \frac{9{,}600 \times 12}{20{,}000 \times .875 \times 5.0} = 1.31 \text{ sq. ins.}$$

5 #5 bars @ 10" ←

Interior columns B-3, C-3

Use 50% M_o = .50 x 48,000
= 24,000 ft#

$$A_s = \frac{24{,}000 \times 12}{20{,}000 \times .875 \times 5.0} = 3.30 \text{ sq. ins.}$$

11 #5 bars @ 9" = 3.37 sq. ins. each way ←

Exterior columns
(as before but steel parallel to edge)

Use 25% M_o = 12,000 ft#

A_s = 1.65 sq. ins.

Use 6 #5 bars @ 8" ←

Design of shear walls:

A change in shear wall and column design occurs @ 4th floor and 8th floor.

Wind loading:

10 floors with floor height of 10', 1st floor 16'

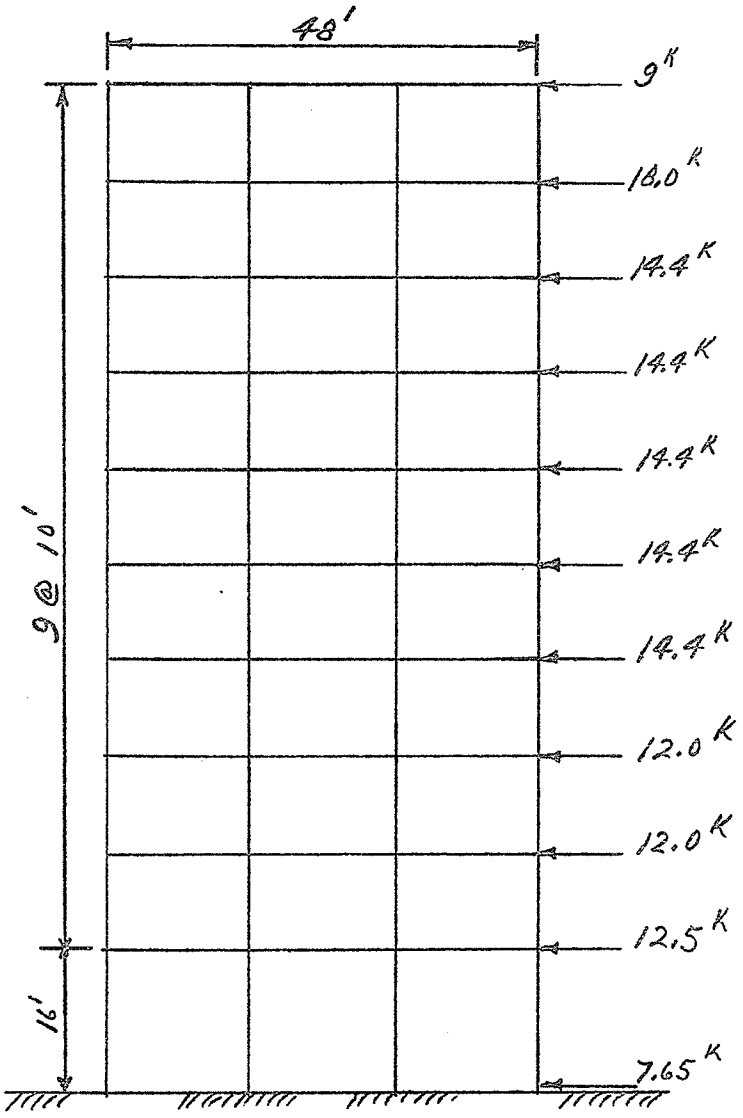

From NBC Supplement #1

q = 17 psf. = uniform lateral loading

From NBC Supplement #3

height variation (C_h)

0' to 20' – 0.8
20' to 40' – 1.0
40' to 90' – 1.2
90' to 180' – 1.5

$F = q \cdot C_h \cdot C_p \cdot A$

height : breadth : length ratio = 106 : 48 : 64
= 2.2 : 1.0 : 1.33

$C_{pe} = 0.9$, $C_{pi} = \pm 0.2$
$\therefore C_p = 1.1$

$F_0 = 17 \times 0.8 \times 1.1 \times 64 \times 8 = 7,650^{\#}$
$F_{16} = 17 \times 0.8 \times 1.1 \times 64 \times 13 = 12,500$
$F_{26} = 17 \times 1.0 \times 1.1 \times 64 \times 10 = 12,000$
$F_{36} = 17 \times 1.0 \times 1.1 \times 64 \times 10 = 12,000$
$F_{46} = 17 \times 1.2 \times 1.1 \times 64 \times 10 = 14,400$
$F_{56} = 17 \times 1.2 \times 1.1 \times 64 \times 10 = 14,400$
$F_{66} = 17 \times 1.2 \times 1.1 \times 64 \times 10 = 14,400$
$F_{76} = 17 \times 1.2 \times 1.1 \times 64 \times 10 = 14,400$
$F_{86} = 17 \times 1.2 \times 1.1 \times 64 \times 10 = 14,400$
$F_{96} = 17 \times 1.5 \times 1.1 \times 64 \times 10 = 18,000$
$F_{106} = 17 \times 1.5 \times 1.1 \times 64 \times 5 = 9,000$

The following design treats the shear walls ←

as two large cantilever beams with a point load @ each floor.

Maximum moment @ base :

$2M = 7.65 \times 4 + 12.65 \times 16 + 12.0 \times 26 + 12.0 \times 36$
$+ 14.4(46 + 56 + 66 + 76 + 86) + 18.0 \times 96 + 9.0 \times 106$
$= 8410^{1K}$
$\therefore M = 4205^{1K}$ (on one shear wall) ←

Maximum moment @ 4nd floor:

$$2M = 14.4(10+20+30+40+50) + 18.0 \times 60 + 9.0 \times 70$$
$$= 3870^{1K}$$
$$\therefore M = 1935^{1K} \text{ (on one shear wall)}$$

Maximum moment @ 8th floor:

$$2M = 14.4 \times 10 + 18.0 \times 20 + 9.0 \times 30$$
$$= 774^{1K}$$
$$M = 387^{1K} \text{ (on one shear wall)}$$

1) 2nd Floor:

Load on each wall = load on two central columns
$= 130 \times 16 \times 32 = 66.5^{K}$

Load @ main floor $= 66.5 \times 10 = 665^{K}$

Dead weight (assume wall 10") $= 150 \times 0^{10}/_{12} \times 16^{10}/_{12} \times 106$
$= 223^{K}$

Allowable stress in wall $= \left[.25 - (0.10 \times \frac{10}{15})\right] f'_c = 540 psi$

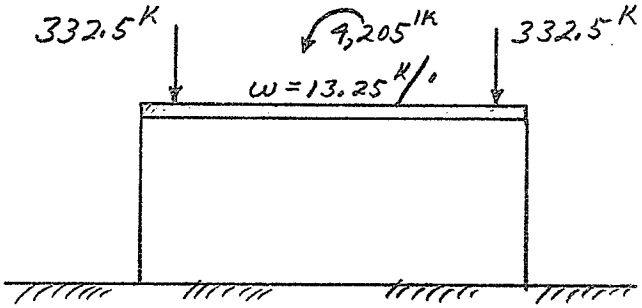

Allowable stresses for bending $= 20,000 \times 1.33$
$= 26,600 psi$

Check for bending as cantilever beam first:

1.) $M = f_s j A_s d$

$$A_s = \frac{4,205 \times 12000}{26,600 \times .875 \times 196} = 11.1 \text{ sq. ins.}$$ ←

2.) Bearing in wall

Total wall load = 665 + 223

= 888 K

$$\text{Bearing} = \frac{888,000}{202 \times 16} = 440 \text{ psi} < 540$$ ←

3.) Check by column design : Section 1109

total load on one shear wall = 888 K

$M = 4205$ IK

$$e = \frac{4205}{888} = 4.73$$

$$e/t = \frac{4.73}{16} = .295 < .667$$

For shear walls and columns:

$f_s = 1.33 (.4 f_y) = 21,300 \text{ psi}$

$$\frac{f_a}{F_a} + \frac{f_b}{F_b} < 1$$

$$f_a = \frac{888,000}{16\tfrac{1}{2} \times 12 \times 10} = 440 \text{ psi}$$

$F_a = .8 (0.225 f'_c + f_s p_g)$ by $p_g = \frac{22.2}{16\frac{1}{2} \times 12 \times 10} = .0113$

$= .8 (675 + 239)$

$= 730 \text{ psi}$

$$f_b = \frac{My}{I}$$

$$I = I_c + I_s = \frac{10 \times 196^3}{12} + 1.26 \times 196^2 \times 20 \times 10$$

$= 15,970 \times 10^3 \text{ ins.}^4$

$$\therefore f_b = \frac{4,205 \times 12000 \times 98}{15,970 \times 10^3} = 310 \text{ psi}$$

$F_b = 1350$ psi

$$\frac{f_a}{F_a} + \frac{f_b}{F_b} = \frac{490}{730} + \frac{310}{1350} = .833 < 1$$ ←

$\therefore$ O.K.

Use 10" wall for 1st to 4th floor

$A_s = 11.2$ sq. ins.

Use 10 #10 bars each end in 12" x 10" area

$A_s = 12.66$ sq. ins. ←

Use #3 ties @ every 10"

For wall itself use minimum horizontal and vertical steel:

Horizontal: .0025 Area = $15\frac{1}{2} \times 12 \times 10 \times .0025$

$= 4.6$ sq. ins.

Use 11 #6 bars — $A = 4.89$ sq. ins.

Use #6 bars @ 11" one face ←

Vertical: .0015 Area = $15\frac{1}{2} \times 12 \times 10 \times .0015$

$= 2.75$ sq. ins.

Use 7 #6 bars $A = 3.08$ sq. ins.

Space #6 bars @ 18" one face ←

Check for total shear in concrete:

$$V = \frac{143.15}{2} = 71.57^{K} / \text{shear wall}$$

$$v = \frac{V}{bjd} = \frac{71,570}{10 \times 16\frac{1}{2} \times 12 \times .875} = 40.5 \text{psi} < 90 \text{psi}$$

$\therefore$ O.K

Supposing vertical steel were to carry all shear:

$$f_v = \frac{V_s}{A_v j d} = \frac{71,570}{3.07 \times .875 \times 16\frac{1}{2} \times 12} = 136 \text{ psi}$$

$\therefore$ OK

Final design 1st to 4th floor:

Area = 10" x 16"

Use 10 #10 bars each end with #3 ties @ 10"

Vertical wall steel – #6 bars @ 18" one face

Horizontal wall steel – #6 bars @ 11" one face ←

2.) Shear wall above 4th floor: (use 8" wall)

M = 1935 IK

Total load = 888 x .7 = 621 K

Bearing = $\frac{621,000}{16" \times 12 \times 8}$ = 385 psi < 540 psi

Bending as cantilever:

$A_s = \frac{1935 \times 12000}{26,600 \times .875 \times 196}$ = 5.08 sq. ins.

Use 7 #8 bars A = 5.50 sq. ins.

@ each end

Use #3 ties @ 8" ←

Vertical wall steel – .0015 x 15' x 12 x 8 = 2.21 sq. ins.

Use #6 bars @ 18" one face

Horizontal wall steel – .0025 x 15' x 12 x 8 = 3.68 sq. ins.

Use #6 bars @ 13" one face

3.) Shear wall above 8th floor: (use 8" wall)

Bearing = $\frac{888,000 \times .3}{16" \times 12 \times 8}$ = 165 < 540 psi

Bending as cantilever

$A_s = \frac{387 \times 12000}{26,600 \times .875 \times 196}$ = 1.02 sq. ins.

Use 4 # 8 bars each end $A_s = 3.14$ sq. ins.
Use #3 ties @ 8"
Verticle wall steel #6 bars @ 18"
Horizontal wall steel #6 bars @ 13"

Design of Columns:

$$f_s = .4 f_y = 16{,}000 \text{ psi}$$

Base to 4th floor:

1) Interior columns

Total load = $130 \times 16 \times 16 \times 10 = 333^K$

Sect. 1004 $M = (130 \times 16 \times 16 \times 16 - 80 \times 16 \times 16 \times 16) \frac{1}{40}$
$= 5.13^{IK}$

NBC Table 4:12 B

Interior columns L.L. $= 50 \times 16 \times 16 \times 10$
$= 128^K$
50% L.L. $= 64^K$
D.L. $= 80 \times 16 \times 16 \times 10$
$= 205^K$

$\therefore$ Total design load @ base $= \underline{269^K}$ ←
$\underline{M = 5.13^{IK}}$ ←

Minimum $I_c = \dfrac{t^3 H}{.5 + \frac{W_D}{W_L}} = \dfrac{6.5^3 \times 16}{.5 + \frac{80}{50}} = \underline{2080 \text{ ins.}^4}$

Trial I:

Column size 20"x20" with 3% steel

Ratio $\frac{H}{t} = \frac{16}{1.67} < 10$ (short column)

$e = \frac{5.13 \times 12}{269} = .229''$

Ratio $e/t = \frac{.229}{20} = .0114 < .67$

(Table 8) Urquhart

Allowable load = $216 + 51(3) = 369^K > 269^K$

Trial II:

Column size 18"x18" with 3% steel

Allowable load = $175 + 41(3) = 298^K$

(Table 9) Actual load = $\frac{269 + 18 \times 18.8 \times 106}{1060}$

$= \underline{305^K}$

Ratio $\frac{H}{t} = \frac{16}{1.5} = 10.65 > 10$

P. 131 Urquhart

Equivalent short column load = $\frac{P'}{(1.3 - 0.3\frac{H}{t})}$

$= \frac{305}{1.3 - .32} = \underline{312^K}$ ←

Trial III:

Column size 18"x18" with 4% steel

Allowable = $339^K > 312^K$

For trial value $P = N(1 + \frac{Be}{t})$

$= 312(1 + \frac{3K \cdot 229}{18})$

$= \underline{324^K}$ ←

From table 8

$$\frac{324-175}{41} = 3.64\% \text{ steel}$$

$A_s = 3.64 \times 18 \times 18 = 11.83$ sq. ins.

Use 10 #10 bars, $A = 12.66$ sq. ins. ←

The exterior and corner colums for the base to 4th floor were desigaed in a similar way as were the columns for the 4th floor to 8th floor and columns 8th floor to roof.

The final design for all columns was tabulated in chapter II in table IIa.

APPENDIX II

Tabulation of Experimental Results

Table VIIa (Trial #1)

Lateral deflection readings for test series I

Floor	Load	Gage readings (inches x 10^{-3})								
		#1	#2	#3	#4	#5	#6	#7	#8	#9
2nd – 3rd	0	0.0	0.0	0.0	0.0	0.0	0.0	0.0	0.0	0.0
	40	1.0	0.6	0.8	0.7	0.7	0.4	0.2	0.0	0.0
	80	1.2	0.9	1.0	1.0	1.0	0.6	0.5	0.0	0.0
	100	1.5	1.0	1.1	1.0	1.0	0.7	0.6	0.0	0.0
4th – 5th	0	0.0	0.0	0.0	0.0	0.0	0.0	0.0	0.0	0.0
	40	0.8	0.1	1.0	0.7	0.8	0.4	0.2	0.0	0.0
	80	2.3	1.6	2.1	1.9	1.7	1.3	1.0	0.2	0.0
	120	3.9	3.0	3.2	3.0	2.6	2.2	1.5	0.7	0.1
	160	5.0	4.1	4.2	4.0	3.4	2.8	2.0	0.9	0.2
6th – 7th	0	0.0	0.0	0.0	0.0	0.0	0.0	0.0	0.0	0.0
	40	2.0	1.6	1.1	1.2	1.2	0.8	0.7	0.0	0.0
	80	5.0	4.1	3.3	3.1	2.9	2.0	1.5	0.5	0.1
	120	8.0	6.6	5.5	5.2	4.5	3.4	2.3	1.0	0.5
	160	11.1	9.1	8.0	7.1	6.1	4.6	3.0	1.5	0.6
8th – 9th	0	0.0	0.0	0.0	0.0	0.0	0.0	0.0	0.0	0.0
	40	4.3	3.2	3.1	2.4	1.9	1.3	1.0	0.6	0.0
	80	9.1	7.3	7.0	5.8	4.0	3.4	2.3	1.4	0.5
	120	15.0	11.5	10.3	8.4	6.5	5.0	3.5	2.0	1.0
	160	19.8	15.0	13.5	11.0	8.3	6.5	4.5	2.6	1.1
10th – ROOF	0	0.0	0.0	0.0	0.0	0.0	0.0	0.0	0.0	0.0
	40	5.8	4.0	3.8	3.0	2.1	1.5	1.3	0.1	0.1
	80	12.3	8.9	7.5	6.0	4.7	3.4	2.5	0.9	0.5
	120	19.0	13.7	11.6	9.0	7.2	5.1	3.6	1.4	0.7
	160	26.0	19.0	16.0	12.7	9.6	7.0	5.0	2.0	1.0

Table VIIa (Trial #2)

Lateral deflection readings for test series I

Floor	Load	Gage readings (inches x 10^{-3})								
		#1	#2	#3	#4	#5	#6	#7	#8	#9
2nd - 3rd		Results discarded due to faulty zeroing of gages								
4th - 5th	0	0.0	0.0	0.0	0.0	0.0	0.0	0.0	0.0	0.0
	40	1.0	0.7	0.8	0.3	0.4	0.3	0.4	0.0	0.0
	80	2.4	1.8	1.9	1.0	1.2	0.9	1.0	0.2	0.0
	120	4.0	3.0	3.0	2.1	2.0	1.8	1.4	0.6	0.0
	160	5.8	4.4	4.1	3.2	3.1	2.7	2.0	1.0	0.2
6th - 7th	0	0.0	0.0	0.0	0.0	0.0	0.0	0.0	0.0	0.0
	40	2.1	1.5	1.5	1.0	1.0	0.5	0.5	0.0	0.1
	80	5.5	4.0	3.9	2.8	2.5	1.9	1.4	0.6	0.1
	120	9.0	7.1	6.5	5.3	4.8	3.5	2.4	1.3	0.5
	160	11.0	8.7	8.0	6.5	5.9	4.3	3.0	1.4	0.5
8th - 9th	0	0.0	0.0	0.0	0.0	0.0	0.0	0.0	0.0	0.0
	40	4.0	2.6	2.5	1.5	1.3	0.9	0.9	0.0	0.0
	80	9.0	6.4	5.8	4.1	3.5	2.5	1.9	0.9	0.0
	120	14.0	10.3	9.0	7.0	5.8	4.1	2.8	1.3	0.4
	160	18.8	14.0	12.5	9.4	7.8	5.8	3.8	2.0	0.6
10th - ROOF	0	0.0	0.0	0.0	0.0	0.0	0.0	0.0	0.0	0.0
	40	7.0	4.7	4.1	3.0	2.4	1.8	1.5	0.8	0.1
	80	13.0	8.8	7.6	5.7	4.6	3.3	2.3	1.0	0.2
	120	19.3	13.6	11.4	8.6	7.0	5.0	3.1	1.8	0.5
	160	26.4	18.8	16.0	12.0	9.5	7.0	4.5	2.3	0.8

Table VIIa (Trial #3)

Lateral deflection readings for test series I

Floor	Load	Gage readings (inches x 10^{-3})								
		#1	#2	#3	#4	#5	#6	#7	#8	#9
2nd - 3rd	0	0.0	0.0	0.0	0.0	0.0	0.0	0.0	0.0	0.0
	40	1.0	0.8	0.8	0.5	0.3	0.4	0.4	0.1	0.0
	80	1.3	1.0	1.0	0.8	0.5	0.5	0.5	0.1	0.0
	100	1.5	1.2	1.0	0.9	0.8	0.6	0.8	0.3	0.0
4th - 5th	0	0.0	0.0	0.0	0.0	0.0	0.0	0.0	0.0	0.0
	40	1.0	0.8	1.0	0.8	0.4	0.4	0.4	0.0	0.0
	80	2.8	2.2	2.1	1.7	1.4	1.2	1.0	0.4	0.0
	120	4.5	3.7	3.6	2.8	2.5	2.0	1.8	0.8	0.3
	160	6.3	5.5	5.0	4.0	3.8	3.0	2.3	1.1	0.5
6th - 7th	0	0.0	0.0	0.0	0.0	0.0	0.0	0.0	0.0	0.0
	40	2.8	2.6	2.0	1.6	1.2	1.0	1.0	0.2	0.0
	80	5.6	4.8	4.0	3.0	2.8	2.0	1.4	0.7	0.0
	120	9.0	7.5	6.5	5.3	4.5	3.5	2.4	1.0	0.4
	160	12.0	10.0	8.9	7.7	6.3	5.0	3.3	1.7	0.8
8th - 9th	0	0.0	0.0	0.0	0.0	0.0	0.0	0.0	0.0	0.0
	40	5.0	3.6	2.5	2.0	2.0	1.0	0.5	0.2	0.0
	80	9.8	7.3	5.8	4.8	4.0	2.5	1.5	1.0	0.2
	120	14.6	11.2	9.0	7.5	6.0	4.2	2.5	1.4	0.5
	160	19.2	15.0	12.1	10.0	8.1	5.8	3.5	2.0	0.9
10th ROOF	0	0.0	0.0	0.0	0.0	0.0	0.0	0.0	0.0	0.0
	40	6.8	5.0	3.3	2.9	2.0	1.6	1.3	0.9	0.2
	80	13.5	10.0	7.4	6.3	5.0	3.5	2.5	1.5	0.5
	120	20.2	15.0	11.9	9.6	7.5	5.5	3.9	2.1	1.0
	160	27.2	20.0	16.0	12.9	10.0	7.5	5.0	2.9	1.2

Table VIIa (Average)

Lateral deflection readings for test series I

Floor	Load	Gage readings (inches x 10^{-3})								
		#1	#2	#3	#4	#5	#6	#7	#8	#9
2nd–3rd	0	0.0	0.0	0.0	0.0	0.0	0.0	0.0	0.0	0.0
	40	1.0	0.7	0.8	0.6	0.5	0.4	0.3	0.1	0.0
	80	1.2	1.0	1.0	0.9	0.7	0.6	0.5	0.1	0.0
	100	1.5	1.1	1.0	0.9	0.9	0.7	0.7	0.2	0.0
4th–5th	0	0.0	0.0	0.0	0.0	0.0	0.0	0.0	0.0	0.0
	40	0.9	0.6	0.9	0.6	0.5	0.4	0.3	0.0	0.0
	80	2.5	1.9	1.7	1.5	1.4	1.1	1.0	0.3	0.0
	120	4.1	3.3	3.3	2.6	2.4	2.0	1.6	0.7	0.1
	160	5.7	4.7	4.4	3.7	3.4	2.8	2.1	1.0	0.3
6th–7th	0	0.0	0.0	0.0	0.0	0.0	0.0	0.0	0.0	0.0
	40	2.3	1.9	1.5	1.3	1.1	0.8	0.7	0.1	0.0
	80	5.4	4.3	3.7	3.0	2.7	2.0	1.4	0.6	0.1
	120	8.7	7.1	6.2	5.3	4.6	3.5	2.4	1.1	0.5
	160	11.4	9.3	8.3	7.1	6.1	4.6	3.1	1.5	0.6
8th–9th	0	0.0	0.0	0.0	0.0	0.0	0.0	0.0	0.0	0.0
	40	4.4	3.1	2.7	2.0	1.7	1.1	0.8	0.3	0.0
	80	9.2	7.0	6.2	4.9	3.8	2.8	1.9	1.1	0.2
	120	14.5	11.0	9.4	7.6	6.1	4.4	2.9	1.6	0.6
	160	19.3	14.7	12.7	10.1	8.1	6.0	3.9	2.2	0.9
10th–ROOF	0	0.0	0.0	0.0	0.0	0.0	0.0	0.0	0.0	0.0
	40	6.5	4.6	3.7	3.0	2.2	1.6	1.4	0.6	0.1
	80	12.9	9.2	7.5	6.0	4.8	3.4	2.4	1.1	0.4
	120	19.5	14.1	11.6	9.1	7.2	5.2	3.5	1.8	0.7
	160	26.5	19.3	16.0	12.8	9.7	7.2	4.8	2.4	1.0

Table VIIa (Results by superposition)

Lateral deflection readings for test series I

Load/Floor	Gage readings (inches x 10^{-8})								
	#1	#2	#3	#4	#5	#6	#7	#8	#9
0	0.0	0.0	0.0	0.0	0.0	0.0	0.0	0.0	0.0
20	15.1	10.9	9.6	7.5	6.0	4.3	3.5	1.1	0.1
40	31.2	23.4	20.1	16.3	13.4	9.9	7.2	3.2	0.7
60	48.4	36.8	31.7	25.6	21.2	15.8	11.1	5.4	1.9
80	64.9	49.0	42.7	34.5	28.3	21.4	14.7	7.5	2.9

Table VIIb (Trial #1 to #3)

Lateral deflection readings for test series II

Load/Floor	Gage readings (inches x 10^{-3})								
	#1	#2	#3	#4	#5	#6	#7	#8	#9
0	0.0	0.0	0.0	0.0	0.0	0.0	0.0	0.0	0.0
20	13.7	9.5	5.0	6.5	5.0	3.5	2.0	1.2	0.2
40	34.0	24.0	19.0	18.2	14.2	11.2	7.2	4.5	1.7
60	55.0	43.0	34.0	30.5	24.3	19.0	13.0	8.3	3.7
0	0.0	0.0	0.0	0.0	0.0	0.0	0.0	0.0	0.0
20	16.5	12.0	10.6	9.0	6.5	5.1	3.5	2.2	1.1
40	38.5	29.3	24.2	22.1	17.0	13.8	9.3	6.0	3.1
60	57.0	45.0	38.5	33.0	25.7	20.5	14.0	9.0	4.5
80	79.7	63.0	54.2	46.0	36.5	28.8	20.0	13.0	6.5
0	0.0	0.0	0.0	0.0	0.0	0.0	0.0	0.0	0.0
20	17.5	13.2	11.5	9.8	7.5	6.1	4.0	2.7	1.2
40	40.0	31.0	27.7	23.0	18.3	14.7	10.0	6.8	3.4
60	58.4	47.0	40.7	34.0	27.0	21.5	15.0	9.5	4.8
80	78.8	62.5	54.3	45.0	36.4	28.5	19.8	12.8	6.4
Average of Trial #1 to #3									
0	0.0	0.0	0.0	0.0	0.0	0.0	0.0	0.0	0.0
40	15.9	11.6	9.0	8.4	6.3	4.9	3.3	2.0	0.8
80	37.5	28.3	27.0	21.1	16.5	13.2	8.8	5.8	2.7
120	53.5	46.0	37.7	32.6	25.7	20.3	14.0	8.9	4.3
160	79.2	62.7	54.2	45.5	36.4	28.6	19.9	12.9	6.4

Table VIIc (Trial #1 and #2)

Lateral deflection readings for test series III

Load/Floor	Gage readings (inches x 10^{-3})								
	#1	#2	#3	#4	#5	#6	#7	#8	#9
0	0.0	0.0	0.0	0.0	0.0	0.0	0.0	0.0	0.0
20	18.0	13.9	11.9	9.6	8.0	6.4	4.2	3.0	1.5
40	39.7	31.0	26.8	22.0	20.9	14.5	9.9	6.7	3.3
60	61.0	49.5	42.0	35.0	29.0	22.2	15.8	10.2	5.0
80	81.0	64.3	55.5	46.0	37.0	29.3	20.7	13.4	6.6
100	109.5	86.2	74.9	62.5	50.0	39.9	28.0	18.3	9.1
120	122.4	96.0	83.0	69.4	55.0	43.6	30.5	20.0	9.9
			Recording permanent set						
0	11.9	11.3	7.7	6.4	5.0	4.5	3.0	2.1	1.0
0	0.0	0.0	0.0	0.0	0.0	0.0	0.0	0.0	0.0
20	18.0	14.0	12.3	11.0	9.0	6.8	5.0	3.1	1.6
40	38.0	30.2	26.4	22.7	18.9	14.4	10.2	6.8	3.5
60	62.3	50.0	43.1	37.0	30.5	23.1	17.0	11.0	5.6
80	83.0	66.0	57.0	48.5	40.0	30.8	22.0	14.5	7.5
100	106.0	84.0	72.8	61.8	50.0	39.0	28.0	18.2	9.5
120	132.5	105.8	91.4	77.5	62.0	49.1	35.3	23.0	12.0
			Recording permanent set						
0	15.5	11.9	10.2	10.0	8.3	6.6	5.0	4.0	2.4

Table VIIc (Trial #3 and #4)

Lateral deflection readings for test series III

Load/Floor	Gage readings (inches x 10^{-3})								
	#1	#2	#3	#4	#5	#6	#7	#8	#9
0	0.0	0.0	0.0	0.0	0.0	0.0	0.0	0.0	0.0
20	15.0								
40	38.0		Readings not taken						
60	63.0	50.5	49.3	36.3	30.1	23.0	16.3	10.9	5.2
80	87.0		Readings not taken						
100	112.0	90.0	78.9	65.2	52.8	41.5	29.8	19.3	9.7
120	132.3	106.4	92.0	77.2	62.0	49.0	35.0	23.0	11.5
			Recording permanent set						
0	5.4	4.3	3.5	2.9	2.2	1.8	1.0	1.0	0.5
0	0.0	0.0	0.0	0.0	0.0	0.0	0.0	0.0	0.0
20									
40									
60			Readings not taken						
80									
100	112.9	91.0	79.7	67.0	55.0	42.7	31.0	20.0	10.5
120	132.1	106.5	92.7	78.0	63.9	49.5	36.0	23.0	12.0
140	162.1	130.0	116.1	95.2	77.3	60.2	44.0	28.5	20.0
160	232.5	187.0	163.2	138.4	120.0	89.5	65.8	43.5	24.0
			Recording permanent set						
0	63.0	58.8	44.1	38.5	35.6	26.0	20.0	15.0	8.5

Table VIId

Lateral deflection readings for test series IV

Floor	Load	Gage readings (inches x 10^{-3})								
		#1	#2	#3	#4	#5	#6	#7	#8	#9
2nd - 3rd	20	1.9	1.9	2.0	1.8	2.0	1.8	2.0	2.2	1.3
4th - 5th	20	4.0	4.0	4.0	3.8	4.0	3.4	3.1	2.8	1.3
6th - 7th	20	6.0	6.0	6.0	5.6	6.0	4.2	3.4	2.8	1.2
8th - 9th	20	8.7	8.5	8.0	6.5	5.6	4.1	3.1	2.6	1.2
10th - ROOF	20	15.0	12.2	10.3	8.6	8.0	6.0	4.6	4.0	1.8
Results by superposition for 10#/floor uniform lateral load										
		35.6	32.6	30.3	26.3	25.6	19.5	16.2	14.4	6.8

Table VIIe

Lateral deflection readings for test series V

Floor	Load	Gage readings (inches x 10^{-3})								
		#1	#2	#3	#4	#5	#6	#7	#8	#9
2nd-3rd	40	5.0	5.0	5.0	4.9	5.0	4.8	5.0	5.2	3.3
4th-5th	40	10.4	10.4	10.1	10.0	10.7	9.5	9.0	6.9	3.8
6th-7th	40	15.2	15.2	15.1	14.6	14.7	10.9	9.2	6.8	3.5
8th-9th	40	22.0	21.5	20.0	17.0	15.0	11.4	9.5	6.9	3.7
10th-ROOF	40	34.0	26.8	22.7	19.3	17.5	13.5	11.1	8.2	4.5
		Results by superposition for 20#/floor uniform lateral load								
		86.6	78.9	72.9	65.8	62.6	50.1	43.5	34.0	18.8

Table VIIf

Lateral deflection readings for test series VI

Floor	Load	Gage readings (inches x 10^{-3})								
		#1	#2	#3	#4	#5	#6	#7	#8	#9
2nd - 3rd	14.07	1.5	1.5	1.5	1.5	1.5	1.5	1.5	1.5	1.1
4th - 5th	22.37	5.7	5.2	5.1	5.3	5.5	5.2	4.1	3.3	1.6
6th - 7th	31.34	11.4	11.5	11.3	11.1	10.1	8.3	6.5	4.2	2.5
8th - 9th	35.30	19.3	18.5	17.3	16.1	13.5	10.6	8.5	5.5	3.3
10th - ROOF	32.91	26.5	21.2	19.0	16.1	14.0	11.0	9.3	6.3	3.6

Table VIIg

Lateral deflection readings for test series VII

Floor	Load	Gage readings (inches x 10^{-3})								
		#1	#2	#3	#4	#5	#6	#7	#8	#9
2nd - 3rd	30.77	4.1	4.1	4.1	4.1	4.1	4.3	4.5	4.0	3.0
4th - 5th	50.18	16.0	15.2	15.6	15.6	15.6	14.5	13.2	9.3	5.2
6th - 7th	68.60	31.2	31.0	30.8	30.0	27.8	28.0	18.0	12.3	6.8
8th - 9th	82.10	52.8	50.8	47.5	41.6	35.8	22.00	22.6	16.0	9.0
9th - Roof	81.30	72.5	56.5	49.5	42.3	36.3	21.0	23.2	16.5	9.1

Table VIIh (Average of 3 trials)

Slab deformations in the plane of the shear wall for test series I

Floor	Load	SR - 4 gage readings (inches/inch x 10^{-6})									
		#1	#2	#3	#4	#5	#6	#7	#8	#9	#10
2nd - 3rd	0	0	0	0	0	0	0	0	0	0	0
	40	-2	-2	-2	-3	-1	-2	-1	-1	-2	-1
	80	-4	-3	-4	-3	-2	-3	-1	-2	-2	-1
	100	-3	-3	-4	-3	-2	-3	-1	-2	-2	-1
4th - 5th	0	0	0	0	0	0	0	0	0	0	0
	40	-2	-1	-2	+1	0	-2	-1	0	+1	+1
	80	-3	-2	-1	0	+1	-3	-1	0	+1	+2
	120	-5	-3	-2	0	+1	-4	-2	0	+1	+3
	160	-6	-3	-2	+1	+2	-5	-2	0	+2	+5
6th - 7th	0	0	0	0	0	0	0	0	0	0	0
	40	0	0	+2	+1	+2	-3	-1	+1	+1	+2
	80	-4	-2	0	+1	+2	-5	-1	+1	+3	+4
	120	-5	-1	+1	+2	+3	-6	-1	+1	+3	+6
	160	-9	-2	0	+1	+4	-8	-1	+1	+5	+3
8th - 9th	0	0	0	0	0	0	0	0	0	0	0
	40	-4	-2	-2	+1	0	-3	0	+1	+1	+3
	80	-6	-3	-1	0	+1	-5	-1	0	+2	+5
	120	-9	-5	-2	0	+2	-8	-2	0	+3	+7
	160	-12	-5	-2	+1	+3	-11	-2	0	+3	+9
10th - ROOF	0	0	0	0	0	0	0	0	0	0	0
	40	-3	-1	+1	+1	+1	-2	0	0	+3	+3
	80	-7	-3	0	+2	+2	-6	0	+1	+4	+6
	120	-10	-4	+2	+3	+3	-8	-1	+1	+4	+9
	160	-14	-6	0	+2	+5	-11	-2	+1	+6	+12

Table VIIh (Results by superposition)

Slab deformations in the plane of the shear wall for test series I

Load/Floor SR - 4 gage readings (inches/inch x 10^{-6})

Table VIIk (Trial #1 and #2)

Slab deformations in the plane of the shear wall for test series III

Load/Floor SR - 4 gage readings (inches/inch x 10^{-6})

	#1	#2	#3	#4	#5	#6	#7	#8	#9	#10
0	0	0	0	0	0	0	0	0	0	0
20	-11	-4	0	+2	+4	-7	-1	0	+4	+6
40	-24	-10	-2	+4	+8	-16	-3	0	+8	+17
60	-33	-14	-2	+6	+13	-23	-4	+1	+12	+26
80	-44	-19	-7	+7	+15	-32	-6	0	+15	+35
100	-50	-22	-5	+6	+20	-38	-8	+1	+18	+43
0	0	0	0	0	0	0	0	0	0	0
20										
40				Readings not taken						
60										
80	-39	-17	-4	+4	+14	-29	-8	0	+10	+28
100	-47	-23	-6	+5	+14	-38	-10	0	+14	+37
120	-58	-28	-16	-5	+14	-45	-12	0	+16	+45

Table VIIk (Trial #3 and #4)

Slab deformations in the plane of the shear wall for test series III

Load/Floor — SR - 4 gage readings (inches/inch x 10^{-6})

	#1	#2	#3	#4	#5	#6	#7	#8	#9	#10
0	0	0	0	0	0	0	0	0	0	0
20										
40			Readings not taken							
60	-34	-18	-8	+1	+10	-24	-7	+1	+8	+20
80			Readings not taken							
100	-54	-26	-10	+1	+11	-38	-10	0	+14	+40
120	-62	-30	-13	0	+12	-44	-12	+1	+18	+46
0	0	0	0	0	0	0	0	0	0	0
20										
40										
60			Readings not taken							
80										
100	-52	-27	-10	+3	+12	-37	-8	0	+16	+39
120	-61	-27	-9	+3	+15	-42	-8	+2	+21	+48
140	-69	-32	-10	+3	+17	-50	-10	+3	+24	+56
160	-86	-40	-18	-2	+14	-61	-14	0	+26	+60

Table VIII (Average of 3 trials)

Joint deformations for test series I

Floor	Load	SR - 4 gage readings (inches/inch x 10^{-6})								
		#10	#11	#12	#13	#14	#15	#16	#17	#18
2nd - 3rd	0	0	0	0	0	0	0	0	0	0
	40	-1	0	-1	-1	-1	0	-1	-1	0
	80	-1	-1	-1	-1	-2	0	-2	-1	0
	100	-1	-1	-1	-1	-2	0	-1	-1	0
4th - 5th	0	0	0	0	0	0	0	0	0	0
	40	+1	-1	0	0	-1	+1	-1	-1	+1
	80	+2	-1	-1	0	-2	+1	-3	-2	+2
	120	+3	-3	-2	-1	-3	+3	-4	-2	+3
	160	+5	-3	-2	0	-4	+5	-6	-3	+4
6th - 7th	0	0	0	0	0	0	0	0	0	0
	40	+2	-1	0	+2	0	+1	-3	-1	+1
	80	+4	-2	-2	+1	-2	+2	-4	-2	+3
	120	+6	-4	-4	+1	-3	+3	-8	-3	+1
	160	+9	-6	-6	0	-4	+5	-11	-5	+3
8th - 9th	0	0	0	0	0	0	0	0	0	0
	40	+3	-1	0	0	0	+1	-3	-1	+1
	80	+5	-3	-3	+1	-1	+2	-6	-3	0
	120	+7	-5	-6	0	-3	+3	-11	-5	+1
	160	+9	-7	-8	-1	-5	+5	-15	-6	0
10th - ROOF	0	0	0	0	0	0	0	0	0	0
	40	+3	-2	-2	+1	-1	+1	-5	-2	0
	80	+6	-4	-5	-1	-3	+2	-9	-5	-1
	120	+9	-6	-8	-2	-6	+3	-15	-7	-2
	160	+12	-9	-12	-3	-8	+4	-19	-9	-3

Table VIII (Results by superposition)

Joint deformations for test series I

Load/Floor SR - 4 gage readings (inches/inch x 10^{-6})

	#10	#11	#12	#13	#14	#15	#16	#17	#18
0	0	0	0	0	0	0	0	0	0
20	+8	-5	-3	+2	-3	+4	-13	-6	+3
40	+16	-11	-12	0	-10	+7	-24	-13	+4
60	+24	-19	-21	-3	-17	+12	-39	-18	+3
80	+33	-26	-29	-5	-23	+17	-53	-24	+4

Table VIIm (Trial #1 to #3)

Joint deformations for test series II

SR - 4 gage readings (inches/inch x 10^{-6})

Load/Floor	#10	#11	#12	#13	#14	#15	#16	#17	#18
0	0	0	0	0	0	0	0	0	0
20	+6	-9	-10	-2	-10	+2	-14	-6	-3
40	+14	-15	-18	-4	-16	+4	-30	-14	-5
60	+21	-21	-26	-6	-23	+4	-42	-19	-5
0	0	0	0	0	0	0	0	0	0
20	+8	-6	-8	-2	-8	+1	-11	-5	+3
40	+18	-12	-18	-4	-12	+6	-26	-11	+2
60	+27	-20	-24	-4	-20	+7	-39	-16	+4
80	+34	-24	-30	-4	-27	+9	-59	-22	-1
0	0	0	0	0	0	0	0	0	0
20	+6	-6	-7	-3	-6	+3	-13	-7	0
40	+14	-12	-18	-5	-15	+5	-29	-14	+2
60	+22	-20	-26	-6	-22	+6	-43	-20	0
80	+30	-28	-33	-8	-30	+8	-60	-24	0
Average of Trial #1 to #3									
0	0	0	0	0	0	0	0	0	0
20	+7	-7	-8	-2	-8	+2	-13	-6	0
40	+15	-13	-18	-4	-14	+5	-25	-13	0
60	+23	-20	-25	-5	-22	+6	-41	-18	0
80	+32	-26	-31	-6	-28	+8	-59	-23	0

Table VIIn (Trial #1 and #2)

Joint deformations for test series III

Load/Floor SR - 4 gage readings (inches/inch x 10^{-6})

	#10	#11	#12	#13	#14	#15	#16	#17	#18
0	0	0	0	0	0	0	0	0	0
20	+6	-6	-5	-2	-5	+3	-14	-6	-2
40	+17	-14	-15	-2	-10	+6	-27	-10	+2
60	+26	-18	-22	-3	-19	+9	-42	-18	0
80	+35	-26	-28	-3	-28	+10	-52	-22	+1
100	+43	-30	-32	-2	-37	+13	-67	-28	-7
0	0	0	0	0	0	0	0	0	0
20									
40				Readings not taken					
60									
80	+28	-25	-30	-5	-28	+6	-52	-22	-2
100	+37	-30	-38	-5	-38	+8	-62	-26	-2
120	+45	-36	-40	-4	-45	+10	-74	-31	-7

Table VIIn (Trial #3 and #4)

Joint deformations for test series III

Load/Floor — SR - 4 gage readings (inches/inch x 10^{-6})

	#10	#11	#12	#13	#14	#15	#16	#17	#18
0	0	0	0	0	0	0	0	0	0
20									
40				Readings not taken					
60	-20	-21	-25	-4	-22	+5	-39	-18	0
80				Readings not taken					
100	+40	-34	-39	-6	-38	+9	-68	-30	-4
120	+46	-37	-43	-5	-46	+12	-78	-34	-5
0	0	0	0	0	0	0	0	0	0
20									
40				Readings not taken					
60									
80									
100	+39	-30	-36	-5	-37	+10	-62	-26	0
120	+48	-33	-40	-4	-44	+13	-74	-31	-3
140	+56	-37	-45	-2	-50	+14	-84	-34	-2
160	+60	-39	-49	-3	-60	+14	-101	-39	-3

APPENDIX III

Computer Application of Kani Method

APPENDIX III

The Kani method of analysis of multistorey frames introduces "a timesaving method of analysis, with consideration of displaceable joints, presenting an iteration procedure with automatic error elimination".*(5) In the Kani method moments produced by rotation, lateral displacement, and direct loading are determined and distributed with the use of appropriate distribution factors. The moments produced by lateral displacement and member rotation were developed by the slope deflection equations. The actual analysis consisted of two simple operations, one for distribution of themoments and a second for side sway, which were repeated until the accuracy required was reached. For a ten storey building, although the process would be simple and repetitive, the time involved in a complete analysis of each frame manually would be practically impossible. However the complete procedure has been programmed for the 1620 computer. All that would be required manually is to feed in the following data:

1. Number of spans and number or stories.
2. Span lengths.
3. Storey heights.
4. Beam moments of inertia.
5. Column moments of inertia.
6. Lateral loads.
7. Modulus of elasticity of concrete.

The location of the point of inflection in the connecting slabs was required. This had been determined experimentally from the

model and was taken as 1/2 the unsupported length. The width of slab acting as a "beam element" was determined as mentioned in Chapter VIII, from work carried out by Khan and Sbarounis*(3).

The computer proceeds to work out the appropriate distribution factors and carry out the iteration process until the desired accuracy is reached. All resulting end moments and lateral displacements were then recorded.

The frame analysis programme was also adapted to frames containing shear walls. The programme allowed the shear wall itself to be analysed as a free cantilever with restraining moments developed at each floor. Thus the rotation at each floor was determined from the analysis of the cantilever under lateral loading and the moment introduced by the slab due to this rotation calculated. Using the combined moments from lateral loading and slab resistance the lateral deflections for the shear walls were determined. The remainder of the frame was then treated as a free frame and a small percent of the total lateral load applied to this frame. The amount of lateral loading attributed to the free frame portion was determined by trial and error. When the assumed lateral load applied to the free frame portion produced lateral deflections which were equivalent to the shear wall the capacity of the free frame portion was determined. Since this was found to be less than 1% of the total load the deflected shape of the shear wall acting alone (including effect of slab restraint) was assumed to represent the entire frame. Once the deflected shape of each shear wall frame and the remaining three free frames was recorded for design load the amount of lateral loading attributed to each

frame could be determined manually by the relative stiffness of the frames. This was carried out as illustrated in Chapter VIII.